American Mineralogist, Volume 61, pages 1059–1116, 1976

Lunar mineralogy: a heavenly detective story. Part II[1]

JOSEPH V. SMITH AND IAN M. STEELE

Department of the Geophysical Sciences, University of Chicago
Chicago, Illinois 60637

Contents

Abstract

This second part is a revised and expanded version of the 1973 Presidential Address, and incorporates new data published up to November 1975.

The earlier list of lunar minerals is expanded to include cordierite, molybdenite, farringtonite, akaganéite, unidentified Cl,Fe,Zn-bearing phases, bornite(?), aluminum oxycarbide(?), monazite, thorite(?), pyrochlore(?), titanite, and graphite.

A general discussion of rock types is set in the context of the phase relations in the silica–olivine–anorthite and Fe–FeS systems, and a model for early primary differentiation followed by partial melting of cumulates. Most of the returned rocks are metamorphosed breccias composed of several materials. Lunar specimens with Mg-rich minerals are reviewed in detail because they may represent early crystalline differentiates. Emphasis is placed on the chemical composition of olivine and pyroxene as a means of sorting out the host rocks, while textures and modes are given less significance because of erratic mechanical and metamorphic processes. Rocks with Mg-rich minerals are classified as *dunitic* [with olivine Fo_{85-89}, Cr,Al,Fe,Mg–spinel, and sometimes a titanate (armalcolite?)], *troctolitic* (Mg-subgroup with olivine Fo_{85-91} and Fe-subgroup with variable olivine mostly Fo_{70-85}), *spinel–troctolitic* (diverse olivine Fo_{97-70}, rare Mg-rich pyroxene, and Mg,Al-rich spinel). Rocks with minerals of lower Mg-content are classified as *high-KREEP material, mostly noritic* (pyroxenes mostly $En_{60-80}Fs_{16-36}Wo_{2-5}$, rare augite, relatively Na-rich plagioclase An_{90-75}), *low-KREEP noritic* (pyroxenes mostly $En_{73-81}Wo_{\sim 3}$ but some $En_{43-48}Wo_{45-48}$, plagioclase An_{92-94}), *anorthositic, granitic and rhyolitic, mare basalts,* and *ANT* group.

Important aspects of the following minerals are discussed.

Feldspars: trace element analysis by ion microprobe; cation vacancy in anorthite; experimental reproduction of textures in basalts; twin distribution; domain textures from electron microscopy; unusual ternary compositions.

Olivines: correlation of Al,Ca,Ti,Cr,Mn, and Ni with type of host rock; slight Mg,Fe ordering; magnetic hyperfine peaks; reaction of olivine clasts in metamorphosed breccias.

Pyroxenes: correlation of Ca,Mg,Fe content with host rock and interpretation in terms of crystal–liquid differentiation; low content of Na and K; content of minor elements including Ti,Al, and Cr; estimation of crystallization and cooling conditions from exsolution phenomena and site populations; interpretation of disorientation and cracking.

Other silicates: possible limit on pressure from occurrence of silica polymorphs; limit on availability of water from rarity and compositions of amphibole; possibility of garnet occurring in deep-seated rocks; uncertain identification of melilite.

Spinels: apparent absence of trivalent iron; new scheme for plotting compositions on a tetragonal pyramid with ulvöspinel at the apex; composition trend from Mg,Al–spinel toward chromite-rich spinel and then to ulvöspinel as the host rock trends from troctolitic to mare basalt; correlation of zoning from chromite to ulvöspinel in mare basalt with relative stage of crystallization of silicates; reduction of Ti-rich spinel to iron plus rutile or ilmenite plus Ti-poor spinel; partition of Zr between ilmenite and ulvöspinel as a thermometer.

Ilmenite: Mg/Fe ratio which probably depends on temperature and Mg content of coexisting (Mg,Fe)–silicates; deformation occurring at low shock pressure; interpretation of intergrowths with rutile, spinel and pyroxene in terms of exsolution, reduction or shock.

Armalcolite: contains about 5 percent $Ti_2^{3+}Ti^{4+}O_5$; breaks down to ilmenite and rutile below about 800–1000°C; has an Mg/Fe ratio which correlates with that of coexisting silicates; has an upper limit for pressure stability at several kbar. Zr-rich and Cr,Zr–Ca-rich grains in breccias were commonly described as armacolite, but may not be isostructural; their Mg/Fe ratios correlate with coexisting silicates; because they are found with Mg-rich silicates they may occur deep in the Moon.

Baddeleyite and *rutile*: Wide compositional ranges.

Phosphate and *phosphide*: relative occurrence depends on the redox conditions. Whitlockite carries substantial REE. Apatite is rich in F and Cl, and OH is probably absent or very low. Schreibersite apparently derived from meteoritic debris and directly from lunar rocks, and the partition of Ni and P between schreibersite and iron mineral gives a useful thermometer for metamorphosed breccias.

Troilite: ubiquitous in lunar rocks; anticorrelation of Fe and S in mare basalts indicates

loss of S; positive correlation of Fe and S in non-mare rocks indicates meteoritic contamination; Ti partitioning with ilmenite is temperature dependent. *Cohenite*: results from meteoritic debris, and probably from solar wind.

Iron metals: ubiquitous; indicate a low redox state; result from both meteoritic contamination and indigenous processes for which Co and Ni contents may provide a fairly reliable clue; occur in veins and vugs indicating presence of vapor.

The sum total of data provides important controls on geochemical and petrologic models. Extensive crystal–liquid fractionation, impact differentiation, shock and thermal metamorphism, vapor transfer and change of redox conditions, and late meteoritic addition are needed to explain the mineralogy. Although considerable uncertainties remain, primary differentiation of an olivine-rich dry Moon is reaffirmed as a valuable model upon which many subsidiary processes including partial melting of cumulates, formation of an Fe,S-rich core, and impact metamorphism can be added as subsidiary parameters. The clues offered to the lunar detective are heavily biased by sampling and confused by multiple processes, and much further research is needed.

Introduction

Part I (Smith, 1974) set lunar mineralogy in the context of a model Moon, crudely classified the rock types, enumerated the observed minerals, and reviewed the properties of feldspar and olivine. Taylor (1975) provided a well-balanced view of the general properties of the Moon, but his detailed geochemical model has some controversial features especially concerning the origin of mare basalts and KREEP-rich rocks. The development of the early Earth and Moon was reviewed by Smith (1975), and a model was developed for origin of the Moon by catastrophic capture followed by accretion of the Earth-orbiting debris. Simultaneous accretion of solar-orbiting material by a proto-Earth and an Earth-orbiting proto-Moon was also considered likely, while origin of the Moon by fission from or volatilization of the Earth was thought to be unlikely. Uncertainties in models for the bulk composition of the Moon were emphasized: in particular, existing estimates for Ca differ four-fold.

The appearance of the review of lunar minerals by Frondel (1975) makes it unnecessary to elaborate here on the strictly mineralogic features, and the present review concentrates on crystal-chemical, petrologic, and geochemical aspects of lunar mineralogy. Minerals not discussed in detail, and not listed in Part I, are given in the appendix.

General discussion of rock types: relation to model of Moon

The confusion in lunar rock nomenclature has been partly reduced as petrologists and geochemists realized that most lunar rocks are hybrids which have undergone sequential changes including erratic shock metamorphism. Most lunar petrologists believe that the outer part of the Moon (perhaps 10 km thick) is dominated by debris produced by repeated impact from −4.5 to −4.0 Gy into a complex assemblage of igneous and metamorphic rocks. Impacts by bodies some tens of kilometers across yielded superimposed Moon-wide blankets ranging from a few kilometers thick at the edge of an impact basin to some meters thick at great distances. The debris consisted of complex mixtures of material excavated down to depths of some tens of kilometers mixed in with dispersed material from the projectile. Secondary impacts and differentiation during transport caused further complication, and could account for the bulk of present regolith. Impact basins were partially filled with hot debris which became modified by metamorphism and volcanism. Mantle material uplifted the basin fill, and late mare basalts provided a cap. The ejecta blankets are dominated by metamorphosed breccias ranging from poorly consolidated material to partly-melted samples. These complex assemblages were further

[1] Note by J. V. Smith. Revised and expanded version of Presidential Address, Mineralogical Society of America, delivered at the 54th Annual Meeting of the Society, 13 November 1973. The first part was published in Vol. 59, p. 231–243, 1974, but various circumstances made it impossible to prepare the second part immediately thereafter. This was actually fortunate because this second part, completed in November 1975, could incorporate the extensive data and ideas which marked the end of the Apollo program. [Final revision of the manuscript in May 1976 allowed addition of references to several papers appearing after November 1975.] The first part is brought up to date, the rock types are evaluated, and the remaining minerals are reviewed. Although a Presidential Address is personal, few recent Presidents could maintain that their work was carried out totally by themselves. Ian Steele has been a remarkably productive colleague since the second year of my lunar program, and it is appropriate that we prepared this article jointly even though it modifies a tradition.

modified by smaller impacts to produce a veneer of regolith.

Most non-mare rocks are inhomogeneous, and some controversy among lunar petrologists arose merely because they had examined different subsamples. Other controversies arose from different interpretations of the same complex texture. Thus some thin sections from rock 14310 show sporadic clots of plagioclase whose irregular grain boundaries are consistent with solid-state annealing, whereas the great bulk of the area is dominated by an undoubted igneous texture. After considerable dispute on fragmentary evidence, most investigators now believe that 14310 was produced by nearly complete melting of regolith in which only the clots and trace elements provide evidence of the earlier hybrid state (see papers by Ridley *et al.*, 1972, James, 1973, Gancarz *et al.*, 1972, and many papers in the *Proc. 3rd Lunar Sci. Conf.* for conflicting ideas: note that Crawford and Hollister, 1974, from the presence of Na-rich clinopyroxene and low-Al hypersthene, interpreted 14310 as a product of melting 200 km deep in the Moon). We accept the general opinion in 14310, and suspect that many lunar rocks with igneous textures are the products of impact melting of complex breccias.

Most Apollo and Luna specimens are metamorphosed breccias in which detailed mineralogical study has revealed extensive chemical and physical changes between mineral grains accidentally thrown together. A good idea of the complexity can be obtained from the following papers: Albee *et al.*, 1973; Anderson *et al.*, 1972; Bence *et al.*, 1973, 1974; Cameron and Fisher, 1975; Chao, 1973; Grieve *et al.*, 1975; Kurat *et al.*, 1974; Simonds *et al.*, 1973, 1974; Steele *et al.*, 1972; Warner, 1972; Warner *et al.*, 1974. All gradations occur from (a) monomict breccias with angular mineral clasts to (b) low-grade polymict breccias with open pores and residual glass to (c) medium-grade polymict breccias with partial recrystallization of the mineral clasts along with complete elimination of the glass to (d) high-grade breccias ranging from ones with hornfelsic textures to ones with igneous textures. As the grade increases, the mineral compositions become homogenized, and information on the primary constituents becomes lost. Partial melting and vapor transport may affect the textures and bulk compositions.

Because so few even-textured rocks occur on the Moon, petrologists and geochemists were forced to use rock terms in a chemical rather than a textural or mineralogical sense; furthermore many acronyms were invented and terrestrial terms were used in a loose or extended way. A glossary is given in pages i–xi of the *Proceedings of the Fifth Lunar Science Conference*. Many names are confusing, and we shall try to use clear terms such as "polymict breccia with anorthosite bulk composition."

Apart from the mare basalts, which can contain large amounts of ilmenite and significant amounts of diopside component, most lunar rock compositions can be represented closely on the ternary plot of silica–olivine–plagioclase. The liquidus relations for the pure SiO_2–Mg_2SiO_4–$CaAl_2Si_2O_8$ system at 1 atmosphere dry conditions (Fig. 1) show crystallization fields for forsterite, Mg,Al-spinel, anorthite, Mg-pyroxene, and tridymite or cristobalite (Andersen, 1915). These crystallization fields change little with substitution of Fe for Mg and NaSi for CaAl (*e.g.* Walker *et al.*, 1975), and a single generalized diagram is sufficient for consideration of melting of lunar highlands material *at low pressure*. Key features of the diagram are (a) incongruent melting of bulk compositions in the region *pqt* to Mg,Al-spinel and Mg,Al-depleted liquid; equilibrium cooling results in reaction of spinel with the liquid to produce olivine and plagioclase below the solidus (Fig. 2) for pressure less than 8kbar; (b) incongruent melting of pyroxene to olivine and Si-rich liquid; with increasing pressure the incongruent melting is reduced, and is finally eliminated at several kilobars; (c) decreasing temperatures along the cotectic curves *qr* and *rs* to the

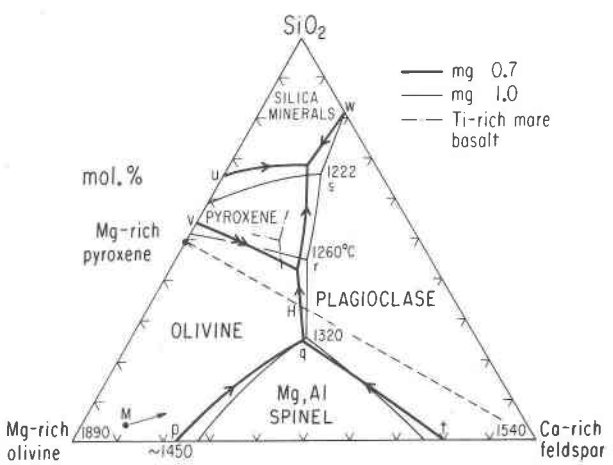

FIG. 1. Crystallization fields of SiO_2–Mg-rich olivine–Ca-rich plagioclase system for dry conditions at 1 atmosphere (Fe-free, Andersen, 1915; *mg* 0.7, Walker *et al.*, 1973b). Temperatures for Fe-free system. See Lipin (1975) for abstract on data for *mg* 0.6. Labels *p*–*w* indicate reference points discussed in the text. *H* and *M* represent possible bulk compositions of the lunar crust and the whole Moon.

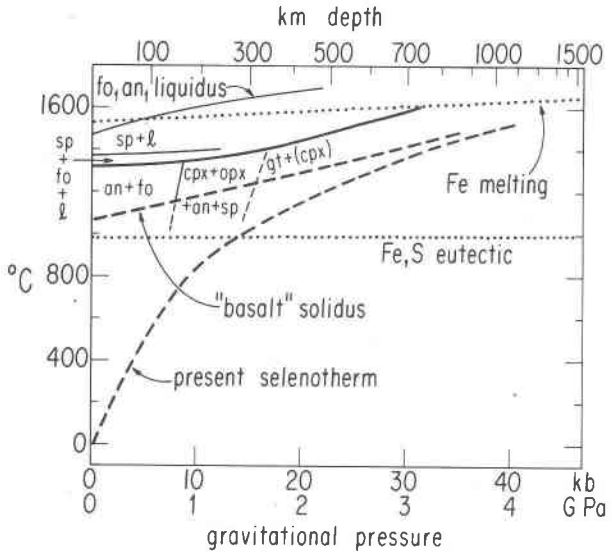

FIG. 2. Some relevant phase equilibria for a Moon with olivine, pyroxene, and plagioclase as the dominant minerals. See text for origin of curves.

eutectic *s* at 1222°C for the Fe-free system; (d) decreasing temperatures over the whole diagram as Fe substitutes for Mg and NaSi for CaAl.

Figure 2 shows some relevant controls on the mineralogy of the Moon. The present-day selenotherm results from interpretation of the electrical conductivity profile deduced from perturbation of the solar wind (*e.g.* Sonett, 1975; Shankland, 1975). Assumption that the mantle consists largely of Mg-rich olivine essentially free of Fe^{3+} leads to a model-dependent estimate of the present temperature profile (Dyal *et al.*, 1974) using olivine data of Duba *et al.* (1974); assumption of Mg-rich pyroxene gives a similar profile (Heard *et al.*, 1975). Although the details are controversial, the general trend of the selenotherm is consistent with seismic evidence for melting below ~1000km depth: if the molten liquid is basaltic, the required temperature for 1000 km depth is ~1500° C which is consistent with the proposed curve. The selenotherm is estimated for the entire early Moon reaching the temperature for extraction of basaltic melt from an ultrabasic bulk composition when account is taken of near-surface cooling over the past 4 Gy. Complete melting of Mg-rich olivine would require temperatures up to 1800–2000° C, which would exacerbate problems of heat sources. Figure 3 is a suggested mineralogical model of the Moon expressed as a density–depth profile. Details will be given elsewhere in a paper on the chemical composition of the Moon. Complete differentiation of the Moon would result in (a) extraction of Fe,Ni,S-rich liquid to form a core, (b) gravitational sinking of Mg-rich olivine and minor amounts of heavy complex oxides to form a mantle, and (c) development of a late liquid rich in plagioclase and pyroxene components which would ultimately form the complex crustal rocks. The Fe-rich core might become a magnetic dynamo. The Fe–FeS eutectic is close to 1000° C for all lunar depths, whereas the melting curve for iron rises from ~1520 to ~1650° (Brett, 1973; Usselman, 1975). A S-rich liquid would be strongly superheated if the supposed selenotherm is correct, thereby reducing the viscosity and easing fluid-dynamical problems of an early lunar dynamo. During progressive crystal–liquid differentiation the Fe content of the liquid would increase, as would the amount of the "incompatible" elements (*e.g.* K, REE, Ba, P, Zr, and U) which enter the octahedral and tetrahedral sites of common silicates only in trivial amounts. Late partial melting and volcanism would confuse the situation greatly, as would the effects of major and minor impacts. Figure 3 shows how the mean density of the Moon could be explained by this kind of petrological model. Even if only the outer part of the Moon melted, as proposed by many workers (*e.g.* Taylor, 1975), many of these

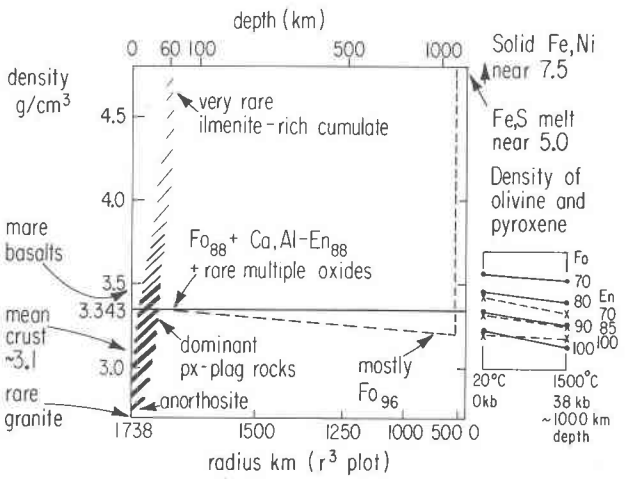

FIG. 3. Mineralogical model of Moon expressed as density profile. The small diagram shows the variation of density of olivine and low-Ca pyroxene from 20°C and 0kbar to 1500°C and 38kbar, the latter of which are possible conditions at ~100km depth. A possible lunar core might consist of either Fe,Ni or Fe,S or a mixture of both. A mantle might consist dominantly of olivine and low-Ca pyroxene. The crust is probably dominated by rocks rich in pyroxene and plagioclase (point *H*, Fig. 1). Mare basalts may result from melting of cumulates including ones rich in ilmenite. Note that many small variants would satisfy the mean density of 3.343 gcm^{-3}, including a mantle whose olivine was uniform at ~Fo_{92}. From Smith (1976).

features of crystal-liquid fractionation would occur (*e.g.* Murthy *et al.*, 1971).

Ignoring the possible Fe-rich core and the minor constituents, the bulk composition of a completely differentiated Moon might approximate to point *M* on Figure 1, which lies in the field outlined by Walker *et al.* (1973a). Olivine would be the liquidus phase whatever the depth in the Moon. Sinking of olivine would result in the bulk composition of the remainder moving away from the olivine corner. Depending on the exact position of *M* and the extent of crystal–liquid reequilibration, the subsequent differentiation could take different paths. Figure 2 shows phase relations for a bulk composition with equal amounts of forsterite and anorthite (based largely on Kushiro and Yoder, 1966). At low pressure, anorthite and forsterite are the subsolidus phases. Anorthite disappears at the solidus (~1320°) giving spinel + forsterite + liquid, then olivine disappears at ~1380° C leaving spinel + liquid, with complete melting at 1500–1600° C. In the subsolidus region, anorthite and forsterite are replaced by anorthite, spinel, and two pyroxenes above about 8kbar, and then by garnet and pyroxene above about 15kbar. The details are controversial, but the general relations are sufficient for the present purpose. Depending on the bulk composition *M* and the temperature profile of the Moon, garnet might form in the lunar mantle. Assuming that the temperature profile of the early Moon is controlled by the "basalt" solidus, garnet should not form at depths less than ~300km. Only half of the lunar volume is inside this depth, and olivine may be the sole crystallizing silicate there, thus eliminating garnet except perhaps for the products of trapped liquid. On the other hand, the liquid may have reached a composition sufficiently rich in An molecule to yield some primary garnet. Further complications can arise in the depth range 100–300 km because of the possible assemblage anorthite + two pyroxenes + spinel.

For depths less than 100 km, crystallization would be controlled principally by the relations in Figure 1. Point *H* on the olivine–plagioclase cotectic would mark the final disappearance of olivine when account is taken of elimination of the incongruent melting of pyroxene at several kilobars pressure (or of subsolidus reaction). The lunar crust would be dominated by Mg-rich pyroxene and Ca-rich plagioclase with a bulk composition near *H*. Subsequent differentiation would terminate at the eutectic *s*. Of course, this ideal theoretical situation could not occur, and many idiosyncratic variations must occur. It is our task to find out whether lunar rocks and minerals give clues on the applicability or otherwise of this model. [Elsewhere we shall consider the validity of models proposed by other workers based on bulk compositions rich in pyroxene (Ringwood) or Ca,Al-rich refractory condensate (D. L. Anderson).]

A simple approach is to examine all the bulk analyses of lunar samples without taking account of the mineralogical features. Wood (1975) separated mare from highlands material by a plot of Ca/Al *vs.* TiO_2. Those specimens with Ca/Al (atomic) > [0.786 −0.229 log TiO_2 (wt.%)] were classified as mare basalts. The remaining samples were split into high-KREEP and low-KREEP varieties by the line $K_2O + P_2O_5$ (wt.% = 0.945 −0.00893 (% normative plagioclase). Figure 4 shows the resulting modal plots of olivine–plagioclase–quartz for the two groups of presumed highlands samples. Many of the bulk analyses by broad-beam electron microprobe analysis are for small lithic fragments, and both the sampling and analytical errors are significant. Nevertheless the data show interesting trends. The KREEP-rich specimens tend to lie near the cotectic *qr* of Figure 1, consistent with proposals for origin from cotectic primary or secondary melts, but the spread is so wide that other origins are indicated as well (*e.g.* hybridism). The KREEP-poor specimens tend to lie in the lower right, and this might be explained by derivation mainly from primary cotectic liquids in the anorthite–plagioclase–silica system, with a bias caused by the tendency for plagioclase to rise to the lunar surface because of its lower density. A few samples are very rich in olivine, and we shall focus attention on them because they may derive from the deep crust or upper mantle.

The remainder of this section will concentrate on evaluation of the rock types in the lunar samples, using the chemistry of olivine, pyroxene and spinel (Figs. 5–12) as the principal mineralogic clues. Because all lunar petrologists assume that the lunar highlands are dominated by Ca-rich plagioclase and low-Ca pyroxene as expressed by rock terms such as highland basalt and noritic anorthosite, we shall deliberately focus attention on the mineralogy of controversial materials which may represent deep-seated rocks. Study of rocks from large igneous complexes and granulite terrains on Earth, together with investigation of xenoliths transported by kimberlites and alkali basalts from the upper mantle, provides an excellent basis for establishing mineralogical and chemical criteria. Under plutonic conditions, the grain size is often coarse, and cumulate texture occurs

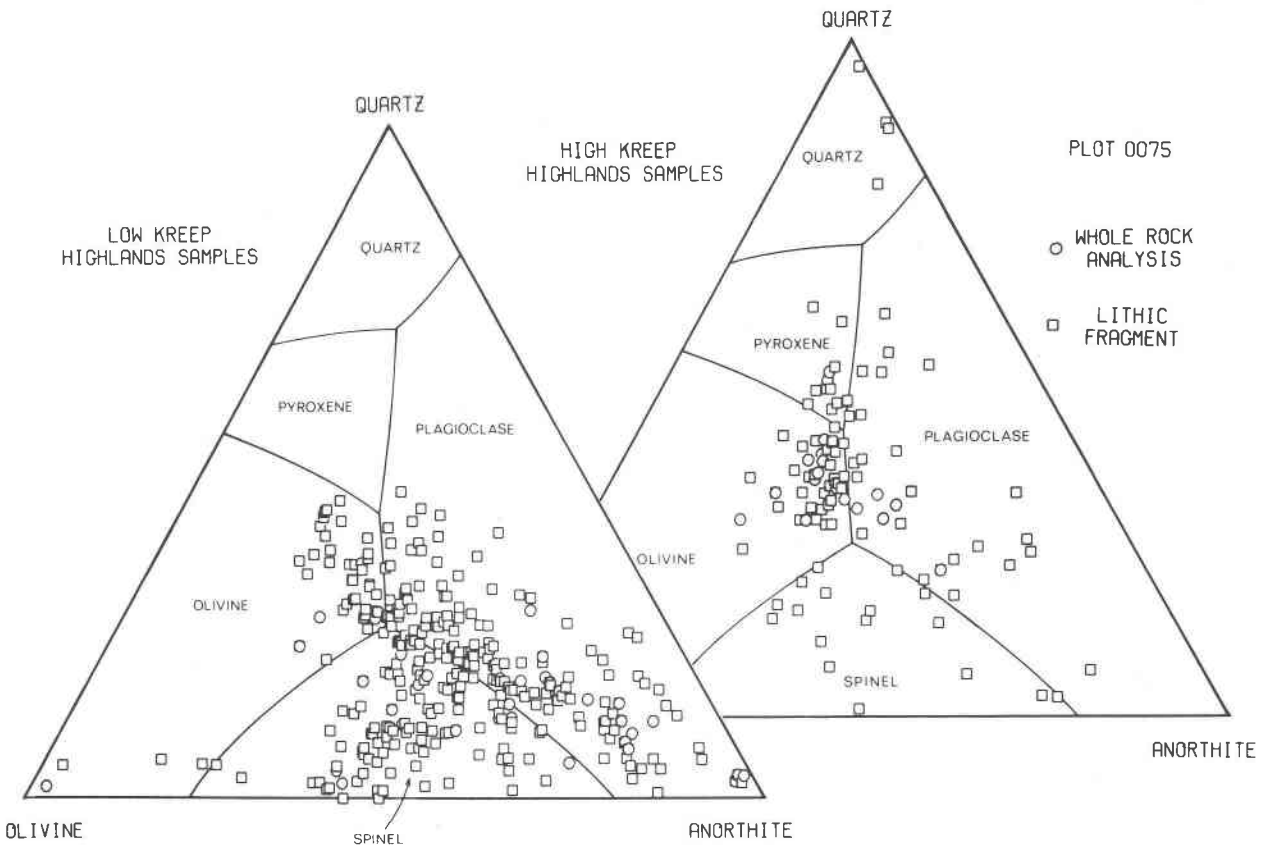

FIG. 4. Principal components of highlands samples selected from computer store. Wood (1975).

in some igneous complexes; however, granulation and recrystallization can lead to a variety of textures from porphyroclastic to equant (*e.g.* Mercier and Nicolas, 1975; many papers in *Phys. Chem. Earth,* Vol. 9). Chemical features should provide easier criteria especially for lunar specimens in which impact metamorphism is so common. The chemical features indicative of deep-seated origin include lack of zoning, presence of high-pressure minerals, chemical partitioning indicative of high-pressure, coarse exsolution and strong cation ordering indicative of prolonged annealing, low content of certain minor elements (*e.g.* Ca in olivine), and chemical features inherited from a high-pressure ancestor. In addition, certain chemical features indicate early crystallization from primitive liquids of which the simplest is the *mg* ratio (= atomic Mg/Mg+Fe) of the ferromagnesian minerals. Rocks composed of early crystals should be low in the "incompatible elements" which tend to end up in granitic residua, and should have accessory minerals rich in most transition metals of the first series (Ti–Ni).

Because there are so few rocks with simple texture and chemistry, the lunar detective is forced to work with complex rocks. As an example Figure 5 shows textural features of 67075, a polymict breccia with anorthosite bulk composition (Brown *et al.,* 1973; Smith and Steele, 1974; McCallum *et al.,* 1975b). The overall view (a) shows the angular clasts of plagioclase, pyroxene, and olivine, while the magnified portions (b–f) show special features described in the figure legend. Particularly interesting is the coarse exsolution of pyroxene clasts (d–f), which indicates prolonged subsolidus annealing (this is the coarsest recorded in lunar pyroxene). Although individual pyroxene grains have uniform compositions (except, of course, for the exsolution) the pyroxenes of different grains in the same thin-section range in composition from $En_{40}Fs_{56}Wo_4$ to $En_{65}Fs_{32}Wo_3$ and from $En_{30}Fs_{27}Wo_{43}$ to $En_{42}Fs_{14}Wo_{44}$ while the olivines range from Fo_{40} to Fo_{55}. The simplest explanation is that 67075 is composed of the compacted debris from different parts of a layered igneous complex which underwent prolonged annealing before disruption

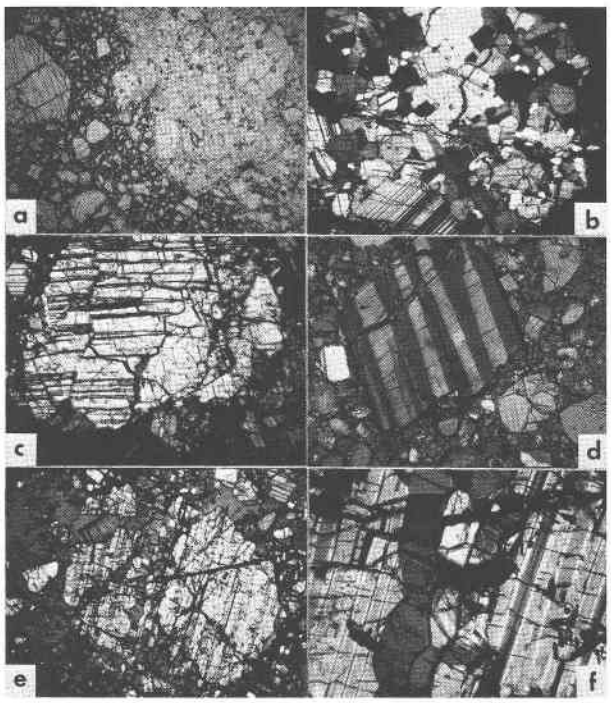

FIG. 5. Photomicrographs of 67075, a polymict breccia with anorthosite bulk composition.

(a) Dark portion at left consists of olivine (~Fo_{80}, fractured) and plagioclase (unfractured) clasts set in plagioclase-rich matrix. Light portion shows various clasts of plagioclase grains plus a larger clast of polycrystalline micro-anorthosite with small equant pyroxenes; minor olivine clasts (~Fo_{50}) also occur.

(b) Polycrystalline micro-anorthosite clast, mostly with triple junctions and polygonal texture. Small pyroxene grains are hard to recognize. Same texture as clast in (a).

(c) Polycrystalline clast dominated by shocked 2 mm grain of anorthite. Matrix shows at upper left, while other anorthite grains with interstitial pyroxene grains occur at the right of the clast.

(d) Pyroxene clast showing coarse and fine exsolution lamellae. The matrix contains angular plagioclase clasts.

(e) Clast composed of 2 mm pyroxene grain with coarse and fine intergrowth (central region) and portion of large plagioclase (dark region at lower left). The composite clast is surrounded by matrix. Matte areas are cracks filled with epoxy. The pyroxene grain is traversed by a band of plagioclase grains with curved boundaries (gray and white grains running NNW through the center). The central part is enlarged in (f).

(f) Central part of (e). Spinel occurs as black inclusions (E-shaped at lower left and rod-shaped at upper and lower right). Pyroxene exsolution lamellae occupy the left and right parts of the field of view. The central one-third consists of plagioclase grains, the outer ones of which tend to be scalloped while the inner ones tend to be ellipsoidal. Similar plagioclase grains occur as dark-gray entities at the margin and just inside the lower edge of the pyroxene grain in (e). The origin of this plagioclase is unknown but injection of plagioclase into fractures followed by prolonged annealing is one possibility. Faint horizontal lines are blemishes on film.

(a) (b) (c) and (e) 2 mm across, (d) 1 mm across, and (f) 0.5 mm across. (a) and (c) plane-polarized light; others crossed or partly-crossed polars. (a) and (c) from 67075,2; others 67075,51.

See McCallum *et al.* (1975b) for other photographs.

(Brown *et al.*, 1973). If 67075 had been strongly metamorphosed or melted, the above evidence would have been lost.

Lunar specimens with high Mg/Fe

All the lunar missions brought back soils and breccias with rare grains of olivine whose highly magnesian composition (~Fo_{90}) is like that of olivines from the Earth's upper mantle (*e.g.* Heiken, 1975). Steele and Smith (1972) located four Apollo 14 fragments with ultrabasic affinities, and many more have since been discovered including some larger specimens with indicative textures. All these specimens are more magnesian (*mg* ~0.9) than the common material (bulk *mg* mostly $\leq$ ~0.75). We first describe some specimens with particularly interesting textures and mineralogy (Table 1 and Figures 6, 7, and 12), and then summarize pertinent mineralogical data for other Mg-rich materials.

(a) Selected specimens of special interest. The clearest textural evidence for deep-seated processes is from 76535 (Gooley *et al.*, 1974), a 155 g rake sample composed mainly of ~5mm grains of plagioclase (58%, An_{96}), olivine (37%, Fo_{88}) and orthopyroxene (4%, En_{86}). Bence *et al.* (1974) found similar 2–4mm fragments in Apollo 17 soils. The grain boundaries are curved and tend to meet at 120°, and the texture is that of a thoroughly annealed rock which has not been brecciated or shock-metamorphosed. The pyroxene has the space group $P2_1ca$ (Smyth, 1974a) which results from unusually effective segregation of Mg and Fe. Although the depth of crystallization inferred from thermodynamic estimates is controversial (Albee *et al.*, 1975), all authors agree that 76535 was annealed in the solid state for a long time at considerable depth: indeed the textural features can be matched in terrestrial granulite rocks. Interesting details are: (a) the plagioclase contains oriented inclusions of iron needles (5–15 wt.% Ni and up to 5% Co), chromite, and an unidentified phase; (b) the olivine contains discrete chromite inclusions and symplectic intergrowths of chromite and pyroxene; (c) symplectic intergrowths of orthopyroxene, diopside and Al–Mg–chromite occur between olivine and plagioclase grains; (d) mosaic clusters of orthopyroxene, diopside, chromite, Fe–Co–Ni metal, troilite, whitlockite, chlorapatite, baddeleyite, plagioclase, and K-feldspar occur sporadically, and are most easily interpreted as the products of trapped primary liquid augmented by exsolved material; (e) some metal particles consist of α–γ assemblages whose

TABLE 1. Analyses of minerals in selected lunar peridotites

	1	2	3	4	5	6	7	8	9	10	11	12	13
SiO_2	39.9	55.9	56.5	52.6	44.9	-	40.1	51.3	52.7	44.8	0.19	42.4	40.8
TiO_2	0.03	0.4	0.3	0.7	0.02	0.9-1.2	<0.01	0.31	0.54	<0.01	0.49	0.0	<0.01
Al_2O_3	-	1.5	1.0	1.5	35.3	14.7-19.4	<0.01	1.07	2.73	35.0	19.9	0.0	0.22
Cr_2O_3	<0.02	0.6	0.5	0.9	-	46.3-52.8	<0.01	0.84	0.85	-	48.3	0.01	-
FeO	12.0	7.4	7.8	2.8	0.06	21.3-24.4	11.9	8.1	3.00	0.14	18.6	8.3	8.6
MnO	0.1	0.1	0.1	0.08	-	0.3-0.3	0.11	0.11	0.13	-	0.75	-	-
MgO	47.1	32.7	33.2	18.1	-	8.2-11.2	48.1	33.7	18.6	0.23	11.1	50.7	50.2
CaO	<0.02	1.5	0.8	23.2	18.8	-	0.13	5.55	21.3	19.3	-	0.05	<0.01
Na_2O	-	-	-		0.4	-	-	<0.01	0.05	0.62	-	-	-
Total	99.2	100.1	100.2	99.9	99.6	-	100.4	101.0	99.9	100.2	99.8	101.5	99.8

	14	15	16	17	18	19	20	21	22	23	24	25
SiO_2	55.0	56.5	46.2	0.0	-	-	-	41.2	53.2	44.5	0.00	0.00
TiO_2	0.78	0.15	-	0.03	0.01	98.0	76.9	-	0.9	-	0.04	57.0
Al_2O_3	5.1	2.44	34.3	57.3	58.0	-	-	0.00	5.9	36.4	61.1	2.85
Cr_2O_3	0.41	-	-	14.0	12.7	0.3	0.5	0.04	0.4	-	8.6	0.43
FeO	5.8	5.70	0.02	9.3	9.4	0.1	9.6	9.8	6.1	0.06	8.9	28.9
MnO	-	-	-	-	0.06	-	-	0.09	-	-	-	0.43
MgO	33.6	35.7	0.02	20.4	20.4	<0.1	13.1	49.3	33.1	0.01	21.4	11.6
CaO	0.0	<0.01	18.4	0.0		<0.1	<0.1	0.04	0.4	19.8	-	-
Na_2O	-	-	0.60	-	-	-	-	-	-	0.38	-	-
Total	100.7	100.5	99.7	101.0	100.6	100.1	100.1	100.5	100.1	100.0	100.0	101.2

1-6 76535 troctolitic granulite (Gooley *et al.*, 1974), 1 olivine $Fo_{87.5}$, 2,3 bronzite as single grains $En_{86.2}Fs_{10.9}Wo_{2.9}$ and in mosaic intergrowths and symplectites $En_{87.2}Fs_{11.6}Wo_{1.3}$, 4 diopside in symplectites and mosaics $En_{49.9}Fs_{4.3}Wo_{45.8}$, 5 anorthite $Ab_{3.7}An_{95.7}Or_{0.6}$, K_2O 0.09 6 Al-Mg-chromite range for all types, V_2O_3 0.6-0.8, also kamacite Co 4.6-6.0 Ni 5.2-6.1, taenite Co 1.8-4.2 Ni 18.0-33.0; 7-11 72415 brecciated dunite (Albee *et al.*, 1974b), 7 olivine Fo_{88}, NiO 0.04, 8 low-Ca pyroxene $En_{81}Fs_{11}Wo_8$, 9 high-Ca pyroxene $En_{54}Fs_5$ Wo_{41}, 10 anorthite $Ab_5An_{92}Or_1$ others 2, K_2O 0.09 BaO 0.04, 11 Al-Mg-chromite, V_2O_3 0.35, ZrO_2 0.08, also Fe-metal Co 1.3-2.2 Ni 24.5-31.8 Mg 1.3 Cr 0.36 Si 0.04; 12-20 brecciated peridotite clasts in 15445 breccia (Anderson, 1973; Ridley *et al.*, 1973) 12 olivine (A) also NiO 0.03, 13 olivine (R), 14 orthopyroxene (A), 15 orthopyroxene (R) 16 anorthite (A) also K_2O 0.12, 17 Cr-spinel (A), 18 Cr-spinel (R) middle of four analyses, 19 rutile (A) also Nb_2O_5 1.6, 20 armalcolite (A); 21-25 brecciated peridotite fragments in 73263 soil (Bence *et al.*, 1974), 21 olivine (mean of 2), 22 pyroxene (mean of first 3 analyses), 23 anorthite (mean of 2, K_2O 0.07), 24 spinel (mean of 2), 25 ilmenite.

composition indicates a cooling rate consistent with some tens of kilometers below the lunar surface.

The origin of the chromite–pyroxene symplectites is controversial. Gooley *et al.* (1974) suggested that they formed by a reaction Ol + An + chromite → Opx + Cpx + Al–Mg–chromite, whereas Albee *et al.* (1975) argued for co-precipitation during magmatic crystallization. Bell and Mao (1975) proposed that similar symplectites in 72415 brecciated dunite and in several lunar olivines resulted from solid-state breakdown of primary garnet trapped in olivine. The garnet would be very Cr-rich ($\sim Ca_{1.9}Mg_{0.6}Fe_{0.5}Cr_{1.3}Al_{0.7}Si_3O_{12}$ for 72415 dunite). Chromite forms vermicular intergrowths with several silicates in terrestrial peridotite xenoliths (Basu and MacGregor, 1975; Dawson and Smith, 1975), and exsolution, especially from pyroxene, combined with solid-state recrystallization provides a plausible but not definitive explanation of the terrestrial occurrences. Perhaps chromite tends to intergrow with silicate under deep-seated metamorphic conditions whatever the source of the silicate; if so, the origin of the lunar symplectites will be hard to discover.

All large grains in 76535 have an inclusion-free rim which results from diffusion of exsolved material to the grain boundaries. Whatever the details of the annealing mechanisms, we endorse the mineralogic implications that 76535 is the product of prolonged

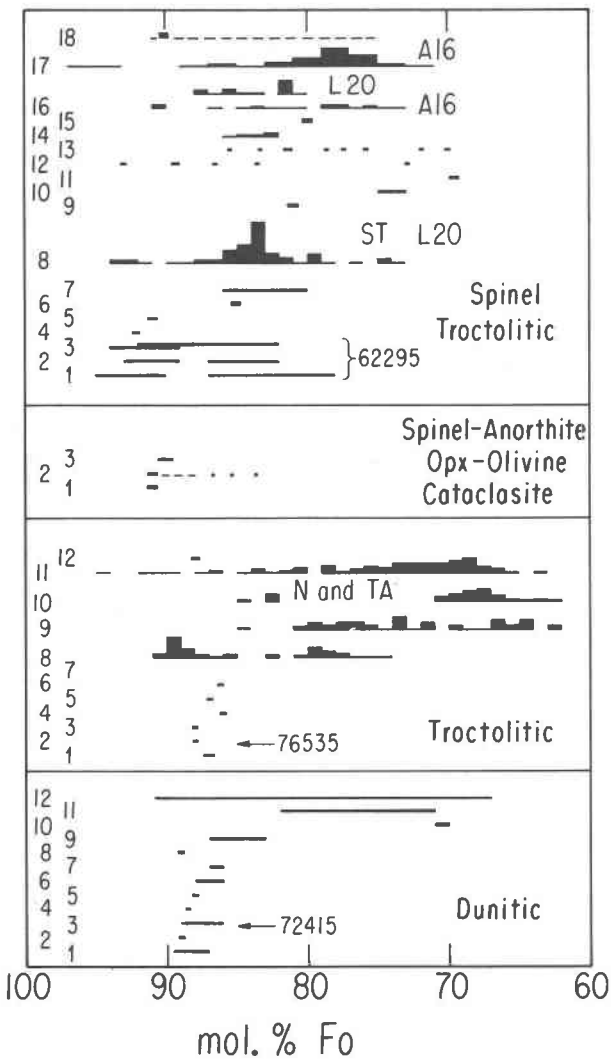

FIG. 6. Compositions of olivine in selected samples, many of *mg*-rich composition.

Olivine-rich ("dunitic")

1. Soil fragment 73242,4,A14: olivine breccia with minor plagioclase and spinel. One clast of pink spinel and plagioclase (Steele and Smith, 1975b). 2. Dunite clast in 14068,10 breccia: polygranular mosaic of olivine Fo_{89} with single chromite grain Helz (1972). 3. Dunite clasts 72415-18: see text (Albee *et al.*, 1974b). 4. Soil fragment 78422,2,A18: olivine breccia, 1 mm across, with minor plagioclase, chromite and armalcolite (Steele and Smith, 1975b). 5. Soil fragment 14002,7,E-1-8: shocked single olivine grain with minor chromite (Steele and Smith, 1972). 6. Soil fragment 78502,17,A34: olivine breccia with minor chromite, armalcolite, and plagioclase (Steele and Smith, 1975b). 7. Soil fragment 78442,2,A15: olivine breccia, 1 mm across, with minor chromite, armalcolite, diopside, and plagioclase (Steele and Smith, 1975b). 8. Soil fragment 78442,2,A16: olivine breccia, 1 mm across, with minor plagioclase and armalcolite (Steele and Smith, 1975b). 9. Breccia 14063,14. Fine-grained clast of 70% olivine, 30% plagioclase An_{88}, and minor bronzite and chromite (Steele and Smith, 1972). 10. Breccia clast 78502,17,B15: olivine breccia with plagioclase clast and minor chromite with $TiO_2 < 1\%$. Unpublished. 11. Polycrystalline inclusion, lmm across, in mare basalt 74275 (Meyer and Wilshire, 1974). 12. Dunitic fragment in polymict breccia 14318. Olivine Fo_{87-91} with average Fo_{86}. Minor plagioclase An_{84-95} with cluster at An_{83} (Kurat *et al.*, 1974).

Olivine–plagioclase-rich ("troctolitic")

1. Clast in rake sample 15335. "Igneous" texture (Steele *et al.*, 1972). 2. Troctolitic granulite 76535 and 2–4 mm fines 76503. See Table 1 and text. 3. Clast in breccia 14321. Granular assemblage of olivine, anorthite An_{95}, and accessory K–feldspar (Compston *et al.*, 1972). 4. Several 2–3 mm fragments in breccia 14320,4. Olivine–plagioclase An_{95} intergrowth with texture similar to crescumulate of layered ultrabasic rocks of Rhum (Brown *et al.*, 1972). 5. Fragment, 1 mm across, in 1–2 mm fines 14166,6. 70% plagioclase An_{96}, 30% olivine, 2% diopside, 8 tiny grains Cr–Zr–armalcolite (Steele and Smith, 1972). 6. Fine-grained annealed clast in recrystallized noritic breccia fragment 76503,6,21. Plagioclase An_{95}, olivine, minor orthopyroxene, and augite (Bence *et al.*, 1974). 7. Troctolitic breccia 77017. Olivine Fo_{81} and plagioclase An_{95}, patches in feldspathic breccia. Interpreted as xenolith in mare basalt (Brown *et al.*, 1974). 8. Clasts in stratified Boulder 1, Station 2, Apollo 17. Most have fractured olivines in granulated groundmass of olivine and plagioclase, but some have basaltic texture. Plagioclase is $An_{84-96}Or_{0.1-1.4}$ with An usually over 88% (Stoeser *et al.*, 1974). 9. Clasts in stratified Boulder 1, Station 2, Apollo 17. Granulated ANT (Stoeser *et al.*, 1974). 10. Luna 20 soil fragments whose bulk composition is noritic or troctolitic anorthosite (Prinz *et al.*, 1973a). 11. ditto for anorthositic norite and troctolite compositions. For specimens 8–11, the analyses are displayed as histograms. 12. "Basalt" fragment 14162,41-1407-11. 30% skeletal olivine Fo_{88} microphenocrysts, 10% Na,Al,Cr-rich pyroxenes $En_{50}Fs_5Wo_{45}$ and $En_{84}Fs_{8.5}Wo_{27.5}$, 50% plagioclase and 10% glassy mesostasis (Powell and Weiblen, 1972).

Spinel–anorthite–orthopyroxene–olivine cataclasite

1. 15445,10 clast in breccia (Anderson, 1973). 2. 15445 Type B clasts in breccia (Ridley *et al.*, 1973). 3. 73263,1,11 2–4 mm soil fragment (Bence *et al.*, 1974). See Table 1 and text for details.

Spinel troctolitic

1. 62295 rock. 1% xenocrysts of olivine Fo_{95-90}, anorthite An_{98-95}, pink spinel (*mg* 0.75, 3.5 mol.% Cr_2O_3) and Fe–Ni–Co metal. 99% fine-scale intergrowth of olivine Fo_{87-78}, plagioclase An_{96-91}, spinel (*mg* 0.9–0.76, 2 mol % Cr_2O_3), and glassy residuum (Walker *et al.*, 1973b). 2. 62295 rock. Olivine phenocrysts Fo_{93-89} with overgrowths Fo_{85-82} set in groundmass of anorthite $An_{90}Ab_{9.2}Or_{08}$ skeletal olivine Fo_{87-82}, spinel, ilmenite, *etc.* (Agrell *et al.*, 1973). 3. 62295 rock. Olivine (xenocrysts Fo_{84-89}, intergrowth Fo_{92-82}), plagioclase (xenocrysts An_{98-92}, intergrowths and quench grains An_{94-89}), spinel (xenocrysts 9–16 mol % chromite, intergrowth 2–4 mol % chromite) (Hodges and Kushiro, 1973). See also Brown *et al.* (1973) and Weiblen and Roedder (1973). 4. 4 mm clast 67435-14 in breccia. Cumulus of olivine $Fo_{91.9-92.4}$ and spinel poikilitically enclosed in plagioclase $An_{96.6-97.4}$ (Prinz *et al.*, 1973b). 5. Luna 20 plagioclase $An_{95,97}$–olivine Fo_{91}–spinel fragment (Tarasov *et al.*, 1973). 6. 1 mm fragment 14321,76 of olivine $\sim Fo_{85}$, anorthite An_{94}, and spinel in breccia (Steele, 1972). 7. Rake sample 65785 with coarse-grained center (65% An_{97}, 30% Fo_{80-86}, spinel zoned outwards from 2.6 to 12.6% Cr_2O_3 and FeO 10 to 12%). Rare pyroxenes, ilmenite, Ni–iron, troilite, Zr–rutile, whitlockite, Cr–Zr–REE armalcolite, K–feldspar, chromite, and farringtonite (Dowty *et al.*, 1974b). 8. Thirty-four fragments of spinel troctolite

metamorphism at considerable depth (tens of kilometers?), probably of an igneous cumulate, in which subtle effects resulted from exsolution, diffusion and reduction. Haskin *et al.* (1974) concluded from analyses of REE, K, Rb, Sr, and Ba that 76535 was originally an olivine–plagioclase cumulate containing 8–16 percent parent liquid with no appreciable Eu anomaly and about 20 times chondritic abundance of REE. The age data are inconclusive (reviewed by Haskin *et al.*, 1974, p. 1214), but original crystallization at −4.3 Gy is indicated.

Five olivine-rich fragments 72415–72418 were collected from a 10 × 20cm clast of metaclastic breccia 72435. Olivine Fo_{86-89} accounts for 91 percent of 72415 as crystals up to one cm set in a granular matrix of olivine with the same composition (Albee *et al.*, 1974b). Some large olivines contain strain bands marked by small recrystallized olivines 50μm across. Plagioclase An_{88-92}, Cr-spinel, high- and low-Ca pyroxene and metal occur as clasts and as inclusions in the olivine, sometimes as symplectic intergrowths. The compositions of the two pyroxenes are closer than for those in 76535 (Table 1, Fig. 7) and the low-Ca pyroxene may be a clinopyroxene ($En_{81}Fs_{11}Wo_8$).

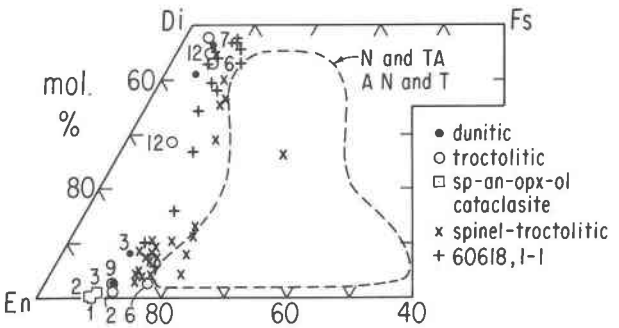

FIG. 7. Compositions of pyroxene in selected samples, many of Mg-rich compositions. Numbered specimens can be identified from the appropriate sub-group of specimens listed in Fig. 6. Specimen 60618,1-1 was described as a spinel–olivine–anorthosite, and is listed as No. 14 in the spinel–troctolitic sub-group. Other data for the spinel–troctolitic group are lumped together without numbered identification. N and TA and AN and T are items 10 and 11 of the troctolitic group.

This evidence plus the relatively high CaO content of the olivine (0.13 wt.%) suggests a higher temperature of equilibration for 72415 than 76535. The 72415 brecciated dunite is particularly important because of the *tentative* conclusion from the Rb–Sr isotopic data that crystallization occurred very early (~ − 4.6 Gy).

Polymict breccia 15445 contains white clasts unusually rich in olivine, spinel, and pyroxene (Anderson, 1973; Ridley *et al.*, 1973) which were called peridotite. Bence *et al* (1974) found similar minerals in 2–4mm fragments in 73263 soil and incorrectly stated that they represented a new rock type, spinel cataclasite, not found in other missions. Although the textures were badly altered by shock, some coarse-grained relics (~ 1 mm) of unbrecciated olivine and Cr–spinel indicate an original coarse texture. The chemical analyses of the minerals differ considerably in detail (Table 1), but the general features are quite similar including the very low CaO and Cr_2O_3 in the olivines, low CaO and high but variable Al_2O_3 in the low-Ca pyroxenes, and the low TiO_2 and moderate Cr_2O_3 in the spinels. Whereas Anderson reported microprobe analyses of rutile (?) and low-Zr "armalcolite" (?), Bence *et al.* reported high-Mg ilmenite. Two Fe-rich pyroxenes in 73263 were ignored because they cannot be in equilibrium with the other minerals, and presumably represent erratic grains incorporated during brecciation. The *mg* ratios of all the other olivines and pyroxenes are mostly 0.90–0.92. Anderson (1973) concluded that the 15445 clasts were igneous cumulates formed at moderate pressure (*e.g.* 2kbar) followed by partial recrystallization during granulation at 950 ± 50°C and $P \geq 1.3 \pm 0.5$ kbar. Bence *et al.* argued that the assemblage of

in Luna 20 sample with plagioclase An_{91-99} mean An_{96}, olivine Fo_{73-94} mean Fo_{84}, low-Ca pyroxene $En_{75-82}Fs_{11-21}Wo_{3-11}$ and spinel *mg* 0.1–0.5 *cr* 0–0.2 (Prinz *et al.*, 1973a). 9. Fragment 10019-22. Plagioclase $An_{95.4}$, olivine Fo_{81}, spinel and glass (Keil *et al.*, 1970). 10. 1 mm clast 14319,11a-3. Plagioclase An_{96}, olivine Fo_{74} and spinel *mg* 0.54 *cr* 0.027 TiO_2 0.3–1.0 wt.% (Roedder and Weiblen, 1972a). 11. 0.5 mm breccia clast 14303,50B. Olivine $Fo_{89.5}$, plagioclase An_{80} and spinel *mg* 0.55 *cr* 0.068 TiO_2 1.1 wt.% (Roedder and Weiblen, 1972a). 12. Type A spinel-brearing lithic fragments in Apollo 16 and 17 soils. Olivine euhedral to subhedral and plagioclase as later laths. Trace metal, troilite (?), mesostasis, and rutile(?). No pyroxene (Weiblen *et al.*, 1974). 13. Type B spinel-bearing lithic fragments in Apollo 16 and 17 soils. Olivine interstitial to plagioclase. Minor spinel, trace metal, troilite (?), ilmenite and 1–8% mesostasis (Weiblen *et al.*, 1974). 14. "Spinel-olivine anorthosite" 60618, 1-1. Rake sample. Photomicrograph shows 4 mm shocked plagioclase grain An_{96} with attached irregular grains of plagioclase, minor olivine, Mg–Al spinel, and pyroxene. Pyroxene also as veins in the large feldspar grain. Assigned to the Mg-troctolite group because of mineral compositions (Dowty *et al.*, 1974d). 15. One Apollo 15 and two Luna 20 fragments. Data for spinels and one olivine (Reid, 1972). 16. Histograms of olivine compositions for spinel troctolite fragments in Luna 20 and Apollo 16 (Taylor *et al.*, 1973). 17. 2–4 mm fragments in A16 soils, denoted Type A Feldspathic Intersertal Igneous Rocks. Quench, diabasic, and poikilitic textures, with rare evidence of thermal metamorphism. An_{93-96}, Fo ≥ 74, pyroxene *mg* ~ 0.2, Mg–Al spinel. Only other mineral data is histogram of olivine compositions (Delano *et al.*, 1973). 18. Luna 20 fragment with very fine-grained igneous texture. 65% An_{99-100}, 15% Fo_{90}, 2% Mg–Al spinel and ~20% interstitial phase. Interpreted as impact melt which lost volatiles (Dowty *et al.*, 1973a).

Al-enstatite, forsteritic olivine, pleonaste, and anorthite is stable from 3 to 5kbar. Whatever the details, the overall evidence suggests that these spinel–plagioclase peridotitic clasts originated at some tens of kilometers depth. Anderson made interesting speculations about the opaque minerals and the minor element content of the silicates, and these ideas should be tested by thorough study of all specimens in this group: in particular the relations between armalcolite and ilmenite need further explanation in view of the stability data obtained by Lindsley *et al.* (1974a). The pattern of rare earths in a 15445 clast was found to be inconsistent with coexistence of olivine, orthopyroxene, and Cr–pleonaste with any known basaltic lunar liquid, and Ridley *et al.* (1973) suggested that garnet had been present by analogy with the pattern found for pyropic garnet in terrestrial peridotites. Further work is needed, but one should ponder the possible presence of garnet peridotite and eclogite on the Moon. For Mg-rich bulk compositions, pressures over 15kbar and depths over 300km would be needed, assuming a temperature over 1000°C (Fig. 2).

(b) Others. From the viewpoint of *bulk composition,* other Mg-rich specimens could be classified mostly as dunitic, troctolitic, and spinel–troctolitic. Figures 6, 7, and 12 show major elements of olivine, pyroxene, and spinel (*s.l.*) from these types.

Dunitic: Polycrystalline olivine-rich fragments occur in breccias and soils, and the legend to Figure 6 lists all the specimens for which chemical compositions and some textural data were given. All are from Apollo 14 and 17. Specimens 1–8 have olivine compositions in the range Fo_{85} to Fo_{89}, suggesting origin from a near-uniform source. Chromite occurs in nearly all these dunitic fragments, and the compositions fall in a single region on a plot of Mg,Al,Cr, and Fe (Fig. 12); furthermore the TiO_2 contents are below 4 weight percent, which distinguishes them from most chromites of mare basalts. Armalcolite occurs in several fragments, and its *mg* value ranges from 0.6 to 0.7 and correlates with *mg* of the coexisting olivine along the trend of Steele (1974). Specimens 10, 11, and 12, and perhaps 9, have olivine compositions which range to lower Fo values.

Troctolitic: Polycrystalline fragments rich in plagioclase and olivine occur in breccias and soils, and the legend to Figure 6 lists all specimens with published chemical compositions and textural data. There are two principal types, one with non-brecciated textures and olivine compositions restricted to Fo_{86-88} (specimens 1–6, 12) and the remainder with a variety of textures (described as fine-grained basaltic, annealed cataclastic, metamorphosed, brecciated, cataclastic, and altered) and a wide range of olivine and pyroxene compositions. One aberrant specimen with Fo_{61} (No. 7) could be interpreted as a cognate xenolith in a mare basalt. The large troctolitic granulite 76535 has the same olivine composition as the first type, and indeed might serve as a guide for interpretation of all the first group. The second group of fragments can be interpreted as the products of impact mixing of diverse materials near the lunar surface. Whereas the CaO content of olivines of the first group is mostly below 0.1 weight percent suggestive of plutonic crystallization, that of the second group is mostly above 0.1 weight percent (*e.g.* Prinz *et al.*, 1973a, Fig. 12) suggestive of near-surface conditions. The first group was found only in Apollo 14 and Apollo 17 samples, whereas the second group was strongly represented in Luna 20 samples as well. Tentatively we define a group of *Mg–troctolites* with unzoned olivines in the range 85–91 Fo and a group of *Fe–troctolites* with diverse textures and olivines less magnesian than Fo_{85}. The Apollo 17 fragments described by Stoeser *et al.* (1974) show a bimodal distribution on the histogram of line 8 in Figure 6, and may represent a mixture of the proposed two types of troctolites. Further study, especially of minor elements, is desirable. Lines 9, 10, and 11 of Figure 6 are histograms for specimens described as "anorthosite," and "ANT." Without further study of textures, mineralogy, and minor elements, it is not possible to interpret these specimens in detail, but we suspect that most of them are polymict breccias which have undergone various degrees of metamorphism. Preferring to rely on chemistry rather than on texture and mode, we shall assume that specimens 8, 9, 10, and 11 are mixtures of several types of material.

Spinel–troctolitic: The olivine compositions in Figure 6 are widely scattered from Fo_{97} to Fo_{70}, with the majority from Fo_{90} to Fo_{75}. Pyroxenes are volumetrically unimportant and tend to scatter widely in composition (crosses in Fig. 7). Spinels are rich in Mg and Al and low in Fe and Cr; their pink color is diagnostic. Rock textures are often igneous, with a distinction between early megacrysts and late groundmass. Most, if not all, of this group can be explained by melting of mixtures of olivine and plagioclase whose bulk composition lies in the area *pqt* of Fig. 1, followed by cooling sufficiently rapid to allow preservation of the spinel. Impact melting of regolith and partial melting of olivine–plagioclase

cumulates near the lunar surface are the two favored mechanisms (*e.g.* Agrell *et al.*, 1973; Hodges and Kushiro, 1973; Walker *et al.*, 1973b). The extensive literature on specimen 62295 provides an excellent guide to the evidence and ideas. In this specimen are two generations of olivine: an early generation variously described as xenocrysts or phenocrysts with composition Fo_{89-95} and a later generation of microcrystals often skeletal and with composition Fo_{80-87}. At least some of the spread of olivine compositions in Figure 6 results from a contrast between early Mg-rich and late Fe-rich crystals, but the total spread is so large that diverse source materials must be involved. Until a thorough study has been made of textures and mineral compositions of all members of this group, we feel that interpretation is difficult. On the whole, we suspect that some are impact melts, while some are the products of rapidly-crystallized magmas from the lunar interior. Perhaps the Fe-rich ones tend to fall into the first group while the Mg-rich ones mostly or entirely fall into the second group.

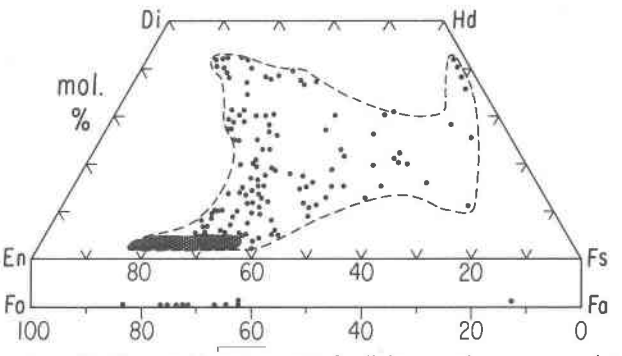

FIG. 8. Composition ranges of olivines and pyroxenes in KREEP-rich rocks. The shading and stippling are qualitative indications of the frequency of analyses of pyroxenes; by far the majority occur in the dark region. Data sources: Apollo 12 gray-mottled breccias (Anderson and Smith, 1971); Apollo 12 feldspathic norites (Brown *et al.*, 1971); 12032,45 lithic fragments (Quaide *et al.*, 1971); noritic clasts in 14313 breccia (Floran *et al.*, 1972); 14053 and 14073 basalts (Gancarz *et al.*, 1971); 14276 basalt (Gancarz *et al.*, 1972); 67749 basalt clast (Steele and Smith, 1973); 4–10 mm Apollo 15 fines with basaltic texture (Powell *et al.*, 1973); basalt clasts in 15465 breccia (Cameron and Delano, 1973); Apollo 12 coarse fines, Type A crystalline norite–anorthosites (Wood *et al.*, 1971); Apollo 12 KREEP fragments (Meyer *et al.*, 1971). Note that many other data are available.

Lunar specimens with lower Mg/Fe

In part I, a crude distinction was made between ANT, KREEP, and mare-type specimens. After 1973, lunar petrologists became increasingly dissatisfied with these simple distinctions, though it was difficult to establish precise criteria for a better classification. The following attempt to sort out the mineralogical evidence is rather subjective.

(a) High-KREEP material, mostly noritic. Essentially all lunar rocks have detectable KREEP components, and the key feature is whether the KREEP content is high or low. Unfortunately the KREEP components (and related ones including Zr and Ba) occur mainly in the interstitial and late phases which are very fine-grained and difficult to characterize. In small and coarse-grained specimens, non-random sampling is a problem. Some bulk analyses were made by broad-beam electron microprobe techniques for which the accuracy of K and P was marginal. Bearing all these factors in mind, it is not certain whether the concentrations of KREEP components show a bimodal or a continuous distribution. The plot of weight percent ($K_2O + P_2O_5$) *vs.* weight percent plagioclase by Wood (1975, Fig. 3) shows a continuous distribution, though there is a strong tendency for the population density to drop abruptly as the KREEP content increases past the line ($K_2O + P_2O_5$) = 0.945−0.00893 (norm. % plagioclase). Orbital data show a marked concentration of radioactivity near the Imbrium region, but until greater areal coverage is obtained it is not certain what is the surface distribution of KREEP-rich materials. Texturally, KREEP-rich materials range from glasses to breccias to rare basalts. Most crystalline specimens have a mineralogy dominated by plagioclase and low-Ca pyroxene (commonly orthopyroxene, but pigeonite occurs), and can be called noritic. Figure 8 summarizes the composition range of pyroxenes obtained from the specimens listed in the legend. Compilation of erratic data from diverse sources cannot give a statistically meaningful frequency distribution. However, when account is taken of the tendency to list unusual compositions, most pyroxenes from KREEP-rich noritic material lie in the range $En_{60-80}Fs_{16-36}Wo_{2-5}$. A fairly strong concentration band extends to augites ~ $En_{45}Fs_{15}Wo_{40}$, while a few scattered analyses extend to Fe-rich compositions. Olivines are uncommon and mostly lie in the range Fo_{63} to Fo_{83}. Plagioclases tend to be sodic compared to other lunar specimens, with a range mostly from $An_{90}Ab_{10}$ to $An_{75}Ab_{25}$ (Part I, Fig. 2).

(b) Low-KREEP noritic material. The legend to Figure 9 summarizes selected specimens. Three Apollo 17 specimens (Civet Cat clast in 72255, rock 78235, and orthopyroxene megacrysts in soils) have minerals with similar compositions: plagioclase An_{92-94}, orthopyroxene $En_{73-81}Wo_{\sim 3}$, and augite $En_{43-48}Wo_{45-48}$. All are coarse-grained, and norite

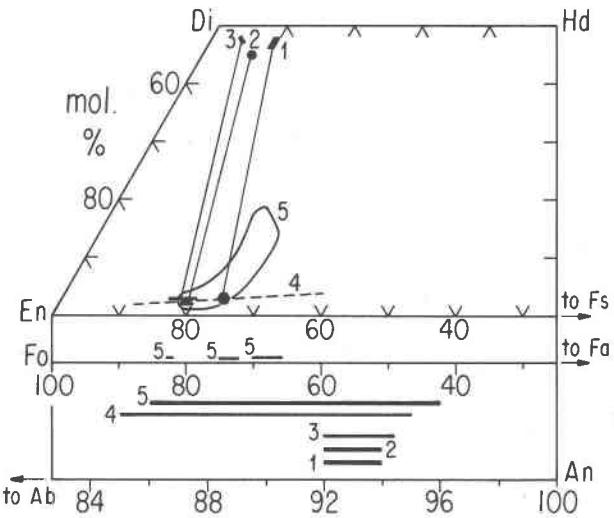

FIG. 9. Compositions of pyroxene, olivine, and plagioclase in low-KREEP norite and 67075 anorthositic breccia. Details of specimens: 1. Civet Cat clast, 2.5 cm long, 72255, Boulder 1, Station 2, South Massif, Apollo 17. 35% light streaks of pure plagioclase $An_{92-94}Or_{0.5-1.0}$ partly shocked to maskelynite. 65% dark streaks of orthopyroxene $En_{72-74}Fs_{23-25}Wo_{2-4}$ with abundant ilmenite plates in cleavages, rare augite $En_{42-45}Fs_{9-10}Wo_{46-48}$ as small grains and lamellae in opx, accessory cristobalite, baddeleyite, ilmenite, chromite, metallic iron, troilite, and Nb-rutile (Stoeser *et al.*, 1974). 2. Norite rock 78235 with 1–5 mm plagioclase and orthopyroxene, chipped from boulder, Station 8, Apollo 17. Cumulate texture. Heavily shocked. 60% anorthite $An_{93.5-94.5}$, 30% $En_{78-80}Fs_{18-20}Wo_{2-3}$, 10% glassy veins, interstitial augite $En_{48}Fs_7Wo_{45}$, silica, whitlockite (MgO 3.6 Ce_2O_3 2.0 wt.%), fluorapatite, rutile (Cr_2O_3 3.0 and Nb?), iron (Co 3 Ni 2), chromite, baddeleyite (TiO_2 4), and troilite (McCallum *et al.*, 1975a; Irving *et al.*, 1974). 3. Six 1–2 mm orthopyroxene crystals $En_{77-81}Fs_{16-20}Wo_3$(Al_2O_3 1.1 Cr_2O_3 0.6 wt.%) with minor attached plagioclase $An_{92-94.5}$ (Fe 0.1 K 0.1 wt.%), mesostasis, and veins of silica mineral, K-Ba feldspar, phosphate, chromite, diopside $En_{48}Fs_{4-5}Wo_{47-48}$, troilite, and iron (Ni 3.9 Co 2.8). Probably related to 78235 (Irving *et al.*, 1974). 4. Micronorite fragments in 14321 polymict breccia. Granoblastic, hornfelsic and vestigial subophitic textures. Unzoned pyroxenes with total composition range $En_{87}Fs_{11}Wo_2$ to $En_{58}Fs_{38}Wo_4$ (TiO_2 0.5 Al_2O_3 0.6 Cr_2O_3 0.3), plagioclase inclusions An_{85-95}, rare high-Ca pyroxene, ilmenite, iron, zircon and whitlockite (Grieve *et al.*, 1975). 5. Nine recrystallized noritic fragments with granular pyroxene occurring as clasts in microbreccias of Apollo 15 soils. Interpreted as monomict breccias. Plagioclase An_{86-96}, pyroxene $En_{60-80}Fs_{15-26}Wo_{2-27}$, olivine Fo_{65-83} (Cameron *et al.*, 1973).

78235 has a definite cumulus texture. An obvious source would be a disrupted plutonic complex. The range of *mg* of the pyroxenes is close to that for pyroxenes in spinel troctolites, but the compositions of the two pyroxenes are more highly separated as befits a lower temperature of equilibration. The orthopyroxenes fall to the extreme Mg-rich end of the compositional maximum for KREEP pyroxenes (Fig. 8). The augite is rare, and occurs as discrete grains and as lamellae in the Civet Cat clast, as interstitial grains in 78235, and as a component of rare KREEP-rich veins in the orthopyroxene megacrysts from soils. Although the bulk KREEP content is low, there are KREEP-rich spots or veins in the specimens. Perhaps these result from permeation of the norites by minor amounts of KREEP-rich fluids, or erratic concentration of residual liquids.

Specimens 5 and 6 in the legend to Figure 9 are clasts in breccias, and the wide range of plagioclase compositions suggests a diverse origin.

(c) Anorthositic. Petrographically, anorthosites should have more than 90 percent plagioclase, but the terms anorthosite and anorthositic have been used loosely. Few photomicrographs have been published of anorthositic specimens, but we suspect that most are polymict breccias. The 19 specimens listed in the legend to Figure 10 probably show the entire range of textures and compositions. Many specimens crudely lumped into the ANT category are rich in feldspar,

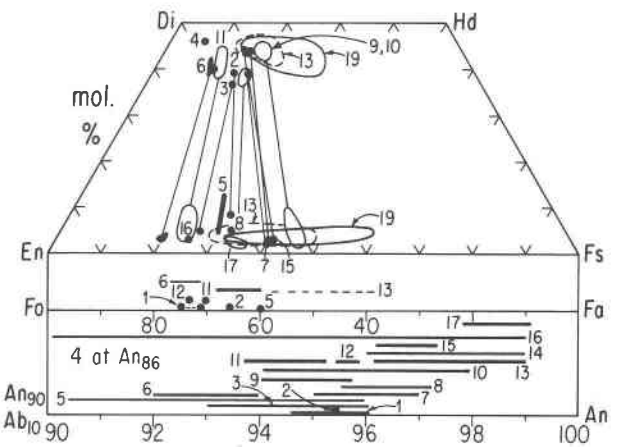

FIG. 10. Compositions of pyroxene, olivine and plagioclase in anorthositic specimens. 1. 2 mm fragments of microanorthosite 10085-4-10a. Microphenocrysts of anorthite $An_{95.5}$ in granulitic mosaic of anorthite, olivine $Fo_{71.75}$, clinopyroxene, ilmenite (9.6 wt.% MgO), rutile, and trace of troilite and iron (Agrell *et al.*, 1970). 2. Anorthositic basalt fragment 10059-27. Anorthite $An_{95.4}$, minor olivine $Fo_{66.1}$, augite $En_{45.6}Fs_{15.2}Wo_{39.1}$, pigeonite $En_{61.4}Fs_{30.3}Wo_{8.3}$, and ilmenite (6.1% MgO) (Keil *et al.*, 1970). 3. Anorthosite fragment 10085-07,6. Anorthite An_{93-96} and orthopyroxene $En_{69.0}Fs_{26.3}Wo_{4.6}$ with lamellae of clinopyroxene $En_{47.0}Fs_{16.6}Wo_{36.4}$ (Reid *et al.*, 1970). 4. Anorthosite fragment 14258,28,1419-7. Bytownite $An_{86.0}Or_{1.7}$, 1% diopside $En_{47.5}Fs_{6.5}Wo_{46.0}$ as inclusions and interstitial grains, and <1% ilmenite (8.2 wt.% MgO) (Powell and Weiblen, 1972). 5. Fragment D of brecciated anorthosite in 14257,2 coarse fines. Anorthite $An_{90.4-95.9}$, minor olivine Fo_{60}, pigeonite $En_{60-66}Fs_{28-30}Wo_{4-13}$ and trace ilmenite (Klein and Drake, 1972). 6. 23 anorthositic fragments of 67712 soils. Anorthite $An_{94\pm2}$, olivine $Fo_{74\pm3}$, and pyroxenes with narrow composition ranges at $En_{48}Fs_{10}Wo_{42}$ and $En_{77}Fs_{19}Wo_4$ (Simkin *et al.*, 1973). 7. Cataclastic anorthosite 61016.

Plagioclase An_{95-97} containing blebs of separate pyroxenes $En_{41}Fs_{15}Wo_{44}$ and $En_{58}Fs_{40}Wo_2$. Trace silica mineral (Steele and Smith, 1973). 8. Cataclastic anorthosite 60215. 97% anorthosite An_{95-97}, orthopyroxene $En_{62-68}Fs_{30-37}Wo_{1-2}$, interstitial to granulated feldspar, very rare iron. Clasts of An_{96}, $En_{63}Fs_{32}Wo_5$ and Cr–spinel (*mg* 0.27 *cr*0.65) (Meyer and McCallister, 1973). 9. Cataclastic anorthosite 60025. 3 mm tablets of plagioclase An_{94-96} in fine-grained recrystallized matrix. 2% $En_{50-52}Fs_{40-47}Wo_{1-10}$ and $En_{37}Wo_{44}Fs_{19}$ occurring partly as crushed grains in matrix, and partly as inclusions and recrystallized grains. Trace silica and opaques (Walker *et al.*, 1973b). 10. Cataclastic anorthosite 60025. 95% An_{98-94}, $En_{50-53}Fs_{44-47}Wo_{2-6}$ and $En_{35-39}Fs_{16-21}Wo_{42-46}$ mostly as discrete grains, trace ilmenite and Cr–spinel (Hodges and Kushiro, 1973). 11. Granoblastic anorthosite 60619. Rake sample. Inhomogeneous distribution of minerals but compositions uniform. $An_{93.6-95.2}$, Fo_{70-71}, $En_{66-73}Fs_{21-26}Wo_{3-11}$, $En_{44-49}Fs_{10-15}Wo_{39-45}$, ilmenite (MgO 5–8 wt.%), chromite (TiO_2 3–5% MgO 5.6% Al_2O_3 12–15%) and rutile (Dowty *et al.*, 1974d). 12. Granoblastic anorthosite 60677. 2 mm clast in rake sample breccia. $An_{95.3-95.9}$, Fo_{74-75} (Dowty *et al.*, 1974d). 13. Nine Apollo 16 ferroan anorthosite rake samples with cataclastic textures and veins of melt, usually recrystallized. 62275 is mostly maskelynite. For brevity, only composition ranges given here. $An_{96.2-97.0}$, except for $An_{97.5-98.9}$ in 62275. Rare olivine mostly Fo_{59-67}, but Fo_{40-65} for 65789. High- and low-Ca pyroxenes as separate grains or intergrowths, with latter most common: most are $En_{50-70}Wo_{\sim 3}$ and $En_{36-41}Wo_{\sim 45}$. Rare chromite in 3 specimens (TiO_2 1–3% MgO 1–4% Al_2O_3 11–21%) and ilmenite in 3 specimens (MgO 2–5%) (Dowty *et al.*, 1974d). 14. Genesis rock 15415. Polymetamorphic texture with evidence of cataclasis and recrystallization. 97–99% anorthite An_{96-99}, 2% $En_{40}Fs_{16}Wo_{44}$, trace $En_{57}Fs_{40}Wo_3$, trace silica mineral, trace ilmenite (MgO 1.0 MnO 0.6 wt.%) (James, 1972; Hargraves and Hollister, 1972; Stewart *et al.*, 1972; Steele and Smith, 1971; Smith and Steele, 1974). 15. Cataclastic anorthosite rake sample 15362. 97% $An_{96.1-97.3}Or_{0.1-0.3}$, 2% $En_{39}Fs_{18}Wo_{43}$, 0.5% $En_{56}Fs_{41}Wo_3$, 0.3% ilmenite (Al_2O_3 1.6 MnO 0.7 MgO 1.9 wt.%), two grains Al–chromite (Al_2O_3 9.1 Cr_2O_3 48.8 FeO 35.1 MgO 1.2) (Dowty *et al.*, 1972a; Nehru *et al.*, 1974). 16. Cataclastic anorthosite 15264,19 fragment. >90% An_{90-99}, average 96, orthopyroxene mean $En_{72}Fs_{25}Wo_3$, trace iron and chromite (Mason, 1972). 17. Cataclastic anorthosites from Apollo 16. Abstract reports various textures, pyroxene and plagioclase compositions, and absence of silica mineral. Specimens 64819, 60215, 61016, 65315 and 60015 have $En_{61.7-65.0}Fs_{32.0-36.5}Wo_{1.5-3.0}$ and $En_{41.4-44.2}Fs_{12.3-14.9}Wo_{42.8-45.1}$ (Dixon and Papike, 1975). 18. Four anorthositic fragments in Apollo 15 soils, one from Luna 20 and three from Apollo 16. Plagioclase An_{93-97}, olivine scattered values between Fo_{45} and Fo_{87}, high-Ca pyroxene $En_{40-49}Fs_{10-20}Wo_{37-43}$ and low-Ca pyroxene mostly $En_{70-85}Fs_{12-27}Wo_{3-5}$. Not plotted in Fig. 10 (Cameron *et al.*, 1973). 19. Anorthositic polymict breccia 67075. Contains clasts of microanorthosite with different amounts of olivine and pyroxene (Fig. 5). Plagioclase is An_{95-98} irrespective of textural state. Olivine as isolated unzoned clasts with bimodal composition range Fo_{40-42} and Fo_{50-55}. Pyroxene as augite, pigeonite, orthopyroxene, and partially inverted pigeonites either as individual grains or lamellar intergrowths up to 40μm across. Composition ranges for clasts and matrix may show clusters. Blue-gray chromites occur as inclusions in olivine or as crushed grains in groundmass, while chromite–ilmenite–iron intergrowths occur as small inclusions in pyroxenes. Data combined from Brown *et al.* (1973), El Goresy *et al.* (1973a), McCallum *et al.* (1975b), Ghose *et al.* (1975) and Smith and Steele (1974).

and show a similar range of mineral compositions. Probably most ANT specimens have bulk compositions corresponding to noritic anorthosite and anorthositic norite. Historically, the Genesis Rock, 15415, is the most interesting, and indeed its texture has been interpreted in different ways. Even on Earth, the origin of anorthosites is very controversial, though most petrologists probably favor origin by cumulation from a liquid followed by solid-state annealing which produces many textural variants. Figure 5 shows several textures in the polymict anorthositic breccia 67075, which was interpreted by Brown *et al.* (1973) as the product of a disrupted layered igneous complex dominated by plagioclase interspersed with minor augite (now exsolved to two pyroxenes). In spite of the problems, we assume that all lunar anorthosites had an igneous origin which has been obscured to different degrees by brecciation, shock metamorphism, mixing and annealing.

Pyroxene, olivine, ilmenite, Cr-rich spinel, silica minerals, rutile, iron, and troilite occur erratically, and sampling problems preclude estimates of modes and mineral associations. Although incorporation of extraneous grains cannot be ruled out, we believe that all these minerals occur in the anorthositic assemblage, though not necessarily in equilibrium. The pyroxenes occur either as separate grains or intergrown lamellae, and the wide composition gap indicates substantial solid-state annealing. Augite predominates several-fold over low-calcium pyroxene, and there is a wide spread of *mg* from 0.8 to 0.4. Olivines occur sporadically, and the range of *mg* is similar to that for the low-Ca pyroxenes. Most plagioclase compositions are between An_{94} and An_{99}, but some analyses go into the bytownite range. The spinels (Fig. 12) are rich in Fe and Cr.

The origin of the pyroxenes and the significance of their *mg* ratio is controversial. Smith and Steele (1974: see also Part I, p. 237) suggested that the plagioclase incorporated substantial $Ca(Fe,Mg)Si_3O_8$ which exsolved at lower temperature to give pyroxene $Ca(Fe,Mg)Si_2O_6$ and a silica mineral. Compilation of available data (*e.g.* legend to Fig. 10) shows that silica minerals occur in only some anorthositic specimens and are always much less abundant than the pyroxenes. Of course, one can suggest that primary olivine combined with exsolved silica to give pyroxene. The *mg* ratio of plagioclase is lower than that for pyroxene crystallizing from the same liquid, and Smith and Steele deduced that the source liquid of lunar anorthosites would be more Fe-rich if the pyroxenes were primary rather than secondary. The

modal and textural data on anorthositic specimens are too poor to give a test, but we now believe that the major part of the pyroxene is primary: the reasons are (a) the olivines in Figure 10 have a similar range of *mg* to the low-Ca pyroxenes in spite of erratic modal variations and (b) the spinels are very Fe-rich (Fig. 12). If this conclusion is valid, the parent liquids of the anorthosites could have been very Fe-rich. Predicted *mg* values are 0.6–0.2 for extreme crystal–liquid fractionation (Part I, Fig. 4), and higher values 0.8–0.4 for complete crystal–liquid equilibration.

Dowty *et al.* (1974d) used the term *ferroan anorthosite* for a "widespread and distinctive lunar rock type," but we are not convinced that a clear distinction has been made from other anorthosites. We deliberately placed their spinel–olivine anorthosite 60618,1-1 with our spinel troctolite group because of chemical similarities and inconclusive texture (their Fig 1b). They distinguished two granoblastic anorthosites whose ferromagnesian minerals are more magnesian than those in the ferroan anorthosites. Hubbard *et al.* (1974) used bulk analyses of minor and trace elements to distinguish between anorthositic rocks, but the relation to the detailed mineralogy and mineral chemistry is not clear. At this time we prefer not to attempt a subdivision of the anorthositic specimens, but agree that the present evidence suggests more than one origin. Because of the mineralogical evidence for a hybrid origin of many anorthositic specimens, we argue that chemical distinctions made from bulk compositions should be less powerful than those made from the individual minerals. Whatever the future of research on anorthositic specimens, the tendency for *mg* to be low in the pyroxenes, olivines and spinels must be explained.

(d) Granitic and rhyolitic. Although no large rocks or fragments are known, numerous tiny clasts (up to 2mm) of granitic material occur on the Moon. Most specimens are quenched melts or fine-scale intergrowths of K-rich feldspar and a silica mineral, but occasional clasts (*e.g.* Anderson *et al.*, 1972, Fig. 3) show coarse grains in a equigranular texture. Because of the small sample size, the number of accessory minerals is hard to determine, but minor pyroxene, olivine, phosphates, zircon, troilite, and iron have been recorded. Ryder *et al.* (1975) reported numerous granitic clasts in Boulder 1, Station 2, Apollo 17, and described various textural variants and unusual ternary feldspars. K-feldspars in granitic specimens usually carry about 1–2 weight percent. BaO and variable but low amounts of Na_2O. The sparse data on olivine and pyroxene compositions (Fig. 11) are scattered and tend to be Fe-rich. The presence of K-rich feldspar, phosphates, and zircon obviously gives a KREEP-like affinity to the granitic and rhyolitic specimens. All workers agree on an origin from highly-differentiated liquids but the relative roles of progressive fractional crystallization (Ryder *et al.*, 1975), partial remelting, and liquid immiscibility are controversial.

(e) Mare basalts. We shall not attempt to review in detail the mineral data for mare basalts. Because mare basalts are undoubted igneous rocks crystallized from magmas, the bulk compositions are meaningful. Readers could consult Taylor (1975, Chapter

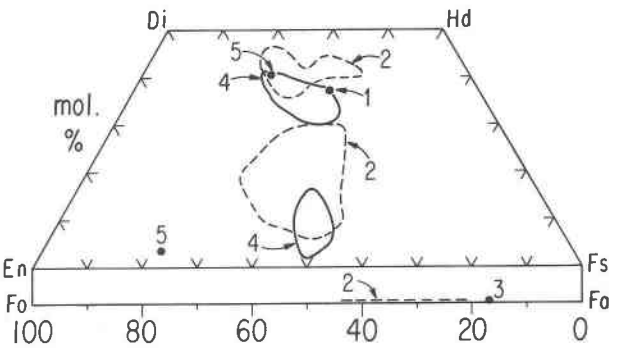

FIG. 11. Compositions of pyroxene and olivine in granitic and rhyolitic specimens. 1. Granitic and rhyolitic fragments in 14306,14321 and 14270 breccias. Several contain cores of K-feldspar and quartz, and one (14306,53) has 0.4 mm grains with planar faces. Most are glassy or have granophyric textures. Analysis of Fe-augite microphenocryst and K-feldspar (Na_2O 0.5 CaO 0.8 BaO 2.6) in 14306,53 granite clast (Anderson *et al.*, 1972). 2. Rhyolitic clasts (0.5–2 mm) in breccias from Boulder 1, Station 2, Apollo 17. Mafic, non-mafic, holocrystalline, and glassy types. Fig. 3 shows total range of pyroxene compositions in all clasts, but individual ranges are smaller. K,Ba feldspars (BaO 1.1–3.6), plagioclase, and unique ternary feldspars near $An_{50}Ab_{10}Or_{40}$. Cristobalite, olivine Fo_{21-44}, ilmenite, troilite, iron, REE-whitlockite, and zircon (Ryder *et al.*, 1975). 3. Rhyolitic fragment in 12070 with granophyric texture, olivine Fo_{87}, ferroaugite and ilmenite (Marvin *et al.*, 1971). 4. Polymict KREEP-rich breccia 12013 permeated by "granitic" component. Distinction between primary and secondary minerals was difficult. Drake *et al.* (1970, Fig. 5g) showed two ranges of pyroxenes associated with granitic areas—$En_{40-50}Fs_{42-51}Wo_{4-16}$ and $En_{28-38}Fs_{21-40}Wo_{30-40}$, K-feldspars $Or_{55-90}An_{2-15}$, quartz and tridymite, ilmenite, Cr-ulvöspinel, troilite, iron, apatite, whitlockite, and zircon. See also Lunatic Asylum (1970). 5. Clasts of granitic composition in 14303, 14319, 14320, and 14321 breccias. Glassy to crystalline. K-feldspars (Na_2O 0.6–1.4 BaO 1–3 CaO 0.2–1.0) and plagioclase (Ab 8–27% Or 1–6%) (Roedder and Weiblen, 1972b). 6. Granoblastic clast of "microgranite" in 14321 breccia. 1 × 1.5 mm. Mosaic of equant grains of K-feldspar (Na_2O 0.3, CaO 0.3 BaO 1.9), silica mineral, minor zircon, apatite, and whitlockite. Also rhyolitic glasses, some devitrified (Grieve *et al.*, 1975).

4) for a useful introduction. Idiosyncrasies in the cooling history of fragments torn out of different levels of the same lava flow produced extreme complexity in the zoning of the pyroxenes. Many of the details are irrelevant from the viewpoint of overall lunar petrogenesis. Mare basalts definitely have diverse bulk compositions and mineralogy requiring different source regions, and partial melting of hybrid rocks is a popular but not fully accepted model. Although there are subtle differences in the chemical zoning which will be mentioned in later sections, pyroxene compositions tend to lie at the left of the region labeled FETI in Figure 3 of Part I: indeed all mare basalts have pyroxenes with $mg \leq \sim 0.7$. Olivines occur only in some mare basalts and also obey the boundary at ~0.7. Strong zoning occurs to very Fe-rich compositions, sometimes with formation of pyroxferroite. Plagioclases tend to lie in the range An_{85-95}. Spinels are very Fe-rich and zoned from chromite to ulvöspinel. KREEP minerals occur at low concentrations in the late residua.

(f) ANT. To conclude this section, a few words are needed on the catch-all acronym for anorthositic, noritic, and troctolitic specimens. Materials with these bulk compositions dominate the non-mare lunar samples, but most are metamorphosed polymict breccias. We have found no simple way of sorting out the mineral properties and in despair refer readers to the summary diagrams in Part I. Most ANT specimens have ferromagnesian minerals with *mg* 0.5–0.8. Pyroxenes dominate over olivines, and low-Ca pyroxenes dominate over high-Ca pyroxenes. Most plagioclases have An > 90 percent. A few specimens can be classified into the groups given earlier. The remainder can be interpreted as a heterogeneous rag-bag of material dominated by plagioclase and low-Ca pyroxene probably produced by mixing up the products of multiple igneous and metamorphic processes. Detailed study of minor and trace elements of mineral and rock clasts should enable progress to be made, but the task is daunting because of the loss of evidence by partial melting and solid-state diffusion.

Origin of rock types

Although very complicated models can be developed, and indeed must be necessary for individual breccias, we suggest that all the data on the rock types and mineral compositions can be accommodated in the following simple framework:

(a) crystal–liquid differentiation of the entire Moon about −4.5Gy with formation of Fe,S-rich core, an olivine-rich mantle, and a plagioclase–pyroxene-rich crust;

(b) intense brecciation of surface rocks, and complex volcanic, plutonic, and metamorphic activity in the upper 200km during the next 0.5Gy; minor amounts of incoming projectiles were incorporated;

(c) KREEP material tended to be dispersed; on the largest scale, Fe-rich ANT rocks would tend to overlie Mg-rich peridotitic rocks with late oxide-rich cumulates in the middle, however, on a smaller scale, layered plutons would develop sporadically in the near-surface region;

(d) after −4.0Gy, consolidation of a lunar crust; igneous activity mostly confined to partial melting and migration of interstitial liquid; extrusion of mare basalts produced by remelting mixtures of early cumulates and trapped liquids; the early melts would tend to become mixed up in the surface debris, and only the later melts would be easily recognizable as the mare basalts.

Some of the above ideas have become widely accepted, but the nature of the lunar interior and the origin of mare basalts are highly controversial. Many of the mineralogical and petrological data can be explained satisfactorily by early melting of only the outer part of the Moon, followed by migration of a molten zone into the interior. All simple models for the origin of mare basalts have apparently been abandoned, and multi-stage models are being explored. At one extreme are models involving remelting of late cumulates produced during primordial differentiation (*e.g.* the use of phase-equilibrium data by Walker *et al.*, 1975, to explain high-Ti lunar basalts from remelting of ilmenite-rich cumulates), and at the other extreme are models involving late melting in the interior of the Moon (*e.g.* Kesson and Ringwood, 1976). We refer readers to the *Proceedings of the 1975 Mare Basalt Conference* (obtainable from the Lunar Science Institute) and of the *Seventh Lunar Science Conference.* Whatever the problems concerning the inside of the Moon, we believe that many petrographic and mineralogic data can be fitted into any scheme involving early differentiation of all or most of the Moon (*e.g.* 76535 and 15445 from a plagioclase peridotite zone, 67075 from a disrupted layered pluton, 62295 from melting of an Mg-rich plagioclase–peridotite zone, 14310 from incomplete melting of plagioclase-rich debris).

We shall consider the petrologic model in detail in a discussion of the controls on the bulk chemical composition of the Moon (Smith and Steele, in preparation). The remainder of this review is devoted to

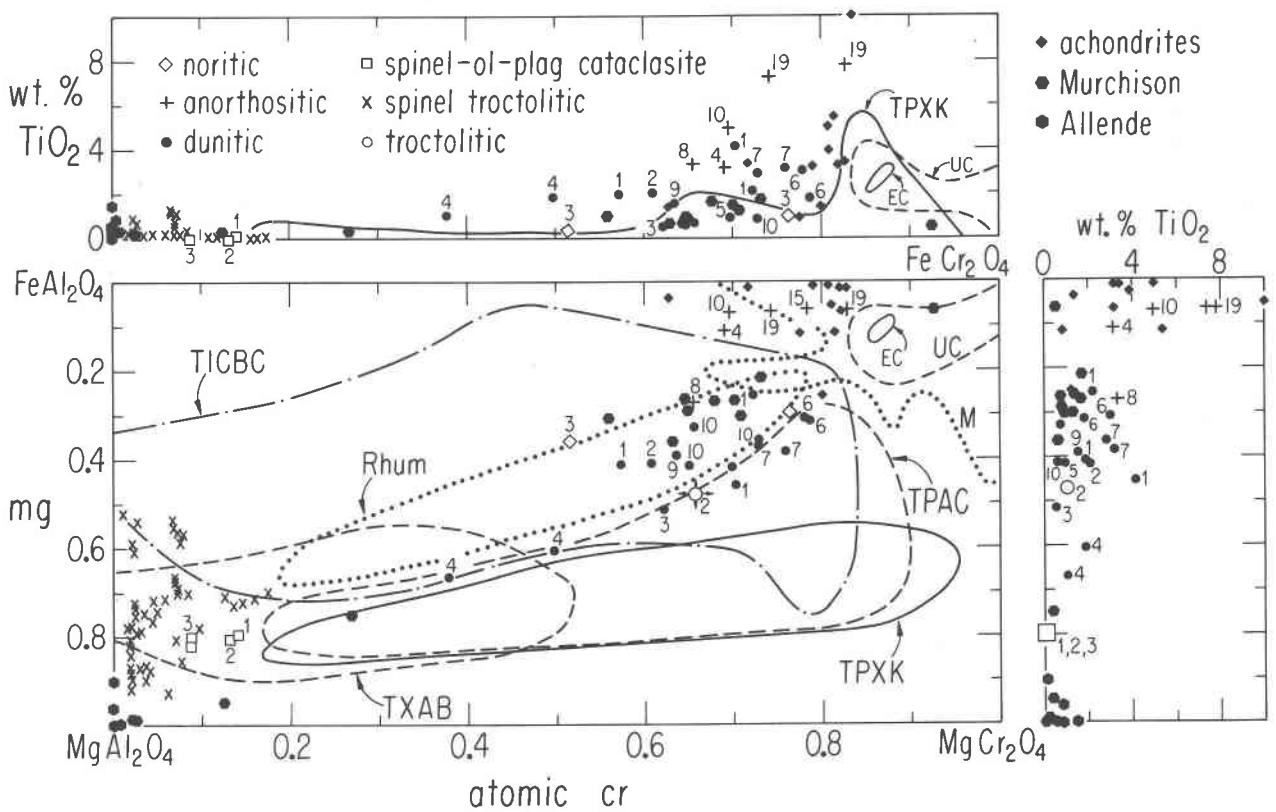

FIG. 12. Major-element composition of spinels from non-mare rocks. *mg* and *cr* are atomic Mg/(Mg+Fe) and Cr/(Cr+Al) respectively. The numbers refer to the specimen sequence in the appropriate figure legend for the rock type (see Fig. 6 for dunitic, troctolitic, spinel–anorthite–orthopyroxene–olivine cataclasite and spinel troctolitic; Fig. 9 for noritic; Fig. 10 for anorthositic). Composition ranges are given for the following: M all meteorites (Bunch and Olsen, 1975), EC equilibrated chondrites (Snetsinger *et al.*, 1967), UC unequilibrated chondrites (Bunch *et al.*, 1967), achondrites (Bunch and Keil, 1971; Lovering, 1975), Murchison C2 meteorite (Fuchs *et al.*, 1973), Type A and B inclusions, Allende meteorite (Grossman, 1975), TPXK terrestrial peridotite xenoliths in kimberlite (Smith and Dawson, 1975), TXAB terrestrial xenoliths in alkali basalts (various sources especially Basu and MacGregor, 1975), TPAC terrestrial podiform deposits in alpine complexes (various sources including those listed by Smith and Dawson, 1975), TICBC terrestrial igneous complexes with basaltic compositions (many sources including those for tholeiitic compositions, *e.g.* Bushveld, and those for metamorphosed Archean complexes, *e.g.* Fiskenaesset: see Smith and Dawson, 1975, for references), Rhum ultrabasic complex (Henderson, 1975). In the auxiliary plots for TiO_2, trends for most terrestrial specimens are omitted to avoid overlap. Most such specimens have less than 1 wt.% TiO_2.

discussion of the mineral groups, especially on the clues they provide to petrologic and geochemical differentiation.

Discussion of minerals

Feldspars

The sections on feldspar and olivine bring up to date the corresponding sections in Part I.

Meyer *et al.* (1974) investigated the potential and limitations of a low-resolution ion microprobe for analysis of trace elements in lunar plagioclase. Only the elements Li, Mg, K, Ti, Sr, and Ba occur in sufficient concentrations to give statistically valid signals that can be corrected accurately for overlapping masses, especially those from troublesome molecular ions. From plots of Li *vs.* Ba and Mg *vs.* Ba, Meyer *et al.* recognized distinct compositional ranges for plagioclases from anorthositic and gabbroic rocks (Li 1–2ppm, Ba 5–25ppm, Mg 150–350ppm), KREEP basalts (Li 10–30, Ba 60–220, Mg 750–1500), mare basalts (Li 2–14, Ba 15–350, Mg > 1700) and a high-Ba group of plagioclase clasts from Apollo 14 breccias (Li 14–50, Ba 200–750, Mg 200–1100). They concluded that these Apollo 14 breccias could not have derived from a pre-Imbrium regolith because they should then have contained more plagioclase of the first type believed to represent the original lunar highlands. [Data for 14063, a fine-grained clastic rock with several components, do not fall with data for the

other Apollo 14 breccias.] Apollo 16 samples with metaclastic texture contain many plagioclase clasts with low content of trace elements even though the bulk content of trace elements is high. Microprobe analysis of minor and trace elements is a powerful tool for deciphering the origin of plagioclase especially in anorthositic rocks and breccias.

Detailed crystal structure refinement by Smyth (1975) of anorthite $Na_{0.036}K_{0.005}Ca_{0.932}Fe_{0.002}Al_{1.927}Si_{2.077}$ from troctolitic granulite 76535 demonstrated 10 percent vacancy in the *M* site of type (000). This result is surprising for a strongly-annealed specimen, though perhaps it is inherited from primary crystallization of a defect anorthite from an earlier igneous melt. Smith suggested that the vacancy might result from expulsion of Fe upon reduction to metal.

Lofgren *et al.* (1974) reproduced experimentally the textures and mineral chemistry of Apollo 15 quartz-normative basalts. Megacryst-groundmass texture could be produced by steady cooling and does not require two discontinuous periods of crystallization. All the synthetic plagioclases were rich in minor elements and were found from electron microprobe analyses to contain 11–23 percent $Ca_{0.5}AlSi_3O_8$ formula-unit. Crawford's (1973) description of the zoning and chemical variation of plagioclase in mare basalts is closely matched by that of Bryan (1974) for quenched oceanic basalts. Delayed growth of plagioclase from basaltic melts is a serious problem for determination of stable phase-equilibria (Gibb, 1974).

Dowty *et al.* (1974a) studied the occurrence of twins in Ca-rich plagioclase of feldspar-rich rocks attributed to the lunar highlands. Carlsbad and Carlsbad–Albite twins as well as Albite and Pericline types were found in rocks with igneous texture which had not been severely brecciated. In cataclastic rocks, only Albite and Pericline twins were found, and Dowty *et al.* suggested that original Carlsbad and Carlsbad–Albite twins had disappeared by breakage along twin boundaries. Albite and Pericline twins commonly showed features attributed to origin by deformation. Anorthites can undergo such twinning very easily and reversibly because the Si,Al order does not block the twin process. Carlsbad and Carlsbad–Albite twins are not infrequent in granoblastic rocks, and probably arise from high-temperature solid-state recrystallization. In terrestrial plagioclase, such twins tend to occur in igneous specimens and are absent in low and medium grades of metamorphism: however, some do occur in the granulite facies. Many other reports of plagioclase twinning occur in the literature: *e.g.* Wenk *et al.* (1972) found that for plagioclase in rocks 12051, 14053, and 14310 the twin frequencies were generally Albite > Carlsbad–Albite ~ Carlsbad ~ Pericline (or Acline) ~ Baveno > Albite–Ala > Manebach, but there were minor differences from rock to rock.

Many papers described the domain textures of lunar plagioclases. Wenk *et al.* (1973) compiled data obtained by electron microscopy on out-of-step domains, and proposed a phase diagram to explain the occurrence of *b* and *c* domains and of the Huttenlocher intergrowth. Subtle features of diffuse X-ray diffractions of both lunar and terrestrial plagioclase were interpreted by Jagodzinski and Korekawa (1973, 1975) in terms of stepped domain boundaries.

Shock and recrystallization produced many complex textures in lunar plagioclase (*e.g.* Heuer *et al.*, 1974), and high-speed particles left tracks. All these effects reported in numerous papers testify to the complex history of the lunar regolith with regard to impact of both meteorites and nuclear particles.

Ryder *et al.* (1975) reported feldspars with unusual ternary compositions from Apollo 17 granitic clasts (see earlier). Those in holocrystalline clasts are compositionally uniform in any clast and lie near $An_{50}Or_{40}Ab_{10}$ whereas those in a rim between plagioclase crystals and granitic groundmass range from plagioclase composition to $An_{51}Or_{34}Ab_{15}$. Some clasts contain intergrown lamellae of K–feldspar and plagioclase, probably the result of unmixing. The ternary compositions lie well within the stability field of two coexisting feldspars, and some kind of non-equilibrium crystallization or metasomatism seems to be necessary.

Niebuhr *et al.* (1973) interpreted the ESR spectrum of 15415 plagioclase in terms of lines from Mn^{2+} and from Fe^{3+} in two structural sites. Only 1 percent of the iron was trivalent.

Olivines

Following up the ideas on minor elements in Part I, Steele and Smith (1975b) measured Al, Ca, Ti, Cr, Mn, and Ni down to the 50ppm level in Mg-rich olivines which may derive from the early lunar crust or deeper environments. Low Ca contents (0 to 0.1 wt.% CaO) consistently occur only in olivines from dunitic and troctolitic rocks, especially breccias, whereas olivines from spinel troctolites, mare basalts, and ANT materials from Luna 20 have CaO over 0.1 weight percent (Fig. 13). Although the effect of bulk composition is not known, simple analogy with terrestrial specimens indicates that high-Ca olivines de-

rive from volcanic environments and low-Ca ones from annealed ones. The distinctly lowest Ca content (0.01 wt.%) is for olivine in 15445 peridotitic cataclasite (see earlier).

The highest contents of Al_2O_3 found in new analyses of lunar olivines are 0.08 weight percent, and most values are below 0.04 weight percent. The high values in the literature, collected in Part I (Fig. 7), should be discarded unless they are confirmed by new analyses. Currently it appears that serious revision of techniques (probably with respect to determination of the background) is needed in some electron microprobe laboratories.

High Cr analyses (up to 0.15 wt.%) and low Ni analyses (up to 0.05 wt.%) in Mg-rich olivines confirm earlier analyses. A weak anti-correlation between Cr and Ni might be explainable in terms of the oxidation state being so low that Ni^{2+} is removed upon reduction to the metallic state while Cr^{3+} is reduced to the divalent state which should favor entrance into olivine. However, the data scatter so much, and there are so many indications of complexities in lunar rocks, that such an idea is presented with great hesitation. Furthermore a weak positive correlation indicates coupled substitution between Cr and Al. Titanium ranges up to 0.1 weight percent and appears to be higher in olivines from plagioclase-rich volcanic rocks; this may result from plagioclase tending to crystallize from later differentiates of the bulk Moon, whose Ti content has been enriched by extensive earlier crystallization of Ti-poor olivine. Systematic study of other transition metals (V,Co) and other minor and trace elements in olivine should place further controls on models for the crystallization of olivine.

Burns *et al.* (1973) concluded that there is no unequivocal optical-absorption evidence for substitution of Cr^{2+} in lunar olivines and pyroxenes because of possible overlap of absorption bands with those for Fe^{2+}. Furthermore they concluded that there is no reliable evidence for assigning bands to Cr^{3+}. If the chromium in lunar olivines is indeed all trivalent, it will be necessary to ascribe the high Cr content of some lunar olivines to high crystallization temperature rather than to low oxidation state. The occurrence of high Cr content in olivine from terrestrial komatiite lavas could be explained in the same way (*e.g.* Green, 1975). Detailed study of olivines synthesized from Cr-bearing systems at controlled temperature, pressure, and oxygen fugacity is badly needed.

Hewins and Goldstein (1974) studied the Ni and Co contents of Ni–Fe metal grains and their olivine host from Apollo 12 mare basalts. Cobalt concentrations in olivine ranged from 300ppm at the core to 70ppm at the rim. The Co/Ni distribution between olivine and metal indicated non-equilibrium, and showed that the metal did not crystallize first. Perhaps late reduction by sulfur loss (see later), affects the distribution of transition elements. Hewins and

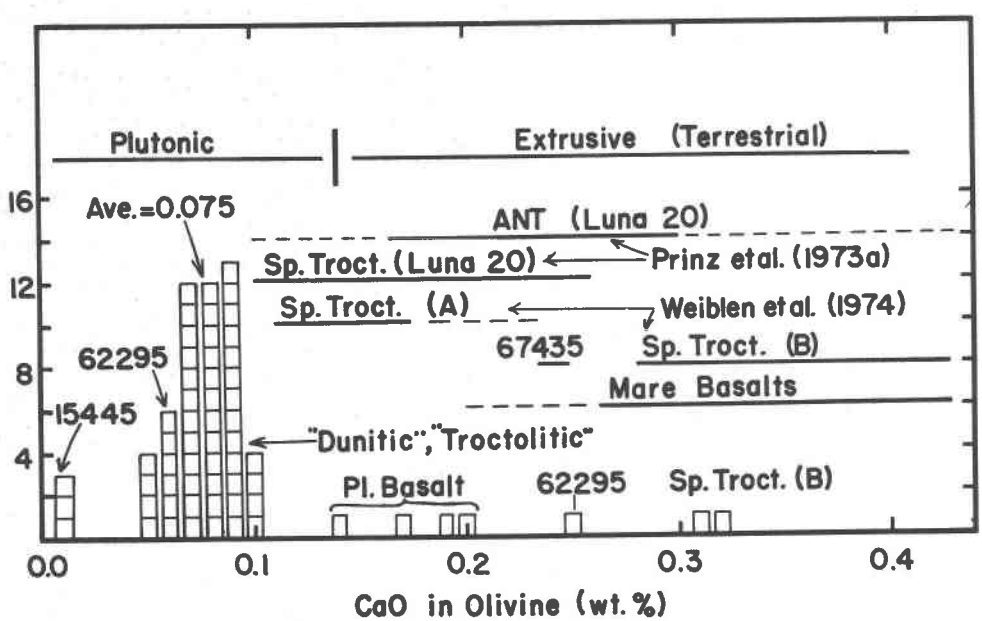

FIG. 13. Calcium in lunar olivines. Steele and Smith (1975b).

Goldstein (1975a) concluded that the olivine and metal of 76535 troctolitic granulite equilibrated at 900 ± 100°C, a range not inconsistent with that deduced from the coexisting pyroxenes.

Ghose *et al.* (1975) observed slight Mg,Fe segregation in olivine from cataclastic anorthosite 67075, a rock which contains orthopyroxene whose Mg,Fe order indicates equilibrium at 640°C. In the olivine, 0.525 ± 0.002 Fe atoms enter the *M*1 site and 0.480 the *M*2 site.

Huffman *et al.* (1975) interpreted magnetic hyperfine peaks of Mössbauer spectra of olivine-rich lunar samples taken at 5°K in terms of superparamagnetic clusters of Fe^{2+} spins in mirror sites. Annealing at 1000°C for 1 day reduced the hyperfine peak intensity by 30 percent in an olivine from a lunar basalt. Terrestrial olivines of unspecified origin showed no hyperfine peaks. When detailed time and temperature studies have been made, the hyperfine spectra may provide another thermometer for high temperatures.

Olivine clasts in high-grade metamorphosed breccias react with the matrix. Cameron and Fisher (1975) described coronas of pyroxene, ilmenite, and plagioclase around olivines in Apollo 14 breccias, and attributed them to diffusion of Ti, Mg, and Fe.

The distribution of *mg* between olivine and basaltic liquid was used by many workers in models for crystal–liquid fractionation in the Moon. Roeder and Emslie (1970) found that *mg* (olivine)/*mg*(liquid) was independent of temperature from 1150 to 1300°C and of oxygen fugacity from $10^{-0.7}$ to 10^{-12} atm. Their ratio of 0.30 was found to apply approximately to synthetic data for lunar basalts except that high ilmenite content caused some displacement. For hydrous systems at 15kbar, the ratio ranges from 0.52 at the iron–wüstite buffer to 0.04 at the magnetite–hematite buffer (Mysen, 1975). Because the oxidation state and water content of the Moon may have changed greatly since its inception, the fractionation between olivine and early liquid may have changed with time.

Pyroxene

Pyroxene is the major mafic phase in the returned samples and the literature is too big for complete review. Selected ideas will be classified under: (a) relation of major elements to rock type and crystallization conditions (b) minor and trace elements (c) exsolution, inversion and site population, and (d) deformation.

(a) Relation of major elements to rock type and crystallization conditions. For classification or characterization of rocks, soils, and breccias, plots of Mg,Fe,Ca on the well-known quadrilateral En–Fs–Di–Hd are useful, as illustrated by Reid *et al.* (1970), Prinz *et al.* (1973a), and Steele and Smith (1973). The use of pyroxene (and olivine) compositions to distinguish rock types was illustrated earlier. In general, the *mg* value decreases with progressive crystal–liquid differentiation, thereby allowing testing of petrologic models. The pyroxene grains from coarse-grained rocks are individually homogeneous except for exsolution, and the bulk composition probably gives a good clue to the original parent liquid. Highly metamorphosed breccias have relatively uniform pyroxenes, whereas poorly-metamorphosed ones have diverse pyroxenes (*e.g.* Warner, 1972, Fig. 10). Rapidly-crystallized pyroxenes show complex zoning trends which are not even uniform over the same thin section or even in different traverses of the same crystal. The details are very complex, and only a brief account can be given here. However, the data are consistent with the general conclusion that pyroxene nucleates easily and that the *mg* value of the first pyroxene depends fairly closely on the bulk *mg*. Subsequent zoning depends on many factors including competition with other minerals for the components in the declining reservoir of liquid, melt temperature, viscosity, and cooling rate.

The main emphasis has been on pyroxenes from mare basalts which show many textures ranging from skeletal crystals in vitrophyres to megacryst-groundmass assemblages. Initially it was believed that the latter texture resulted from early slow crystallization (perhaps in a deep-seated magma chamber) followed by rapid crystallization (perhaps upon extrusion at the lunar surface as a lava flow). However, Lofgren *et al.* (1974) were able to reproduce all the textures of Apollo 15 quartz-normative basalts merely by varying the rate of monotonic cooling. Indeed many specimens of lunar basalts probably came from the same individual lava flow and differ merely in their closeness to the surface; of course, initial quenching combined with multiple extrusion could give complex cooling histories. The observations by Dowty *et al.* (1973b, 1974c) on Apollo 15 basalts illustrate the complexities.

Sector zoning, often associated with skeletal growth, produces quite different chemical trends in the same crystals (*e.g.* Hollister *et al.*, 1971; Bence *et al.*, 1971; Boyd and Smith, 1971). Delayed crystallization of plagioclase (see earlier) results in a higher content of $CaAl_2Si_2O_8$ in the residual magma, while onset of plagioclase crystallization results in a sharp

drop of Ca and Al in the zoning trend of the pyroxene (*e.g.* Hollister *et al.*, 1971; Bence *et al.*, 1971; Dowty *et al.*, 1974c). After about two-thirds of the basaltic liquid has crystallized, the remainder tends to be trapped in pockets, and the composition of the crystallizing pyroxenes is affected by the idiosyncrasies of the local environment. Most pyroxene crystallization occurs just above the vault-shaped solvus, but discontinuities in some zoning trends from pigeonite to augite compositions suggest straddling of the solvus. Finally, very fine oscillatory zoning probably results from diffusion effects at the crystal-liquid surface. After the initial surge of studies of pyroxene zoning, most investigators have settled for random analyses which provide a statistical averaging of the above effects. Bence and Papike (1972) gave details of zoning trends for Apollo 11, 12, 14, 15, and Luna 16 specimens.

Random Ca, Mg, Fe plots of pyroxenes from mare basalts mostly fall in the region labeled FETI in Part I, Figure 3. There are many dozens of such plots, and those of Dowty *et al.* (1973b) are good examples. Although there are slight differences from one textural type to another, all plots show $mg \leq \sim 0.7$ with the major population between 0.7 and 0.6. Extreme zoning trends ultimately produced the pyroxenoid pyroxferroite. Relative concentrations of Ca-rich and Ca-poor pyroxenes definitely vary from one type of mare basalt to another: thus Ti-rich basalts 70215 and 75035 are strongly dominated by Ca-rich pyroxenes (Longhi *et al.*, 1974) whereas most basalts have both Ca-poor and Ca-rich pyroxenes.

To summarize: the peridotite suite is characterized by high-Mg, low-Ca pyroxenes accompanied by only sporadic rare diopside, the KREEP suite is also dominated by low-Ca pyroxenes, but these are somewhat less rich in Mg and are accompanied by rather more Ca-rich pyroxenes, the mare basalt suite is even poorer in Mg and has a greater proportion of Ca-rich pyroxene, and the ANT conglomeration occupies a middle region. This general trend from Mg-rich, Ca-poor to Fe-rich, Ca-medium compositions can be explained by cotectic crystallization moving off the simple olivine–plagioclase–silica ternary towards a Ca-rich pyroxene end-member. Of course, partial melting is involved as well as progressive crystal-liquid fractionation, metamorphism, and hybridism.

(b) Minor and trace elements. In conformity with the low content of volatile elements in the Moon, Na and K are much lower than for terrestrial pyroxenes. Potassium is below detection in routine electron microprobe analyses ($\sim < 0.05$ wt.%) and probably is below 0.01 weight percent in most samples. Sodium is rarely reported and is usually much less than 0.1 weight percent. Crawford and Hollister (1974) emphasized the occurrence of Na,Al-rich augite blebs ($En_{43}Fs_{13}Wo_{44}$, Na_2O 0.16,Al_2O_3 8.2 wt.%) in cores of hypersthene in 14310 KREEP basalt (see earlier), and suggested that the unusual content of Na and Al resulted from crystallization at high pressure. Detailed analyses of Na and K are needed.

Broad overall correlations between the major, minor and trace elements are rather similar to those found for terrestrial pyroxenes; *e.g.* Cr tends to correlate with Mg, while Al, Ti, and Cr tend to prefer augite to coexisting low-Ca pyroxene. Most investigators concentrated on Al, Ti, and Cr which are easy to determine with the electron microprobe (apart from fluorescence error from adjacent ilmenite and spinel) and which show large variations. Unfortunately the details are very complex because of the wide variation of crystallization conditions. In the near-absence of Na and K, the substitutions of Ti, Al, and Cr can be interpreted in terms of the following components (Bence and Papike, 1972): $M^{2+}Ti^{4+}Al_2O_6$, $M^{2+}Cr^{3+}SiAlO_6$, and $M^{2+}AlSiAlO_6$. The components $M^{2+}Ti^{3+}AlSiO_6$ and $Cr^{2+}SiO_3$ have also been invoked. Zoning trends of pyroxenes from mare basalts were plotted by many investigators and interpreted in terms of factors such as: beginning of plagioclase crystallization involving decrease of $M^{2+}AlSiAlO_6$ component and approach to the 1:2 ratio of Ti to Al for the $M^{2+}Ti^{4+}Al_2O_6$ component; presence of Ti^{3+} by a Ti/Al ratio greater than 0.5; early removal of Cr^{3+} leaving Cr-depleted liquid; correlation with crystallization of ilmenite or spinel; and changes in crystallization rate. Early pyroxenes from 14310 (see earlier for references) are enriched in $M^{2+}Al_2SiO_6$ probably because of the high Al_2O_3 of the bulk rock, but crystallization at high pressure has also been invoked. Most ANT rocks are metamorphosed breccias with diverse origins and textures, and the significance of minor elements has not been evaluated. Careful evaluation of the minor and trace elements in the pyroxenes from unusual Mg-rich rocks is needed: perhaps the most noticeable feature in Table 1 is the high Al_2O_3 content of pyroxenes in 15445 and 73263 cataclasites.

Qualitative areal scans with an ion microprobe showed trends for Mg, Ca, Ti, Al, Mn, Li, Na, K, and Ba in some pyroxenes from mare basalts (Bence and Autier, 1972). Higher concentrations of some elements were found at crystal edges or at pigeonite–augite interfaces, probably from liquid trapped in defects.

(c) Exsolution, inversion and site population. Prior

to the Apollo program, the phase relations and polymorphism of the pyroxenes were only partly understood, and major new discoveries were made on lunar samples. The state of knowledge in 1969 is exemplified by *Special Paper Number Two* of the Mineralogical Society of America, J. J. Papike, Ed. Papike *et al.* (1973) interpreted pyroxene structures from the viewpoint of topology and structural linkages.

Ross *et al.*(1973) delineated the augite–pigeonite solvus at 1 atm, using pyroxenes from mare basalt 12021. Lindsley *et al.* (1974b) determined the compositions of augite and hypersthene coexisting at 810°C and 15kbar under hydrothermal conditions, and found that the composition gap was similar to those observed for coexisting augite and either pigeonite or hypersthene in various lunar specimens (augite–pigeonite–orthopyroxene intergrowths in crystals from 67075 anorthositic breccia, Brown *et al.*, 1973, McCallum *et al.*, 1975b; inverted pigeonite clasts from 14082 and 14083 breccias, Papike and Bence, 1972; inverted pigeonite in fractured clast of "anorthositic gabbro" in breccia 15459, Takeda, 1973). All these specimens with coarse intergrowths of augite and low-Ca pyroxene(s) are the result of high-temperature crystallization followed by prolonged annealing in the solid state. Inversion from pigeonite to orthopyroxene is sporadic. Although precise conditions cannot be determined, the cooling history and other evidence require burial at some kilometers depth probably of gravitationally-layered plutonic bodies. Analogies were drawn with the well-known Skaergaard and Bushveld complexes on Earth.

Low-Ca pyroxenes with Mg-rich compositions have orthorhombic symmetry (*e.g.* those in the Mg-rich specimens described earlier, and in fragments ascribed to KREEP-rich rocks, Fuchs, 1971). These pyroxenes show no evidence of inversion from pigeonite, and presumably crystallized directly with orthorhombic symmetry. This is consistent with the occurrence of low-Ca, Mg-rich pyroxenes in terrestrial rocks. However, bronzites from troctolitic granulite 76535 and norite 78235 (Smyth, 1974a; Steele, 1975) have the space group $P2_1ca$ rather than *Pbca* in terrestrial bronzites. Crystal-structure analysis by Smyth (oral communication, 1975) showed segregation of Mg and Fe into four sites instead of the usual $M(1)$ and $M(2)$ sites. The new space group was also found in pyroxene from the Steinbach meteorite. Prolonged subsolidus annealing must be needed to promote the strong ordering of Mg and Fe, as was inferred from the textural features of the lunar and meteoritic specimens. Perhaps the new space group developed only in pyroxenes annealed at some tens of kilometers depth in rocks ascribable to a peridotitic facies.

Coarse exsolution of lunar pyroxenes is uncommon, and most specimens have exsolution which is so fine that X-ray diffraction and electron microscopic techniques are needed. In general for mare basalts, the pyroxenes crystallized mostly as augite or pigeonite (often as zoned crystals) which exsolved small amounts of pigeonite and augite, respectively, during cooling. Pigeonites crystallize with $C2/c$ symmetry and invert to $P2_1/c$ symmetry upon cooling below a temperature ranging from 1000°C for Mg-rich specimens to 500° for Fe-rich ones (Prewitt *et al.*, 1971). Passsage through the inversion results in an antiphase domain texture which is revealed by dark-field electron micrography (*e.g.* Champness and Lorimer, 1971; Champness *et al.*, 1971; Christie *et al.*, 1971; Lally *et al.*, 1972; Ghose *et al.*, 1972). Very complex lamellar structures were observed which require several stages of exsolution (*e.g.* Ghose *et al.*, 1973). In slowly cooled rocks, inversion from pigeonite to orthopyroxene may occur. Unfortunately it is difficult to determine from textures whether exsolution proceeded by spinodal decomposition or heterogeneous nucleation. Lally *et al.* (1975) suggested that the following experimental data yield the best information on the cooling rate: difference of β angle for exsolved pyroxenes in quickly-cooled rocks, textural evolution and domain size in moderately-cooled rocks, and the width of diffusion zones and the domain morphology in slowly-cooled rocks.

Finally, the distribution of cations between the $M(1)$ and $M(2)$ sites depends on temperature, and can be examined by either Mössbauer resonance study of the Fe distribution or by X-ray crystal structure analysis of the electron density. Interpretation of both types of data is difficult for various technical reasons (*e.g.* Dowty *et al.*, 1972b; Schürmann and Hafner, 1972), but the evidence for equilibration of cations between the $M(1)$ and $M(2)$ sites down to temperatures of around 600°C even for pyroxenes from mare basalts seems convincing (*e.g.* Hafner *et al.*, 1971; Ghose *et al.*, 1972; Brown and Wechsler, 1973; Yajima and Hafner, 1974). Such low temperatures have appeared surprising in view of the persistence of pigeonite and the expected rapid cooling of thin basaltic flows. However, the Mg, Fe distribution can be modified by atomic diffusion on a unit-cell scale, whereas polymorphic inversion requires major structural changes over much larger distances. Suggestions of a late episode of metamorphic heating of basaltic specimens may require further thought.

Some non-pyroxene phases were found as inclusions in pyroxenes and probably result from exsolution: oriented ilmenite and green spinel in orthopyroxene clasts from 14321 breccia (Gay *et al.*, 1972); oriented ilmenite lamellae in orthopyroxenes from Apollo KREEP-rich soils (Fuchs, 1971); platelets of chromite in pyroxene $En_{88}Fs_{11}Wo_1$ grains of 14258 soils (Haggerty, 1972a); chrome–spinel lamellae parallel to (001) and perpendicular to (001) in pigeonite from Luna 20 soil (Ghose *et al.*, 1973); oriented lamellae of ilmenite in a hedenbergite crystal from Luna 20 soil (Haggerty, 1973a). A cluster of iron needles in pyroxene from 12021 basalt was interpreted by Walter *et al.* (1971) as the result of late-stage introduction of Fe rather than from exsolution.

(d) Deformation. Disorientation and cracking of lunar pyroxenes were explained by several factors: differential thermal contraction of pigeonite and augite (Carter *et al.*, 1971), inversion from *C* to *P* lattice symmetry of pigeonite (Brown *et al.*, 1971), rapid growth (*e.g.* Carter *et al.*,1970), and shock deformation (*e.g.* Dence *et al.*, 1970; Engelhardt *et al.*, 1970). Careful study is needed to separate all these factors as emphasized by Carter *et al.* (1971). Although some lamellae in pyroxenes are reasonably ascribed to shock deformation, most arise from exsolution. Even the most casual study of breccias reveals that pyroxenes are much less affected by shock than plagioclases: indeed some soil fragments contain plagioclase which was converted completely to maskelynite glass whereas the pyroxene was merely fractured. Although the possibility should be considered that a plagioclase-rich magma might be produced by filter-pressing the liquid produced by shock deformation of plagioclase–pyroxene rocks, no evidence has been adduced.

Other silicates

The silica minerals cristobalite and tridymite occur as late crystals in mare basalts. Several papers in the *Proceedings* of the Apollo 11 and 12 conferences describe stacking faults and complex inversion twinning of cristobalite. Quartz is very rare in basalts, but is a characteristic mineral in granitic fragments where it is usually intergrown with a barian sanidine. Electron microprobe analyses report 0.0*n*–0.*n* weight percent of Al_2O_3, TiO_2, FeO, CaO, Na_2O, and K_2O in cristobalite and tridymite, but the accuracy is unknown because of problems from secondary fluorescence and small grain size. On Earth, cristobalite and tridymite have not been found in ancient rocks because of inversion to quartz. Persistence of cristobalite and tridymite on the Moon (and in meteorites) might be explained by absence of the catalytic effect of water, but other effects cannot be ruled out. Rare quartz grains in lunar soils may be relics from coarse-grained granites. Charles *et al.* (1971) suggested that quartz in granitic specimens implies crystallization at over 400 bars for a dry system, so long as the quartz crystallized from a melt and did not invert from tridymite or cristobalite. This pressure corresponds to a depth of over 10km.

Pyroxferroite, a pyroxenoid with a seven-repeat silicate chain, commonly crystallized instead of pyroxene from the late residua of mare basalts. Its composition range was not delineated precisely because of complex textural relations with Fe-rich pyroxene, but is probably $Mg_{0-0.15}Fe_{0.7-0.9}Ca_{0.1-0.25}SiO_3$. Table 2, No. 1, gives a representative analysis. Crystal-structure refinement showed cation disorder (Burnham, 1971), and the number of tetrahedra in the chain repeat was not controlled by the cation stoichiometry. Pyroxferroite crystallized metastably (Lindsley and Burnham, 1970).

Tranquillityite, $Fe_8(Zr,Y)_2Ti_3Si_3O_{24}$, also occurs in the late residua of mare basalts and is important for its high content of REE and U (Table 2, No. 2). The crystal structure is unknown, but hexagonal geometry was indicated in preliminary X-ray work (Lovering *et al.*, 1971). Tranquillityite broke down to baddeleyite, ilmenite, and pyroxene in 75055 basalt (El Goresy *et al.*, 1974).

Zircon promises to provide useful clues to the origin of soils and breccias. As pointed out by G. M. Brown, Zr is always high in KREEP-rich material, and indeed he tried to popularize the acronym KREPZ. The most abundant minor element is Hf which ranges from 0.*n* to about 3 weight percent in some dozen analyses (*e.g.* Table 2, Analysis 4). Terrestrial zircons carry similar amounts of Hf, which tends to increase from gabbroic to granitic rocks. Various other minor elements including Al, P, Ti, Fe, Mg, and Ca were reported, and the P-rich zircon from 14321 polymict breccia is noteworthy (Table 2, Analysis 3). Pink, colorless, and brown grains were found in lunar soils, and several types in breccias. A detailed study of zircon from all rock types is urgently needed to test whether it can be used to disentangle components of polymict breccias. Unlike terrestrial zircon, the lunar varieties are unzoned, and there is no evidence for more than one stage of growth.

Amphiboles are extremely rare in lunar samples in conformity with the absence or near-absence of hy-

TABLE 2. Some representative analyses of lunar minerals

	1	2	3	4	5	6	7	8	9	10	11	12	13	14	15	16	17
P_2O_5	-	-	0.60	-	-	-	-	-	-	-	-	-		-	-	41.2	39.8
SiO_2	46.0	14.0	32.7	32.6	54.5	42.1	39.9	36.1	0.25	-	0.1	0.2	0.24	0.18	0.61	1.33	1.22
TiO_2	0.4	19.5	-	-	0.16	0.1	4.0	0.1	27.5	71.2	71.3	62.1	42.3	1.82	85.3	-	-
ZrO_2	-	17.1	66.9	63.5	-	-	-	-	32.8	-	1.5	6.2	30.2	94.7	0.70	-	-
HfO_2	-	0.2	-	3.4	-	-	-	-	0.89	-	-	-	-	1.65	-	-	-
Al_2O_3	0.3	1.1	0.20	-	0.75	16.7	12.3	21.4	0.43	1.9	0.8	1.2	0.15	0.54	0.82	-	
Cr_2O_3		0.1	-	-	-	-	-	nf	0.24	1.3	1.7	10.3	0.29	0.13	2.65	-	
FeO	46.0	42.5	0.09	0.4	12.2	14.2	19.6	31.5	7.44	16.2	13.4	8.1	22.0	0.45	0.61	3.88	0.70
MnO	0.8	0.3	-	-	0.16	0.2	0.4	1.2	0.08	0.02	0.04	0.09	0.30	0.17	0.12	0.07	<0.01
MgO	0.7	0.0	0.02	-	16.3	9.9	8.2	0.4	0.03	8.8	9.2	2.8	4.33	0.14	0.03	1.95	0.10
CaO	6.0	1.3	0.15	-	2.13	12.0	11.6	8.7	3.55	-	0.4	3.2	0.32	0.16	0.52	42.2	51.3
Y_2O_3	-	2.8	-	nf	-	-	-	nf	10.5	-	-	-	-	-	-	1.95	0.57
Nb_2O_5	-	0.3	-	-	-	-	-	-	1.62	-	-	-	0.25	0.49	7.1	-	
Na_2O	-	-	-	-	8.69	1.3	2.7	nf	-	-	-	-	-	-	-	0.09	<0.01
K_2O	-	-	-	-	1.49	0.6	1.8	nf	-	-	-	-	-	-	-	-	
Total	100.2	99.2	100.6	99.9	97.1	97.7	100.5	99.4	99.7	99.4	98.8	95.0	100.3	100.5	98.8	98.3	99.1

1 Pyroxferroite, Table 4, Chao et al. (1970). 2 Tranquillityite, Table 2, Lovering et al. (1971), U 70ppm. 3 Zircon, micronorite clast in 14321 polymict breccia, Grieve et al. (1975). 4 Zircon, 12013 polymict KREEPy breccia, Haines et al. (1971), U ~ 100ppm. 5 Amphibole, 10058 basalt, Gay et al. (1970), F 1.2 ± 0.3. 6 Amphibole, grains from 12021 basalt, Dence et al. (1971), F 0.4 Cl 0.2. 7 Amphibole, breccia fragment in 14319 fines, Mason et al. (1972). 8 Garnet, loose grains from 12021 basalt, Traill et al. (1970). 9 Zirkelite, basalt 15538, Wark et al. (1973), La_2O_3 0.29 Ce_2O_3 1.63 Pr_2O_3 0.43 Nd_2O_3 2.13 Sm_2O_3 1.08 EuO 0.09 Gd_2O_3 1.45 Tb_2O_3 0.42 Dy_2O_3 2.09 Ho_2O_3 0.38 Er_2O_3 1.48 Tm_2O_3 0.11 Yb_2O_3 1.24 Lu_2O_3 0.44 UO_2 0.14. 10 Armalcolite, basalt 10022, Table 2, Anderson et al. (1970). 11 "Zr-armalcolite", breccia 78442, Steele (1974). 12 "Cr-Zr-armalcolite", breccia 78442, Steele (1974). 13 "Cr-Zr-armalcolite", breccia 78442, Steele (1974). 13 Z1, 15102 soil fragment, Haggerty (1972c). 14 Baddeleyite, Luna 20 grain, Brett et al. (1973), V_2O_3 0.06. 15 Rutile, inclusions in ilmenite of KREEPy 14162 microbreccia, Hlava et al. (1972), V_2O_3 0.22. 16 Whitlockite, 14310 basalt, Griffin et al. (1972), F <0.1 Cl 0.01 La_2O_3 0.74 Ce_2O_3 2.15 Pr_2O_3 0.35 Nd_2O_3 1.11 Sm_2O_3 0.30 Gd_2O_3 0.51 Dy_2O_3 0.50. 17 Apatite, 14310 basalt, Griffin et al. (1972), F 3.35 Cl 0.29 La_2O_3 0.31 Ce_2O_3 0.51 Pr_2O_3 0.09 Nd_2O_3 0.52 Sm_2O_3 0.14 Gd_2O_3 0.09 Dy_2O_3 0.11.

drous fluids which have such strong effects on Earth. Gay *et al.* (1970) chipped a small grain from a vug in mare basalt 10058 and reported the electron microprobe analysis No. 5 of Table 2. This magnesioarfvedsonite composition is surprisingly high in Na and low in Ca with respect to other lunar minerals. An ion microprobe analysis for H and an electron microprobe analysis for Cl would be interesting. Charles *et al.* (1971) synthesized the hydrous equivalent, and discussed the stability relations for lunar amphibole. Dence *et al.* (1971) reported aluminotschermakite grains from a bag containing 12021 mare basalt, and suggested that the amphibole together with garnet (see later) crystallized metastably. The electron microprobe analysis (Table 2, No. 6) shows low but significant alkalies, low F and Cl, and near-equal CaO, MgO, and FeO. Mason *et al.* (1972) observed loose grains in 14163 fines with chemical and optical properties indicative of Fe-rich richterite (Table 2, No. 7) and argued against it being a terrestrial contaminant. It is surprising that further amphiboles have not turned up in the extensive scanning-electron micrographs of vugs and in mineralogical studies of lunar fines. Further work is needed. Amphiboles from enstatite chondrites are richterites with a general similarity to the lunar magnesioarfvedsonite, except for their very low FeO and very high MgO (Olsen *et al.*, 1973b). A fascinating speculation is whether amphibole occurred in an early hydrous Moon which ultimately lost its water, or whether amphibole was always very sparse in a Moon which was always dry.

Existing reports of mica and layer silicates in lunar samples are too sketchy to have any genetic significance. The possibility of meteoritic input into lunar fines must be borne in mind.

Loose grains of almandine-rich garnet (Table 2, No. 8) from mare basalt 12021 were interpreted as rare constituents of late differentiates (Traill *et al.*, 1970). Of more general interest is the speculation that a garnet precursor was involved in the generation of ol–opz–plag cataclasite 15445 (Ridley *et al.*, 1973). For all models of the Moon which involve compositions dominated by olivine, pyroxene, and plagioclase, garnet must be considered as a possible constituent at depth (see earlier). As the outer part of a hot Moon cooled to the present estimated selenotherm, the boundary for garnet stability could have moved up by 50 to 100 km. Many interesting speculations can be made on possible changes of lunar density and radius with implications for surface morphology (*e.g.* lineaments) and heat content. If the

lunar interior is dominated by olivine, these effects could be rather small, but if plagioclase coexisted with olivine at substantial depth, the reaction of ol + an → gt + px could be important. The possible role of the basalt–eclogite transition was discussed extensively, *e.g.* by Ringwood and Essene (1970) and Anderson (1975).

The speculation that the Moon was derived from a high-temperature condensate of the solar nebula was forcefully advocated by D. L. Anderson (*e.g.* 1975), but runs into severe problems from phase-equilibrium constraints. Melilite is one of the minerals typical of high-temperature condensates, as exemplified by åkermanite-rich ones from the Allende meteorite (*e.g.* Grossman, 1975). Eleven uniaxial grains, five and six respectively with optical properties similar to those of åkermanite and gehlenite, were reported by Masson *et al.* (1972) in Apollo 14 fines, but no melilites have been reported in lunar rocks. Further study is needed to verify whether these grains are indeed melilite, and whether they have compositions like those of the Allende melilites. Whether melilite occurs in the lunar interior is purely speculative. Relevant phase relations were given by Yoder (1973). Of course, the chance of hypothetical melilite from the deep interior of the Moon being found in surface rocks is very small. However, a detailed study of lunar fines is desirable to identify the crystals reported by Masson *et al.*

Spinels

(a) General chemistry. There are no direct chemical analyses for Fe^{2+} and Fe^{3+} in lunar spinels, but electron microprobe analyses can be calculated to AB_2O_4 compositions without invoking substantial Fe^{3+}. This is consistent with the generally reduced state of lunar rocks, and indeed Haggerty (1972a) suggested that some Cr is divalent in lunar spinels though firm evidence is lacking. The major elements are Mg, Al, Ti, Cr^{3+}, and Fe^{2+}. Manganese increases from 0.0*n* to 0.*n* weight percent as Fe increases. Vanadium (expressed as V_2O_3) has a similar range but there are insufficient data upon which to base correlations. Calcium and silicon were reported at the 0.0*n* to 0.*n* weight percent level (*e.g.* Nehru *et al.*, 1974), and presumably enter the crystal structure, though analytical error must be considered for small spinel crystals. Most published analyses of lunar spinels omit one or more minor elements, and a systematic study is badly needed. There is no valid evidence for deviation of any lunar spinel from the AB_2O_4 composition.

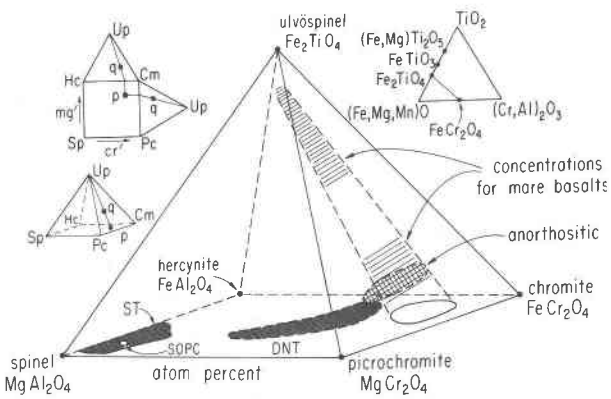

FIG. 14. Graphical representations of lunar spinels and composition ranges for spinels from several lunar rock types. ST spinel troctolitic, SOPC spinel–olivine–plagioclase cataclasite, DNT dunitic, noritic, and troctolitic. See Figs. 12, 16, and 17 for details.

The following scheme for calculating end members is based on that of Busche *et al.* (1972) and is unambiguous: (a) calculate the number of metal atoms for 4 oxygens; (b) add Si to Ti, V to Cr, and Ca + Mn to Fe giving TI, CR, and FE; (c) use up the TI as Fe_2TIO_4 (all lunar spinels contain enough FE); (d) calculate $FECR_2O_4$ and assign either excess CR to $MgCR_2O_4$ or excess FE to $FEAl_2O_4$; (e) calculate remaining Mg as $MgAl_2O_4$; (f) note whether residual Mg or Al occurs; (g) recalculate end members to 100 percent.

Both Busche *et al.* (1972) and Haggerty (1971a) plotted analyses on a Johnston type of trigonal prism with rectangular base between spinel (sensu stricto) $MgAl_2O_4$ (Sp), picrochromite $MgCr_2O_4$ (Pc), chromite $FeCr_2O_4$ (Cm), and hercynite $FeAl_2O_4$ (Hc), and a roof-line between Fe_2TiO_2 (Up) and Mg_2TiO_4. Unfortunately this geometry is unnecessarily complex because the Mg_2TiO_4 end-member is not needed in lunar spinels (except for skeletal crystals in a shocked basaltic glass, Sclar *et al.*, 1973), but is implied by the method of plotting. The simplest geometry is a tetragonal pyramid with Fe_2TiO_4 at the apex (Fig. 15). To plot an analysis (a) calculate the metals to a total of 4 oxygens; (b) calculate Up from Ti(+Si); (c) add Mn and Ca to Fe and subtract 2 (Ti + Si) to give Fe′, then calculate $mg' = Mg/(Mg + Fe')$; (d) add V to Cr to give Cr′, then calculate $cr' = Cr'/(Al + Cr')$; (e) plot point *p* in either of the two diagrams at the upper left of Figure 14 using *mg′* and *cr′*; (f) plot point *q* between *p* and the end member Up using the Up component. Because data points on a perspective drawing of the tetragonal-pyramid (middle left diagram) are not located unambiguously

unless the line *pq*Up is drawn, the triple projection (upper left diagram) is usually best for detailed study. When Ti is low, Figure 12 shows an easy approximation. Calculate *mg* = atomic Mg/(Mg + Fe) and *cr* = atomic Cr/(Cr + Al), and plot on a rectangle rather than a square in order to fit lantern slides better. Then plot TiO_2 on adjacent rectangles as weight percent. For specimens rich in $FeCr_2O_4$, 1 weight percent TiO_2 corresponds to about 3 mole percent Up. For spinels from mare basalts, a simple approximation is the line between (Fe, Mg, Mn) (Cr, Al, V)$_2O_4$ and (Fe, Mg, Mn)$_2$(Ti, Si)O_4 in the upper right diagram of Figure 14. The positions of lunar ilmenite (Fe, Mg) TiO_3 and armalcolite (Fe, Mg) Ti_2O_5 are also shown.

The large diagram in Figure 14 summarizes the principal composition trends of lunar spinels. Those from non-mare rocks lie in two clusters, one near spinel (*s.s.*) and one trending towards chromite. As Fe and Cr increase, so does the ulvöspinel component. Spinels from mare basalts tend to lie in a tube between magnesian-aluminian chromite and ulvöspinel with relatively low population in between.

Crystal-structure refinements of chromite, ulvöspinel, and a pink Mg, Al-rich spinel showed that Cr^{3+} and Ti^{4+} enter the octahedral *B* site, that Mg^{2+} enters the tetrahedral *A* site, and that Fe^{2+} enters both sites with a strong preference for the *A* site (Takeda *et al.*, 1974). There are no X-ray data indicating lower than isometric symmetry for spinels, but several authors (*e.g.* Haggerty, 1972a) reported anisotropic optical reflectivity for Ti-rich spinels.

(b) Spinels from non-mare rocks. Figure 12 coordinates the data which have already been discussed in relation to petrologic differentiation of non-mare rocks. The analyses tend to lie in a band from Mg, Al-rich spinels to Fe, Cr-rich ones with higher concentrations at the two ends. Titanium tends to increase with increasing Fe and Cr content but there is a wide scatter which should be much greater than experimental error. Detailed data for an anorthosite and an anorthositic norite from Apollo 15 are shown in Figure 16.

Ranges for various types of meteoritic and terrestrial spinels are shown for comparison.. Chromites from equilibrated chondrites (EC) and unequilibrated ones (UC) are richer in $FeCr_2O_4$ than any lunar spinel, thereby providing a possible criterion for characterizing such types of meteoritic spinels in lunar regolith; however metamorphism might change the composition in breccias or grains broken out of breccias. Spinels from achondrites have lower $FeCr_2O_4$, and their range partly overlaps that of spinels from lunar anorthosites and mare basalts: other aspects of the mineralogy of achondrites, of course, resemble those of lunar minerals. Some compositional overlap occurs with lunar spinels and Cr-rich spinels from other meteorites whose compositions were reviewed by Bunch and Olsen (1975). The Allende and Murchison meteorites carry spinels which are mostly very rich in Mg and Al, but a few have substantial Fe and Cr (*e.g.* Fuchs *et al.*, 1973; Grossman, 1975): further study may extend the composition range.

Terrestrial spinels carry substantial Fe^{3+} and tend to zone to magnetite rather than ulvöspinel. Specimens with low Fe and Ti are summarized in Figure 12, and most have only a few weight percent of Fe_2O_3 and TiO_2. Spinels from deep-seated rocks, terrestrial peridotite xenoliths in kimberlite (TPXK) and terrestrial xenoliths in alkali basalt (TXAB), lie in bands at lower *mg* than for lunar spinels except for Al-rich compositions where overlap occurs. Podiform deposits in alpine complexes give spinels (TPAC) which range to lower *mg* values at higher Cr-content. Spinels from terrestrial igneous complexes of basaltic composition cover a very wide range, and the factors which govern their composition are not fully understood. Probably the oxygen fugacity, water content, and extent of later metamorphism have important effects. Spinels from layered complexes produced under reducing conditions from tholeiitic basalt or ultramafic composition tend to have *cr* ~0.6–0.8 and *mg* ~0.2–0.7 (*e.g.* Irvine, 1974), while those from metamorphosed Archean complexes tend to have spinels with lower *cr*. The closest fit to low-Ti spinels

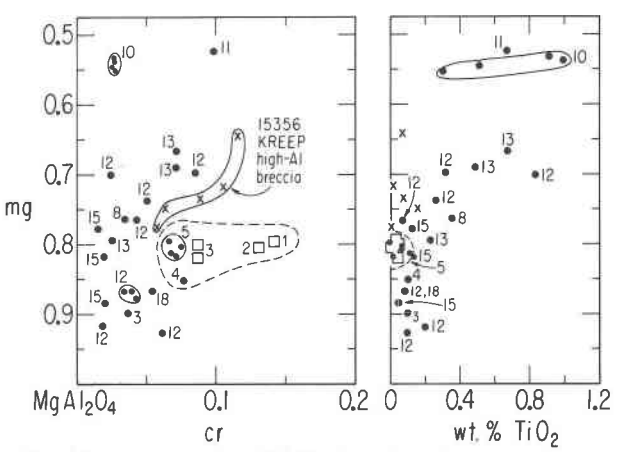

FIG. 15. *mg* vs. *cr* and wt.% TiO_2 for spinels from spinel troctolitic samples (dots) and from spinel–anorthite–orthopyroxene–olivine cataclasites (squares). The numbers are keyed to the legend of Fig. 6.

from lunar dunitic, noritic, and troctolitic rocks is with spinels from the Rhum layered complex whose dominant rock is allivalite (*i.e.* mostly bytownite and olivine): however, facile comparison is to be eschewed especially in view of the textural and compositional complexities reported by Henderson (1975) and Cameron (1975): several other papers in Volume 39, Number 6/7, *Geochim. Cosmochim. Acta* are pertinent.

With this background one can hazard a model for the origin of the lunar spinels. Those from anorthositic rocks are remarkably high in $FeCr_2O_4$ and lie at the opposite end from the spinels from spinel troctolites and the spinel–olivine–plagioclase cataclasites, while those from dunitic, noritic, and troctolitic rocks lie in between. A possible explanation is that during primary differentiation of the Moon, the early liquids were low in Fe, Cr, and Ti. Prolonged precipitation of low-Cr, Mg-rich olivine joined later by plagioclase resulted in ultimate build-up of liquids relatively rich in Fe, Cr, and Ti. The oxidation state would be high enough to prevent formation of substantial Cr^{2+}. The sp–ol–pl cataclasites represent the early mineralogy, while the anorthosites represent cumulates crystallizing from the later liquids. Spinel troctolites with Mg,Al-rich spinels might result from remelting of early cumulates, while the noritic, dunitic, and troctolitic spinels would represent intermediate stages. Mare basalts would result from remelting of late cumulates rich in ilmenite and Fe,Ti-rich spinel, and would precipitate the chromite–ulvöspinel series upon reaching the lunar surface (see later). This proposed explanation is simpler than that for terrestrial spinels because of the absence of complications from change of oxidation state in response to change of water pressure, and because of a simpler mineralogy for the lunar compared to the terrestrial interior (but see earlier for comments on garnet).

The composition of spinels may provide a clue to the origin of spinel troctolites. Although the available data are scattered and probably of variable accuracy, Figure 15 shows interesting trends. On the *mg,cr* plot, the spinels from sp–ol–px cataclasites have relatively high *cr*. Specimen 5, a fragment of anorthite, olivine, and spinel from Luna 20, and Specimen 4, an olivine–spinel–plagioclase clast from an Apollo 16 breccia have mineral compositions similar to those from the cataclasites, and differ only in the absence of pyroxene. On the *mg*,TiO_2 plot of Figure 15, the spinels from all these materials have low TiO_2. The other spinels tend to lie in broad bands in which *cr* and TiO_2 increase as *mg* decreases. Specimens 10 and 11 from breccia clasts have unusually low *mg* for low-*cr* spinels. Detailed investigation should be made of minor and major elements of spinels from all specimens listed under spinel troctolitic in the legend to Figure 6.

Mg,Al-rich spinel crystallizes from the liquid in the system SiO_2–anorthite–olivine (Fig. 1), but should react completely with the liquid *at equilibrium* to produce anorthite + forsterite at lower temperature (Fig. 2) *unless* cumulation of spinel moves the bulk composition out of the system. Walker *et al.* (1973b) and Hodges and Kushiro (1973) interpreted rock 62295 as the rapidly quenched partial melt from a parental olivine–spinel–anorthite rock, in which melt some phenocrysts or xenocrysts of spinel, olivine, and plagioclase were carried. Metamorphism of this and similar spinel troctolites should result in partial or complete elimination of the Mg,Al-spinel. Because spinel is much denser than silicates, it should sink rapidly in lunar liquids thereby causing depletion of Al_2O_3 and MgO.

Mg,Al-rich spinels from Apollo 14 and other polymict breccias commonly show reaction rims against the matrix; these rims are richer in Ti, Cr, and Mn than the parent spinel (Roedder and Weiblen, 1972a).

(c) Spinels from mare rocks. Numerous composition plots exist for spinels from mare rocks (*e.g.* Haggerty, 1972b, 1973a, Nehru *et al.*, 1974), but the situation is confusing because of incomplete correlation between the zoning trends of the spinel and co-crystallizing silicates. In general, early spinels are Mg,Al–chromites which are euhedral and enclosed in olivine when that mineral is present. Late spinel has ulvöspinel composition and occurs either in the groundmass as separate crystals or more commonly as rims on earlier spinels. The intermediate history varies from one rock to another and from one place to another in the same rock. The morphology of the zoning depends on whether crystallization is progressive or whether resorption or reaction occurs. The composition depends on competition with other minerals.

In broad outline, the composition range is shown in Figure 14, but the details can be very complex as shown by several plots in Figure 16. Basalt 12051 contains spinel which apparently zones continuously from Mg,Al–chromite to ulvöspinel with a snake-like trend which should be checked against zoning in the pyroxene.

Many mare basalts contain spinels which zone discontinuously (*e.g.* those from Apollo 15 basalts). Nehru *et al.* (1974) discussed the existing ideas for the

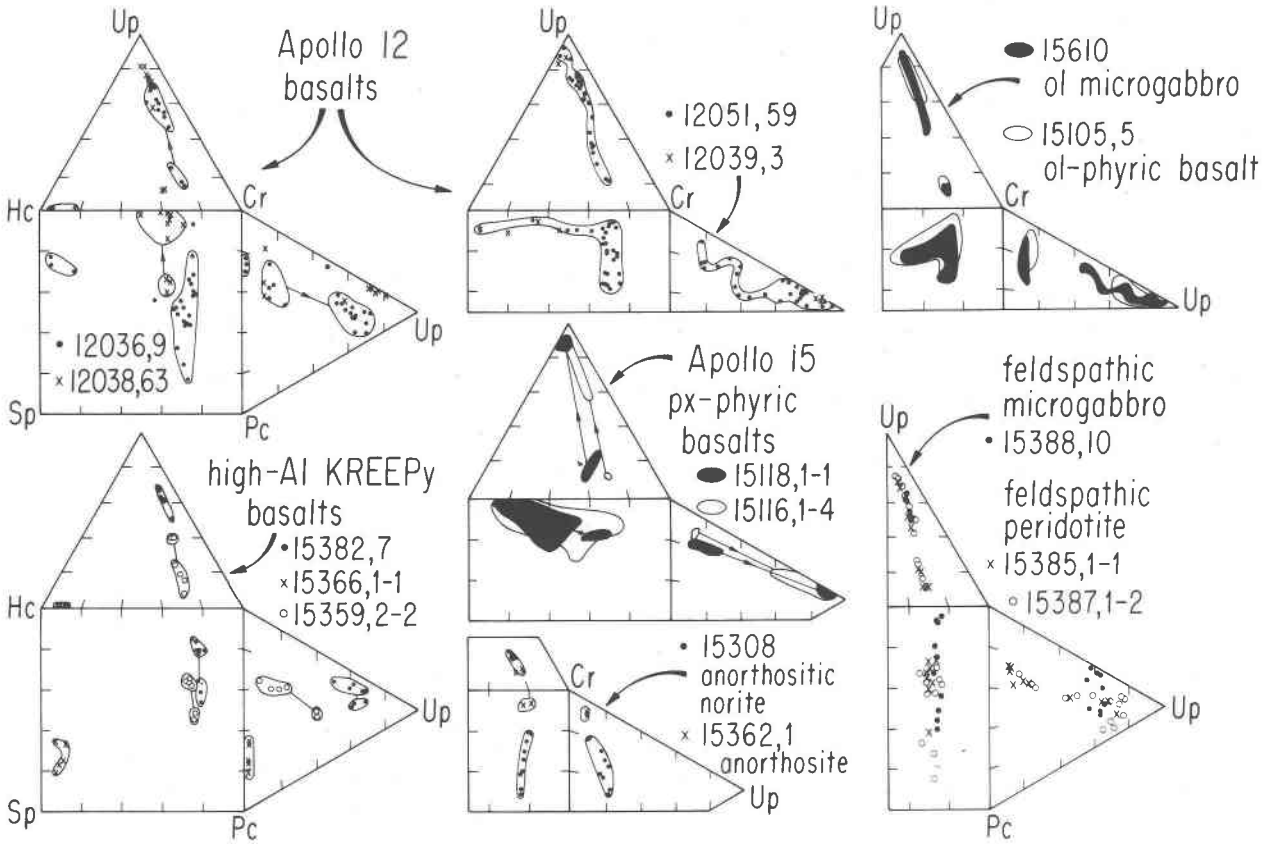

FIG. 16. Composition ranges of spinels in selected lunar rocks. Apollo 12 and Apollo 15 data were calculated from atomic fractions given in Busche *et al.* (1971) and Nehru *et al.* (1973) using the procedure described in the text.

discontinuity and favored early crystallization of chromite followed by cessation of spinel growth, while pyroxene continued to crystallize followed by resumption of spinel growth producing an ulvöspinel rim. Laboratory syntheses show that the solvus in the Fe_2TiO_4–$FeCr_2O_4$–$FeAl_2O_4$ system (Muan *et al.*, 1972) crests below 1000°C for compositions with $cr > 0.6$, thereby ruling out exsolution as a possible explanation for spinels growing above 1100°C from lunar basaltic melts. Nehru *et al.* (1974) correlated the presence or absence of a composition gap with texture and composition of Apollo 15 rake samples, and for pyroxene-phyric basalts suggested that the gap is smaller for rocks which cooled more slowly. Dalton and Hollister (1974) found that in 15555 basalt the $M^{2+}CrSiAlO_6$ content of pyroxene decreased and the $M^{2+}Al^2SiO_6$ content increased when Cr-rich spinel crystallized, and that $M^{2+}TiAl_2O_6$ content increased sharply when ulvöspinel crystallized. El Goresy *et al.* (1975) used spinel zoning as an indicator of the crystallization relations with olivine, pyroxene, and plagioclase in Apollo 12 and 15 mare basalts.

Figure 16 shows details for several unusual rocks. Basalt 12036,9 (upper left) contains three types of spinel, one of which is unusually rich in hercynite (Busche *et al.*, 1972): the unusual spinels occur as 3 grains in early Al-rich pyroxene melt inclusions. Two of the high-Al, KREEPy basalts from Apollo 15 have spinels falling in the general range from chromite-rich to ulvöspinel-rich compositions, but the third one has Mg,Al-rich spinels like those from spinel troctolites.

(d) Miscellaneous. Ulvöspinel in mare basalts is often reduced to ilmenite + iron (*e.g.* Haggerty, 1971b) and very rarely to rutile + iron (El Goresy *et al.*, 1972). Ti-rich spinels frequently were reduced to Ti-poor spinel + ilmenite + iron, and Haggerty (1972a) suggested a reduction indicator TAC = $TiO_2/(TiO_2 + Al_2O_3 + Cr_2O_3)$. Experimental studies by Taylor *et al.* (1972) showed that the former reaction can proceed under slightly less reducing conditions than the latter. The stability curves range from log oxygen fugacity ~ -16 at 1000°C to ~ -18 at 850°C. McCallister and Taylor (1973) concluded from laboratory studies that the reduction of ulvöspinel to iron and ilmenite usually involves nucleation

and growth, and that ilmenite lamellae develop in ulvöspinel only under conditions slightly more reducing than for equilibrium of all three phases.

The partition of Zr between ilmenite and ulvöspinel in the presence of iron and ZrO_2 depends on temperature, and favors ilmenite 3-fold near 1100°C and 1.5-fold near 850°C (Taylor and McCallister, 1972). The highest reported concentrations for lunar basalts are 0.4 weight percent Zr in ilmenite and 0.2 weight percent in ulvöspinel. Observed ratios for Apollo 15 rocks indicate that some contain ilmenite and ulvöspinel which equilibrated down to ~ 850°C whereas others were quenched from near-liquidus temperatures.

El Goresy *et al.* (1972) suggested that the partition of Mg between ilmenite and ulvöspinel approaches equilibrium more closely during subsolidus reduction than during initial crystallization, and interpreted chemical analyses in terms of phase equilibrium data of Johnson *et al.* (1971).

Spinel lamellae occur in ilmenite (see later). Gay *et al.* (1972) reported trails of beads about 1μm across in olivine from Apollo 14 breccia, and Roedder and Weiblen (1971) reported rosettes up to 10μm across in olivine in 12018 basalt. Both types of inclusion may be spinel, but definitive identification awaits electron-optical study.

The occurrence of magnetite in lunar specimens is highly controversial. Trace element data for bulk lunar soils indicate incorporation of ~1 percent carbonaceous chondrite which should bring in some magnetite: indeed Wood *et al.* (1971) found magnetite spherules in a fragment of carbonaceous chondrite in 12037 fines. However, Jedwab and Herbosch (1970) did not find any crystals in Apollo 11 soils with the peculiar morphology of magnetite from Type 1 carbonaceous meteorites. Numerous studies by magnetic, Mössbauer, and electron spin resonance techniques reported in Volume 3 of the *Proceedings* of both the Fourth and Fifth conferences are subject to various interpretations. Magnetite may have been incorporated into lunar soils but destroyed by reduction involving solar protons or lunar-derived reducing materials.

Ilmenite

Ilmenite can be found in essentially all types of lunar specimens ranging from scattered grains in anorthosite and ultrabasic materials to about 20 percent of ilmenite-rich mare basalts. Particularly important are its relations to armalcolite, rutile, and Ti-rich spinel, while the partition of elements between ilmenite and silicate may provide useful indicators of physical conditions when laboratory calibrations have been made.

The crystal structures of lunar and terresterial ilmenites are essentially the same in being based on highly ordered Fe^{2+} and Ti^{4+} (Raymond and Wenk, 1971). Whereas terrestrial ilmenites commonly contain Fe_2O_3 in solid solution, lunar ilmenites show no definitive evidence for such substitution, and indeed there is evidence for minor substitution of Ti_2O_3. Pavićevic *et al.* (1972) interpreted the *L* X-ray spectra of ilmenites from 10047 and 12063 basalts in terms of Fe^{2+} and Ti^{4+}, but small intensity differences with spectral lines for ilmenite from 14053 basalt were interpreted in terms of Ti^{3+} substitution. Bayer *et al.* (1972) interpreted electron microprobe, X-ray and Mössbauer data of terrestrial and lunar ilmenites, and concluded that Fe^{3+} was present in the former and Ti^{3+} in the latter. These and other data on the occurrence of Ti^{3+} in lunar ilmenites should be augmented by systematic study to check for possible correlation with paragenesis and oxidation state. Electron microprobe analyses of ilmenites from nonchondritic meteorites showed no excess or deficiency of Ti (Bunch and Keil, 1971). Most lunar ilmenites appear to be stable towards reduction, but Mao *et al.* (1974) reported breakdown to ferropseudobrookite and iron, and to rutile and iron in Apollo 17 soils. These reactions indicate very reducing conditions (*e.g.* log oxygen fugacity below −16 if the temperature were 1000°C), perhaps resulting from incoming solar protons.

The main compositional substitution is Mg for Fe^{2+}. In ilmenites from mare basalt, MgO ranges from about 2 to 0.2 weight percent, the amount apparently decreasing from early arborescent crystals to tiny ones in the late residuum (*e.g.* Cameron, 1970; Smith *et al.*, 1970). Ilmenite rims on armalcolite contain up to 5 weight percent MgO, and the presence of oriented rutile lamellae indicates decomposition of armalcolite. Steele (1974) found that the ilmenites from metamorphosed Apollo 17 breccias were consistently higher in MgO (4.6–7.6, average 6.5 wt. %) than those from ilmenite basalts (0.8–3.5, average 1.8); this confirms the interpretation of Brett *et al.* (1973) for Luna 20 specimens. The former ilmenites were chemically homogeneous and had apparently equilibrated with the silicates during metamorphic recrystallization. Ilmenites from unmetamorphosed breccias showed considerable compositional scatter, and presumably have diverse origins. Nehru *et al.*

(1974) plotted histograms of MgO for ilmenites from Apollo 15 rake samples. The wide scatter of data for most rocks indicates disequilibrium but nevertheless MgO of the ilmenite tends to increase with bulk *mg* of the host rock. Ilmenite from brecciated peridotite fragments in 73263 soil (Table 1, analysis 25) contains 11.6 weight percent MgO. Under equilibrium, the principal factor which determines the partition of Mg between ilmenite and coexisting silicates (*e.g.* pyroxene and olivine) is temperature. Anderson *et al.* (1972) proposed a thermometer for the distribution of Mg/Fe between ilmenite and pyroxene, and gave a tentative calibration based on thermochemical calculation and some observations on natural minerals. F. C. Bishop (personal communication) confirmed the general relations from laboratory syntheses, but found considerable shifts in the proposed relations. The Mg/Fe ratio of the ilmenite increases with bulk Mg/Fe ratio of the rock and with increasing temperature as Mg is transferred from the silicate to the ilmenite. The lunar data can be explained satisfactorily by the new calibrations, and values for equilibration temperatures in metamorphic lunar rocks will ensue. Interpretation of ilmenite from mare basalts will require careful examination of textures to coordinate the crystallization times of the ilmenite and silicates.

The reported ranges of minor elements in ilmenite are MnO ~ 0.2–0.6 weight percent, Cr_2O_3 ~ 0–1.0, CaO ~ 0–0.4, Al_2O_3 ~ 0–2.8, ZrO_2 ~ 0–0.4, but some values may be too high because of fluorescence or overlap onto other minerals during electron microprobe analysis. The high values of Al_2O_3 especially should be investigated in view of the errors found in analyses of olivine. No reliable patterns emerge from correlation of the minor element concentration with rock type, but systematic study may well prove fruitful when erratic errors are eliminated.

The partitioning of Zr between ilmenite and ulvöspinel was mentioned earlier, and interpretation of observations for several well-known basalts (*e.g.* 12052 and 14310) indicated cooling rates near the solidus in the region of 100°C per day. Arrhenius *et al.* (1971) noted that lunar ilmenites contain 6 to 8 times more Zr than terrestrial ones, but the several proposed explanations remain untested by laboratory syntheses. El Goresy *et al.* (1974) found that Cr_2O_3 was higher (0.93–1.05 wt. %) in secondary ilmenite rims around armalcolite than in primary ilmenite (0.39–0.65) of ilmenite basalt 74243. The CaO content of ilmenite may correlate positively with that of the bulk rock, but careful measurements are needed to test this. Because of overlap between the TiK_β and V K_α lines, V is difficult to detect in Ti-rich minerals, but reported values range up to 0.4 weight percent.

Shock deformation of ilmenite produces multiple twinning, which can be seen in ilmenite from many lunar breccias. X-ray study of natural and experimentally deformed ilmenite by Minkin and Chao (1971) showed that distortion is greatest in reciprocal lattice directions perpendicular to *a*. Sclar (1971) produced sigmoidal bending and microfaulting in experimentally-shocked ilmenites; these features are common in ilmenite from lunar breccias. Sclar *et al.* (1973) obtained further evidence on the twinning produced by shock deformation of terrestrial ilmenite, and found that optically visible twins were produced at 35–75 kbar peak pressure, and that initial twinning on {0001} was followed by twinning on $\{10\bar{1}1\}$. This peak pressure is much lower than for production of twinning in pyroxenes and feldspars. Sclar *et al.* also obtained evidence of shock-induced reduction and cation disordering.

Ilmenite frequently occurs with oriented rutile, and textural studies suggest that most intergrowths result from breakdown of armalcolite upon falling temperature (see next section) rather than reduction. However, Sclar *et al.* (1973) attributed some occurrences to shock reduction. Exsolution of spinel from ilmenite was reported by several investigators *e.g.* Dence *et al.* (1971). Haggerty (1973a) noted ilmenite exsolution in pleonaste spinel. Fuchs (1971) and Gay *et al.* (1972) interpreted oriented ilmenite plates in orthopyroxene as exsolution products. Ilmenite inclusions in plagioclase from anorthosites were ascribed to exsolution of Ti from plagioclase by Smith and Steele (1974).

Ilmenite of euhedral shape occurs in vugs (*e.g.* in Apollo 14 breccias: McKay *et al.* 1972). Scanning electron microscopy of specimens from 10072 basalt showed growth steps and globular over-growths of silicate and sulfide (Jedwab, 1971). These observations, and those on other mineral types testify to the presence of a widespread vapor phase in the outer part of the Moon.

Armalcolite, zirkelite and possible related phases

The identification of some fine-grained Ti- and Zr-rich minerals in the lunar rocks is uncertain because of lack of diffraction data. Peckett *et al.* (1972) made considerable progress by plotting compositions on a ZrO_2–FeO–TiO_2 ternary diagram, and Brown *et al.* (1975) extended the data to eight contrasted compositions. There is no problem with ilmenite

$(Fe,Mg)TiO_3$ described in the preceding section. The minerals zircon ($ZrSiO_4$; HfO_2 0–3 wt. %), baddeleyite (ZrO_2; FeO 0–7, TiO_2 2–3, HfO_2 1–3, Y_2O_3 0.2), rutile (TiO_2, Nb_2O_5 0.*n*–7, Fe_2O_3 0–8, Cr_2O_3 0–3, ZrO_2 0–2) and tranquillityite $Fe_8^{2+}(Zr + Y)_2Ti_3Si_3O_{24}$ are well established (see next section) by electron microprobe and optical methods though systematic study with diffraction techniques is needed. Zirkelite and zirconolite are two names assigned to a mineral which occurs in the late residuum of mare basalts and in the groundmass of KREEP-rich breccias. The terrestrial equivalents have not been fully established, and there may be only one actual mineral for which the name zirkelite may have priority. Chemical analyses of the lunar mineral show ZrO_2 30–45, TiO_2 25–35, CaO 3–11, FeO 4–11, and Y_2O_3 3–11 weight percent with substantial amounts of REE, Th, and U (*e.g.* Table 2, Analysis 9). Wark *et al.* (1973) gave the general formula $A^{2+}B_2^{4+}O_7$ based on data for natural and synthetic specimens. X-ray study showed monoclinic symmetry. The above Zr-rich minerals occur late in the differentiation when Zr and other "incompatible" elements have been concentrated by prior crystallization of silicates. For details, see Frondel (1975).

The name armalcolite was used for several kinds of lunar minerals with about 70 percent TiO_2 (Haggerty, 1973b). The kind occurring as a primary phase in Ti-rich mare basalts from Apollo 11 and 17 definitely has the pseudobrookite type of structure and contains little Zr. Because of the reduced state, it contains no significant Fe^{3+}, and its composition $(Fe,Mg)Ti_2O_5$ is obtained from the terrestrial equivalent $Fe_2^{3+}TiO_5$ by substituting Ti + (Fe,Mg) for $2Fe^{3+}$. This armalcolite exists as two textural variants (a) in both Apollo 11 and 17 ilmenite basalts as blue-grey discrete grains with or without a mantle of Mg-rich ilmenite; (b) only in Apollo 17 medium- to coarse-grained ilmenite basalts as tan-colored discrete grains, either in mutual and sealed but cuspate grain-boundary contact with ilmenite or in cores mantled by ilmenite. Type (b) is frequently twinned. Haggerty (1973d) invented the terms "ortho" and "para" which were not accepted by other workers because (a) single-crystal X-ray data were indistinguishable (Smyth, 1974b), and (b) the ranges of chemical composition overlap (Papike *et al.*, 1974; Taylor and Williams, 1974). However, the grey variety apparently tends to have higher MgO and Cr_2O_3 and lower FeO than the tan variety (Taylor and Williams, 1974; El Goresy *et al.*, 1974). The terms grey and tan low-Zr armalcolite appear suitable.

El Goresy *et al.* (1974) noted a correlation between the type of armalcolite and the bulk composition and crystallization path of the host basalt. Perhaps the morphology depends on the nucleation conditions. Armalcolite shows Mg/Fe zoning which may be correlatable with the composition of the host liquid and the crystallization temperature. Taylor and Williams (1974) correlated the Co/Ni ratio of coexisting iron with the presence of armalcolite, and suggested that armalcolite occurs only in rocks depleted in Ni.

The low-Zr armalcolites (*e.g.* Table 2, Analysis 10) range from about $Mg_{0.62}Fe_{0.38}Ti_2O_5$ to $Mg_{0.35}Fe_{0.65}Ti_2O_5$, and carry minor Cr_2O_3 (1–2 wt. %) and Al_2O_3(1–3 wt. %). Traces occur of MnO, V_2O_3, CaO, and ZrO_2, probably always <0.2 weight percent. The trivalent elements Cr and Al should substitute as $M_2^{3+}TiO_5$, thereby reducing the atomic fraction of Ti. High contents of Ti in electron microprobe analyses suggest substitution of Ti^{3+} as the $Ti_2^{3+}Ti^{4+}O_5$ component (Lindsley *et al.*, 1974a) as a consequence of the highly reduced state of mare basalts, perhaps to the extent of 5 to 10 mole percent. The alternative of structural vacancies is inconsistent with crystal structure analyses of lunar and synthetic armalcolites (Wechsler *et al.*, (1975). Preliminary analyses suggest considerable disorder of Fe, Ti, and Mg between the two cation sites, but similarities in ionic radii and X-ray scattering factors caused severe problems in estimation of site population. Terrestrial armalcolites from kimberlites may contain some ferric iron (Cameron and Cameron, 1973; Haggerty, 1973c, 1975) in response to a more oxidizing environment.

The stability relations of low-Zr armalcolite were included in the study by Lindsley *et al.* (1974a) of the join ferropseudobrookite $FeTi_2O_5$–karrooite $MgTi_2O_5$. Armalcolite is stable at higher temperature, whereas ilmenite solid solution and rutile are stable at lower temperature. Armalcolite begins to break down at 1130°C for *mg* 1.0 and 1000°C for *mg* 0.5, and breakdown is complete at 800°C for *mg* 0.5. Lipin and Muan (1974), Lindsley *et al.* (1974a), and Kesson and Lindsley (1975) showed that M^{3+} ions (Al, Cr and Ti) stabilize armalcolite to lower temperatures at low pressure (approx. by 100°C for lunar armalcolites). Pressure raises the stability limit for armalcolite with an increase of 300°C for pure $MgTi_2O_5$ at 7.5kbar and about 100–150°C for armalcolites containing substantial Al, Cr, and Ti^{3+} (Kesson and Lindsley, 1975). Phase relations for Ti-rich mare basalts were highly controversial, but the original problems appear to have been largely resolved by Walker *et al.* (1975) and O'Hara and Humphries (1975). Armalcolite is a primary phase on the liquidus only at

low pressure for certain bulk compositions rich in TiO_2 component. Papike *et al* (1974) observed zoning in armalcolite from Apollo 17 basalts in which *mg* decreased outwards in response to decreasing *mg* of the crystallizing basalt. Because the low-temperature limit of armalcolite solid-solution decreases faster than the temperature of the basaltic liquid, armalcolite ceased to crystallize at the "suicidal" value of *mg* = 0.66.

Anderson (1973) reported microprobe analyses consistent with low-Zr armalcolite and rutile occurring in ol–sp–opx–plag cataclasite 15445, while Bence *et al.* (1974) reported ilmenite in similar cataclasites from 73263. These occurrences need further study because the oxides may provide limits on crystallization conditions. For example, the Mg-rich composition of the 15445 armalcolite(?) would be unstable below 1100°C at 0kbar and about 1400°C for 7kbar.

Low-Zr armalcolite underwent several post-crystallization reactions in ilmenite basalts (many papers: *e.g.* El Goresy *et al.*, 1974; Haggerty, 1973b). Some armalcolite reacted with liquid to form ilmenite. Some underwent solid-state breakdown to Mg-rich ilmenite + rutile (*e.g.* Haggerty, 1973b, p. 781) while some reacted with ulvöspinel to form ilmenite. Reaction of ulvöspinel with iron to form ilmenite and Ti_3O_5 has also been observed. Haggerty (1973b) described the reaction of niobian rutile and ilmenite to form a vein of armalcolite in grain 12070,35.

Usselman *et al.* (1975), on the basis of cooling rate experiments, suggested that armalcolite rimmed by an oriented intergrowth of equimolar ilmenite + rutile formed at depth, but with a maximum of 100 km. Ringwood and Essene (1970) found that low-Zr armalcolite was not stable in compositions similar to those of ilmenite basalts above pressures of ~4kbar. It seems fairly safe to conclude that low-Zr, Fe-rich armalcolite is not present in the lunar mantle though further experiments are desirable. Walker *et al.* (1975) concluded that ilmenite rather than armalcolite was in the source region of mare basalts. See later for comments on Mg-rich armalcolites.

Sclar *et al.* (1973) reported armalcolite rich in Fe(*mg* 0.26) and Al_2O_3 (7 wt. %) as minute skeletal crystals in a fragment of shocked basalt.

The last group of Ti-rich minerals occurs as tiny grains in breccias from Apollo 14, 16, and 17. The maximum size is only about 50μm, and no X-ray diffraction data have been obtained. Several reports emphasize complex textural relations (*e.g.* Haggerty, 1973b; Albee *et al.*, 1973) and the correlation between *mg* of the silicates and the complex oxides indicates that a metamorphic equilibration has occurred (Steele, 1974). Haggerty (1973b) classified these Ti-rich minerals as Type 2 and Type 3 armalcolites and distinguished them chemically by relatively high contents of Cr, Zr, and Ca for Type 2 and Zr for Type 3. The principal ranges of analyses are as follows (Cr,Zr,Ca-rich first; Zr-rich second): SiO_2 01.–0.6, 0.1–0.3; TiO_2 65–71, 68–72; ZrO_2 4–8, 0.5–4; Al_2O_3 1–2, 0.5–1.3; Cr_2O_3 4–11, 1–2; FeO 6–13, 8–18; MnO 0.1–1.3, 0–0.1; MgO 2–4, 7–12, CaO 3.1–3.7, 0.3–0.7; REE 0.5–1.5, not detected; Nb_2O_5 0–0.4, 0–0.6. Representative analyses are given in Table 2, Nos. 11 and 12. These ranges can be calculated approximately to $M^{2+}M^{4+}_2O_5$ formulae when Zr^{4+} is added to Ti^{4+} and account is taken of substitution of the trivalent elements as $M^{3+}_2M^{4+}O_5$. However, the cation totals tend to lie about 0–0.15 below the ideal value of 3, perhaps because some Ti is trivalent. Steele (1974) obtained low oxide totals especially for the Cr,Zr,Ca-rich specimens, and Peckett *et al.* (1972) had a similar problem which led them to suggest presence of light elements particularly Li; however, other analysts obtained good totals. Perhaps choice of standards and correction formulae is responsible. The simplest proposal is that these two composition clusters represent variants of the pseudobrookite structure, perhaps with a strong tendency to formation of an ordered superstructure. However, armalcolite and other pseudobrookites are stable only at high temperature, whereas the Zr- and Cr,Zr,Ca-rich specimens appear to be stable under metamorphic conditions, perhaps occurring in the range 500–900°C. Levy *et al.* (1972) reported isometric symmetry for reflection optics of the Ca–Cr–Zr variety, instead of the biaxial optics for a pseudobrookite structure, but this may result from metamictization (unpublished X-ray data of I. M. Steele). Analogies have been drawn between the Cr,Zr,Ca-rich specimens and zirkelite, but the latter contains much more Ca and less Ti. Steele (1974) used inverted commas for the terms "Zr–" and "Cr–Zr–armalcolite", but the rules of the IMA Commission on New Mineral Names indicate the need for neutral terms. Peckett *et al.* (1972) used the term Phase X for the Ca–Cr–Zr-rich mineral, while Haggerty (1973b) used the term Zr–armalcolite for the Zr-rich one. Only structural data can resolve the problem, but in the meantime, we shall use "Zr–" and "Ca–Cr–Zr–titanate" as neutral terms. Haggerty (1972c) reported phase Z1 in 15102, and discussed its possible relation to zirkelite (1973b); see Table 2, Analysis 13.

Both "Zr–" and "Ca–Cr–Zr–titanate" occur in complex intergrowths with other oxides. Albee *et al.* (1973) showed the minerals occurring within 50μm of

each other, but not in contact, in metaclastic fragment 61156; Mg-rich ilmenite, Nb-rich rutile and silicates formed part of the cluster. Haggerty (1973b) described complex assemblages including (a) "Ca–Cr–Zr–titanate", Mg-rich ilmenite, chromite, rutile, and iron and (b) "Zr–titanate", ilmenite, chromite, and Zl. Other assemblages were reported which involved zirkelite, but not the unknown titanates. All these assemblages, and ones involving baddeleyite are explainable by a sequence of solid-state reactions involving Ti–Cr–Zr–Fe–Mg oxides affected by changes of temperature and oxidation state. Steele (1974) deliberately selected some Apollo 17 metabreccias with narrow composition ranges of silicates. These showed a regular partition of *mg* between titanate and olivine with K_D (oxide/olivine) ~0.3 for "Zr–titanate" and ~0.1 for "Ca–Cr–Zr–titanate." Ilmenites had similar K_D to the latter. These partition data may be relevant to the possible coexistence of complex Ti–oxides and Mg-rich silicates in the lower crust or upper mantle, but the effect of pressure must be evaluated.

The titanates carry a substantial amount of rare elements including up to 0.6 weight percent Nb_2O_5. The "Ca–Cr–Zr–titanates" are characterized by about 1 weight percent total REE. Other minerals such as rutile and apatite, however, contain greater quantities of one or more of these rare elements.

Baddeleyite, corundum, and rutile

These three oxides are much less abundant than the multiple oxides.

Baddeleyite (ZrO_2) is found in the KREEPy assemblages. Although there are no systematic studies, scattered electron microprobe analyses reported HfO_2 1–3 weight percent, FeO 0–7, and TiO_2 1–8 weight percent (*e.g.* Table 2, Analysis 14). Brown *et al.* (1975) reported from an Apollo 17 basalt a Ti–Fe–baddeleyite with Y_2O_3 1.8 weight percent and HfO_2 0.8.

Rutile (TiO_2) generally occurs in association with ilmenite. Lamellae parallel to $\{01\bar{1}2\}$ of ilmenite indicate exsolution, whereas irregular intergrowths of Mg,Fe-rich rutile and Mg–ilmenite indicate breakdown of armalcolite (Haggerty, 1973b). Primary rutile tends to occur as twinned, randomly-oriented, euhedral crystals associated with ilmenite. Some analyses of primary rutile are rich in Nb, and Marvin (1971) reported Nb_2O_5 6.4 weight percent, Cr_2O_3 3.2, Ta_2O_5 0.2, V_2O_3 0.4, La_2O_3 0.4, and Ce_2O_3 0.8 in rutile grains from microbreccia fragment 12070,35, while Hlava *et al.* (1972) reported Nb_2O_5 7.1, Cr_2O_3 2.6, ZrO_2 0.7 but no REE in rutile from an Apollo 14 KREEP fragment (Table 2, Analysis 15). Stoeser *et al.* (1974) reported a mineral from the Civet Cat norite clast with TiO_2 73 percent, Nb_2O_5 20, Cr_2O_3 4, ZrO_2 2, and FeO 1 percent. The highest reported content of ZrO_2 is for a rutile spinel troctolite 65785 (ZrO_2 3.8, Nb_2O_5 not found, Cr_2O_3 0.6, FeO 0.7, Al_2O_3 1.1; Dowty *et al.*, 1974b). Probably all Nb-rich specimens occur in KREEPy rocks or patches of rocks, but the factors which govern the other elements are unknown. The rutile(?) in the 15445 sp–ol–opx–plag cataclasite contained 1.6 weight percent Nb_2O_5, but only trivial amounts of other elements. Jedwab (1973) reported several types of rutile in lunar soils including a blue rutile with no detectable Nb and Zr. The blue rutile occurred as an 0.5mm aggregate of micrometer grains, and may have resulted from condensation.

Corundum aggregates from 10084 fines were intrepreted as condensates of impact-derived vapor (Kleinmann and Ramdohr, 1971). A 200μm crystal was found in 14163 fines by Christophe-Michel-Levy *et al.* (1972), but no corundum has been reported in lunar rocks.

Apatite and whitlockite

Whitlockite ~$Ca_3(PO_4)_2$ is apparently more abundant than apatite ~$Ca_5(PO_4)_3(F,Cl)$ in lunar rocks. Both phosphates occur in the high-KREEP rocks or in KREEP-rich areas of low-KREEP rocks, sometimes as intergrowths readily characterized by cathodoluminescence. Particularly beautiful are the scanning electron micrographs of vugs containing hexagonal prisms of apatite or hexagonal tablets of whitlockite (*e.g.* McKay *et al.*, 1972). Many breccias and lunar rocks contain veins and vugs lined with phosphates, silicates, ilmenite, and iron; these testify to ubiquitous vapors penetrating the surface rocks.

Prewitt and Rothbard (1975) compared terrestrial, lunar, and meteoritic whitlockites by X-ray and chemical methods. Whitlockite from the Estacado meteorite yielded a crystal structure with one phosphate tetrahedron inverted with respect to the crystal structure of a terrestrial whitlockite: the ideal formula is $Ca_{18}Mg_2Na_2P_{14}O_{56}$. A terrestrial whitlockite from the Palermo quarry had the formula $Ca_{18.2}(Mg,Fe)_3H_{1.6}P_{14}O_{56}$, while synthetic ones could be made either with or without hydrogen ($Ca_{18}Mg_2H_2P_{14}O_{56}$, $Ca_{18}Mg_2P_{14}O_{55}$). Unfortunately Prewitt and Rothbard could not locate a lunar whitlockite large enough for single-crystal X-ray

study. About 80 electron microprobe analyses of lunar whitlockites record up to 25 elements with weight concentrations up to two atomic percent (*e.g.* Table 2, Analysis 16). Lunar whitlockite may have inverted from a high-temperature polymorph (Griffin *et al.*, 1972), which would tolerate excess Ca and extensive substitution of REE. Prewitt and Rothbard (1975) believed that the old name *merrillite* should be used for the meteoritic mineral, and that a new name would be needed for the lunar mineral when detailed X-ray work had given a proper characterization. In the meantime, however, the name whitlockite is retained for the lunar mineral. Columns 16 and 17 in Table 2 contain analyses of whitlockite and apatite from 14310 basalt, for which special care was taken with standardization. Fluorine and chlorine are always low in lunar whitlockites; SiO_2 is consistently reported at the 0.*n* percent level or greater; FeO ranges from 0.*n* to 6 weight percent, while MgO tends to vary inversely from 4 to 0.*n* weight percent; Y_2O_3 ranges from 1 to 3 percent; Ce_2O_3 and Nd_2O_3 occur up to 3 percent, while other REE occur at the O.*n* to 1 percent level; Na_2O ranges from 0.0*n* to 0.6 weight percent; SrO usually was not reported, but 1 percent in 15475 whitlockite (Brown *et al.*, 1972). Probably the composition of lunar whitlockite depends on local idiosyncrasies during the crystallization of late residua, and the *mg* ratio for example may be a guide to the degree of fractionation during such crystallization. Vapor-deposited whitlockite may have a different composition than whitlockite crystallized from liquid: in particular, the REE may be absent in the former.

Some 40 electron microprobe analyses of lunar apatites record 0.0*n*–2 weight percent Cl and ~2.5–4 percent F, and when account is taken of the high error for F there is no need to invoke the presence of OH. However, ion microprobe analyses for H would be very interesting to check for the relative availability of Cl,F, and OH. Apatites from recrystallized soils exposed to solar protons might incorporate significant OH, and vapor-deposited apatite might also have a distinctive composition. The ranges of other elements are: SiO_2 0.*n*–2 weight percent indicating substantial replacement of P by Si; FeO 0.0*n*–2; MgO 0.0*n*–0.*n*; Y_2O_3 0.*n*–2; Ce_2O_3 0.0*n*–3; Nd_2O_3 0.0*n*–1, U 20–1000 ppm. The high U contents might permit age determination by ion microprobe techniques.

The relative occurrence of phosphate and phosphide (*e.g.* schreibersite) depends on the redox conditions (next section). Fuchs (1968) recorded several other types of phosphates in meteorites, of which only one (farringtonite) has been observed in lunar rocks so far.

Sulfides, carbide, phosphide and metals

The detailed review by Frondel (1975) emphasized the crystallographic and mineralogic aspects of these minerals and allows us to concentrate on petrologic and geochemical features. Many papers discussed whether the minerals have a lunar, meteoritic, or hybrid origin, but simple answers cannot be expected because of complex effects produced by shock and thermal metamorphism and by melting of polymict breccias. Furthermore the bulk Moon was itself probably accreted from early bodies, and many types of such bodies were available, not necessarily the same as those now represented by meteorites in museums. The extensive evidence for precipitation of iron and troilite in vugs, for reduction of Fe^{2+} to Fe° by sulfur volatilization and carbon oxidation, and for redox conditions allowing movement of phosphorus between oxidized minerals (phosphate and silicate) and metallic phases (schreibersite and iron minerals) adds to the problems. However, considerable progress has been made in establishing possible criteria for distinguishing lunar from meteoritic phases, and at least some specimens can be assigned with considerable confidence. In addition, various textures and element partitionings are useful as indicators of metamorphic equilibration. An understanding of the metallic minerals and alloys is important for interpretation of magnetic phenomena.

(a) Sulfides. The principal sulfide is troilite, essentially FeS. In mare basalts, troilite can occur with blebs of iron mineral, and Skinner (1970) interpreted troilite–iron intergrowths in 10072 basalt as products of an immiscible liquid which separated at 1140° C from the silicate magma after substantial crystallization of ilmenite and pyroxene. In Apollo 12 basalts, troilite commonly occurs with ilmenite and spinel rather than with metallic iron, but does occur intergrown with iron as a late product of crystallization (*e.g.* Taylor *et al.*, 1971). Probably its occurrence depends on a combination of factors including the bulk S content and the state of oxidation. Troilite is one of the minerals occurring in cracks in norite 78235 (Irving *et al.*, 1974) and in the mosaic assemblages interpreted as the final products of crystallization of troctolitic granulite 76535 (Gooley *et al.*, 1974), to mention just two occurrences in coarse-grained rocks. Indeed troilite seems to be ubiquitous in lunar rocks (except perhaps for some anortho-

sites). This is not surprising when consideration is given to the factors governing the migration of S on the Moon.

During primary differentiation of the Moon, a liquid rich in Fe, FeS, and the metal- and sulfur-seeking elements would form wherever the temperature exceeded about 1000° C (Fig. 2), and its high density would cause it to sink. Coexisting silicate liquids should contain sulfur at the level of at least 0.0*n* weight percent by analogy with data for terrestrial rocks (summarized by Bishop *et al.*, 1975); indeed the S content of mare basalts indicates 0.*n* percent (Brett, personal communication). Crystallization could lead to rocks relatively richer or poorer in S depending on the efficacy of differentiation. Particularly important for interpretation of the sulfide and iron minerals is the extent of post-crystallization migration of S and Fe, especially the escape of S vapor and associated reduction of Fe^{2+} into Fe°. Gibson and Moore (1973) noted a negative correlation between S and Fe° (*not* total iron) in Apollo 15 and 17 basalts, and Brett (1975) found similar correlations for Apollo 12 basalts. The incremental ratio $\Delta S/\Delta Fe°$ was close to but substantially less than the theoretical ratio of unity for atom-for-atom reduction of Fe^{2+} in basaltic melt as follows:

S^{2-}(melt) + Fe^{2+}(melt) = S° (vapor) + Fe° (crystal). Disproportion of troilite to iron mineral + S would also require a unit ratio. Brett supported the suggestion by Gibson and Moore that the observed correlations resulted principally from outgassing of S, but the ultimate fate of the S is unknown. Sato *et al.* (1973) made detailed measurements of the redox conditions of lunar basalts and argued from thermochemical calculations and the expected presence of C in the Moon that reduction of lunar rocks by conversion of carbon or carbide to carbon monoxide would be a second plausible mechanism at the lunar surface. Probably more than one process occurs in the reduction of lunar rocks, but the extensive evidence of migration of S in lunar surface rocks and the greater abundance of S than C suggest that S volatization plays the stronger role in determining the *present* redox state. Gibson and Moore (1973) found that 12 to 30 percent of the S and C in lunar breccias could be volatilized under vacuum in 1 day at 750° C and almost all at 1100° C. The extensive observations of troilite in vugs (*e.g.* in Apollo 14 breccias; McKay *et al.*, 1972) testify to the migration of S-bearing vapor. On an even larger scale, the migration of S in the lunar mantle and especially from the hypothetical lunar core must be considered seriously. For the Moon model in Figure 3 and the possible selenotherm in Figure 2, S could exist as an Fe, FeS eutectic liquid at depths greater than 300km in the present Moon and at even shallower depths before the Moon cooled down.

Troilite is a significant constituent of many types of meteorites, but the contribution of impact debris to the S content of lunar surface rocks, especially impact breccias, is hard to evaluate because of the ease of volatilization of S. About 5 percent (range 1 to 7%) of coarse metal-rich particles from Apollo 14 and 16 soils contain sulfide (Goldstein and Axon, 1973). Although the Co and Ni contents of metallic iron may not distinguish rigorously between meteoritic and lunar sources, the wide range of Co and Ni contents of metallic iron mineral associated with sulfide in these coarse particles indicates both lunar and meteoritic sources. Spherules, 50μm to 5mm across, showed S contents from 0.05 to 26 weight percent, and had complex textures which were reproduced experimentally by rapid cooling of drops of synthetic liquid (Blau and Goldstein, 1975). These spherules occur in most lunar soils, and were interpreted as the products of shock melting of metallic and non-metallic material, probably of both lunar and meteoritic origin. Synthetic compositions rich in both S and P apparently yielded two immiscible liquids, one of which crystallized to troilite with small inclusions of nickel–iron while the other crystallized to nickel–iron grains surrounded by schreibersite $(Fe,Ni)_3P$ and a few blebs of troilite: rare lunar fragments showed evidence of similar textures. Brett (1975) observed a strong positive correlation between S and Fe° (*not* total iron) in non-mare rocks, and suggested that meteoritic material with approximately 10 times Fe° to S had been incorporated.

Troilite from a vug was found to have a superstructure with *a* and *c* doubled over those for the simple NiAs structure type (Evans, 1970).

Electron microprobe analyses of minor elements in troilite are questionable because of problems from secondary fluorescence and overlap into inclusions. Published data show Mg 0.02–0.13 weight percent, Si 0–0.8, P not detected, Ca 0–0.6, Ti 0–0.7, Cr 0–0.1, Mn 0–0.4 but mostly <0.05, Co 0–0.3, Ni 0–6.3, Cu 0–0.4. High values of Co (0.3) and Ni(6.3) were found only for troilite occurring with iron in a globule in 12001 fines (Champness *et al.*, 1971), and all other values are 0–0.1. High values of Cu were reported only for troilite coexisting with copper metal in 10045 basalt (Simpson and Bowie, 1970). High values of Mg, Si, Ca, and Mn should be rechecked,

but consistently high values of Si and Ca were obtained for troilite from 12051 basalt by Keil *et al.* (1971).

The Ti content of troilite is greater (up to 0.5 wt.%) when it coexists with ilmenite or ulvöspinel than when it coexists with metallic iron (0.0*n*) in lunar basalts, and although fluorescence error cannot be ruled out, exchange reactions may be responsible (El Goresy *et al.*, 1971; El Goresy *et al.*, 1972; Taylor *et al.*, 1971). Troilite annealed with iron, ulvöspinel, and vapor at 700 to 1000° C showed systematic reduction of Ti content from 0.8 weight percent at 1000° C to 0.3 at 700° C, while the Ti content of metallic iron dropped from 0.8 to 0.4 (Taylor *et al.*, 1973a). Observed Ti contents of lunar troilite coexisting with ilmenite could be interpreted as the result of metamorphism to temperatures from about 900 to substantially below 700° C.

Mackinawite was tentatively identified from its strong bireflectance as tiny spots associated with troilite from basalts 12018 and 12063 (El Goresy *et al.*, 1971; Taylor *et al.*, 1971). Subsolidus reaction below 150° C is indicated. Taylor and Williams (1973) reported optical and chemical identification of chalcopyrite and cubanite along cracks and grain boundaries of troilite in 12021 basalt. Both Cu–Fe–sulfides may have exsolved at low temperature from Cu-bearing troilite, and both contain 0.9 weight percent Co. Clanton *et al.* (1975) reported that in vugs of 76015 breccia the order of crystallization from vapor was silicate, ilmenite, Ni–Fe mineral, troilite, chalcopyrite (Cr 0.5 wt.%), pentlandite (Fe 35.5 Ni 29.1 Cu 0.3 Cr 0.2), and chromite (?). Sphalerite in "rusty" rock 66095 contained 28 mole percent FeS and occurred as reaction rims in and around troilite grains (El Goresy *et al.*, 1973a,b) or as individual grains attached to or enclosed by troilite grains (Taylor *et al.*, 1973b). The latter authors argued that the uniform composition and the latter texture were inconsistent with the idea of alteration by a Zn-bearing solution proposed by the former authors. The identification of all other species of lunar sulfides is tentative.

(b) Cohenite and schreibersite. The carbon chemistry of lunar samples is extremely complex because of the input of carbon from the solar wind and because reaction of carbon with iron in silicates involves oxidation–reduction processes. Grains of cohenite large enough to be visible by optical microscopy were reported only in a few fragments in fines and 66095 "rusty" breccia. The coexisting minerals and textures indicate that the host fragments were derived from iron meteorites. Electron microprobe analyses showed Ni 0.8–1.7 weight percent, Co <0.02–0.25, P 0.03–0.08 (Goldstein *et al.*, 1972; El Goresy *et al.*, 1973a,b; Goldstein and Axon, 1973; Taylor *et al.*, 1973b). Carbide from a melted fragment of iron meteorite had 6 percent Ni and up to 8 percent P (Goldstein *et al.*, 1970). Carbon from the solar wind should tend to reach a steady level on mineral surfaces as proton stripping balances the incoming carbon. Meteorite impact should result in transfer of some carbon from surface to interior of grains, while some could be converted to gaseous species especially carbon monoxide. Sputtering and erosion by micrometeorites should change the grain size. Many papers (*e.g.* Moore *et al.*, 1974) have reported the C and S contents of lunar specimens. Pillinger *et al.* (1974) found that the content of iron carbide in lunar fines (as measured by evolution of CD_4 upon dissolution by deuterated acid) is proportional to the amount of fine-grained (<1μm) iron metal measured by ferromagnetic resonance spectroscopy. Both the carbide and iron metal when normalized to the solar wind exposure are proportional to the bulk iron content of the fines, which indicates that carbide synthesis occurred only with Fe^{2+} reduced to Fe° by the solar wind. In general, lunar carbide tends to be higher in the fines, and only a small part is of meteoritic origin.

Schreibersite, $(Fe,Ni)_3P$, is important because it forms only under fairly reduced conditions, and its relationship to phosphate should place a limit on the oxygen fugacity–temperature relation. Furthermore it is a common constituent of meteorites, especially irons, and its occurrence in lunar rocks might provide a measure of meteoritic contamination. Unfortunately solid-state reactions cause problems. The distribution of Ni between schreibersite and metallic iron provides a thermometer.

The Type 1 enstatite meteorite fragment in an Apollo 15 soil (Haggerty, 1972d) contains 1 percent schreibersite together with kamacite, troilite, and niningerite (Mg,Fe,Mn,Cr)S. A fragment from Apollo 11 fines containing iron mineral with Neumann lines, schreibersite, cohenite, and troilite is probably meteoritic, and Widmanstätten lines were probably removed by shock (Frondel *et al.*, 1970). A fragment from breccia 10046 contained symplectic intergrowths indicative of crystallization from a P-rich eutectic (Goldstein *et al.*, 1970). A particle from Apollo 12 fines contained coarse kamacite grains plus an intergrowth of small kamacite grains set in schreibersite matrix, while another particle showed den-

drites of kamacite and taenite surrounded by schreibersite and troilite (Goldstein and Yakowitz, 1971). For the latter particle, the Ni distribution between the taenite, kamacite, and schreibersite (Fig. 17) indicated equilibration to 500–600° C based on experimental data of Doan and Goldstein (1970) for the Fe–Ni–P system. Metamorphism in an ejecta blanket followed by mechanical removal would be a possible explanation of the equilibration to relatively low temperature. These and other data (*e.g.* Goldstein *et al.*, 1972) indicate that iron meteorites were impacting the lunar surface and that their debris was undergoing complex reactions including melting and metamorphism.

The state of oxidation of some iron meteorites was estimated by Olsen and Fuchs (1967) using calculations for the assemblage chlorapatite–metallic iron–pyroxene. These showed that schreibersite is stable for conditions more reducing than the iron wüstite buffer, while phosphate is stable for more oxidizing conditions. McKay *et. al.* (1973) heated synthetic silicate glass doped with $Ca_3(PO_4)_2$, NiO, and Co_3O_4 in a controlled stream of H_2 and CO_2. Charges quenched from 1250° at oxygen fugacities lower than 10^{-13}–10^{-14} atm contained spherical intergrowths of schreibersite and metallic iron interpreted as the product of immiscible Fe–P liquid. The oxidation conditions in lunar rocks probably range over several orders of magnitude around the iron–wüstite buffer, and straddle the phosphide–phosphate equilibrium. Because of the possibility of growth of schreibersite from calcium phosphates, Ridley *et al.* (1972) argued that presence of schreibersite was not a sufficient criterion for meteoritic contamination. Lunar schreibersite could result from one or more of three processes: (a) simple incorporation of meteoritic schreibersite, (b) shock heating of meteoritic phosphate (Goldstein *et al.*, 1972), and (c) conversion of lunar phosphate. Conversely meteoritic schreibersite could be converted to lunar phosphate.

Gooley *et al.* (1973) studied the occurrence of schreibersite and iron in Apollo 16 rake samples, and their data were supplemented and endorsed by those of Brown *et al.* (1973), El Goresy *et al.* (1973a), Grieve and Plant (1973), McKay *et al.* (1973), Misra and Taylor (1975), and Reed and Taylor (1974) for other Apollo 16 rocks. Figure 17a shows the data on Ni and P distribution obtained by Gooley *et al.* (1973), and Figure 17b shows tabulated data for many types of specimens given by various authors. Coexisting schreibersite and metallic iron in samples quenched from high temperature (open circles in Figs. 17a and b) show low P in the schreibersite and high P in metallic iron (except for Item 8, Fig. 17b); these compositions are close to those for the 1000° C isotherm in the synthetic Fe–Ni–P system (Doan and Goldstein, 1970). The insert to Figure 17b shows the

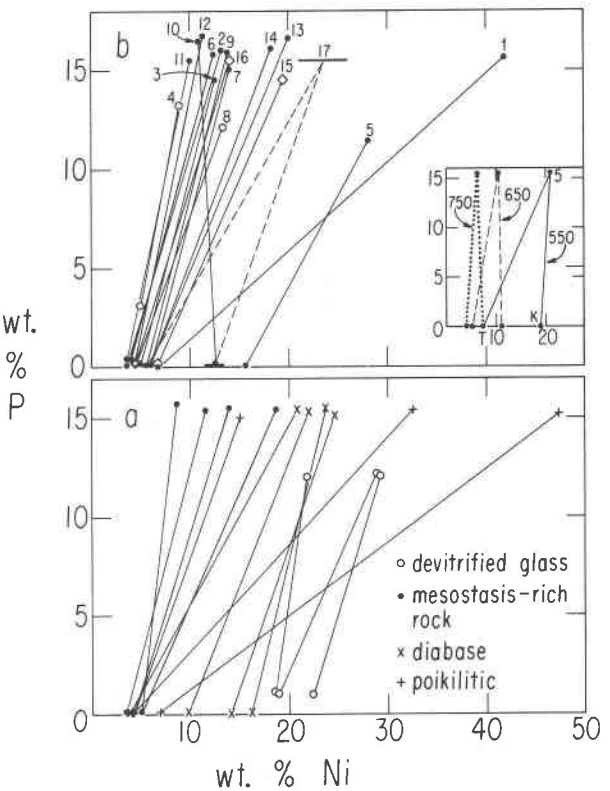

FIG. 17. Partition of P and Ni between coexisting metallic iron and schreibersite. (a) Apollo 16 rake samples, Gooley *et al.* (1973). (b) Other data: 1–4 Brown *et al.* (1973), 1 62295 spinel troctolite, 2 60335 feldspar-phyric troctolite, 3 15082 soil fragment, 4 68815 troctolite clast in remobilized breccia (phosphide interpreted as product of liquid quenched from 1080°C). 5 14310 basalt, El Goresy *et al.* (1972). 6 64455 highland basalt, Grieve and Plant (1973). 7 66095 metamorphosed breccia, mean of several analyses, El Goresy *et al.* (1973a). 8 66065 breccia, typical analyses for spherical intergrowths, McKay *et al.* (1973). 9 66095 metamorphosed breccia, metal–schreibersite–cohenite association, Taylor *et al.* (1973b). 10 14310 basalt, Axon and Goldstein (1972). 11–14 phosphide–metal particles in 14003 and 14163 fines, Axon and Goldstein (1972). 15 Type 1 enstatite meteorite in Apollo 15 fines, Haggerty (1972d). 16 Apollo 12 soil particle F2, kamacite–schreibersite eutectic, Goldstein and Yakowitz (1971). 17 Apollo 12 soil particle F3-2, kamacite–taenite dendrites in schreibersite–troilite matrix, Goldstein and Yakowitz (1971). See Misra and Taylor (1975, Fig. 5) and Reed and Taylor (1974, Fig. 9) for graphical data on Apollo 16 samples. Data for 7 particles from soil 78501 in which iron–phosphide assemblages coexist with anorthosite, basalt, or agglutinate were given by Goldstein *et al.* (1974): equilibration temperatures of 375–475°C were indicated. Inset diagram shows 3-phase triangles between taenite, kamacite, and schreibersite at 550, 650, and 750°C, Doan and Goldstein (1970).

experimental data for the three-phase triangle for taenite, kamacite, and schreibersite at 750, 650, and 550° C. For bulk Ni contents to the right of the kamacite–schreibersite side of the triangle, the tie lines between kamacite and schreibersite stay almost parallel, whereas for bulk compositions to the left of the taenite–schreibersite join, the tie lines between taenite and schreibersite are also almost parallel. The data of Gooley *et al.* (1973) indicate that schreibersite and iron exchanged Ni to ~600° C in mesostasis-rich rocks, to ~550° C in diabases, and to various temperatures from 600 to below 550° C for rocks with poikilitic texture. Reed and Taylor (1974) reported a similar temperature range for 100 metallic particles from Apollo 16 soils and rocks. Both Gooley *et al.* (1973) and Misra and Taylor (1975) emphasized that schreibersite was rare or absent in the poikilitic rocks, and Misra and Taylor noted that whitlockite was unusually abundant in them. Gooley *et al.* suggested that this resulted from conversion of phosphide to phosphate as a result of slower cooling, while Misra and Taylor pointed out that the distinctly high P contents of the metallic iron in poikilitic rocks indicated a different thermal history which included equilibration at a higher temperature. No phosphide–phosphate intergrowths have been reported. Reed and Taylor (1974) stated that the P contents of metallic iron minerals in the Apollo 16 rocks were higher than those for metallic iron minerals from meteorites, and suggested that P was incorporated into metallic iron minerals from meteoritic debris upon reduction of lunar phosphate.

Spinel troctolite 62295 has a quench texture, but the Ni distribution between schreibersite and taenite (Brown *et al.*, 1973; Misra and Taylor, 1975) indicates equilibration below 550° C (Fig. 17b, No. 1).

The coarseness of schreibersite grains (called rhabdite when occurring as needles and elongate crystals) provides an estimate of time-temperature relations. Axon and Goldstein (1972) concluded that several metal–phosphide fragments from Apollo 14 soils had been annealed to 500–600° C for periods up to 1 month to 50 years. Gooley *et al.* (1973) concluded that rhabdite lamellae, 4μm wide, in poikilitic rock 64657 would have required growth for about 2 months at 600° C.

Basalt 14310 was controversial because of the high content of trace elements characteristic of meteoritic contamination. Axon and Goldstein (1972) and El Goresy *et al.* (1972) presented evidence for more than one generation of schreibersite, one type occurring as coarse grains in contact with iron, troilite, and Ca phosphate while a second type occurs as tiny grains. The assemblage plotted as Number 10 in Figure 17b apparently annealed at 700° C while assemblage Number 5 may not be in equilibrium. When account is taken of metamorphism and oxidation–reduction reactions, the complex data are not inconsistent with derivation of 14310 by melting of a regolith (but see Crawford and Hollister, 1974, p.416).

In summary, the coexistence of schreibersite and iron provides a useful parameter on thermal annealing, while the relative amount of schreibersite and phosphate provides information on the redox conditions. Meteoritic schreibersite can apparently be either augmented by lunar-derived schreibersite or dissipated by conversion to phosphate; unless it is accompanied by other iron-bearing minerals in recognizable textural or chemical assemblages, it is not a reliable indicator of meteoritic contamination.

(c) Metallic Fe,Ni,Co minerals. **Introduction.** Most metallic minerals in lunar specimens are Fe,Ni,Co alloys with up to 100 percent Fe, 60 percent Ni, 8 percent Co, and small amounts of other siderophile elements. Trivial amounts of metallic copper occurring in some specimens (listed by Dwornik *et al.*, 1974) appear to be indigenous, while indium and aluminum metal probably are contaminants. Most of the Fe,Ni,Co alloys were characterized only by optical and chemical methods, and distinction between kamacite (α type with low Ni) and taenite (γ type with high Ni) varieties was not always made. Although details of interpretation were controversial, magnetic techniques yielded much additional chemical information, especially for submicroscopic iron produced by reduction. The literature is confusing because early data were interpreted in terms of simple ideas now seen to require further evaluation, and because it is difficult to cross-relate the data obtained by the different techniques. By 1975, it was certain that iron minerals derived from at least four partly interrelated sources: (a) rocks and magmas from the lunar interior in which the composition of the iron minerals correlates with the silicates, sulfide, and vapor phase, (b) simple meteoritic contamination in which the iron minerals survived the impact, (c) complex meteoritic contamination in which the iron minerals were transmuted during the impact and mixed with material already on the Moon, (d) reduction of Fe^{2+} in silicates, sulfide, and magma by various processes involving shock, escape of S vapor, addition of H and C from the solar wind, and conversion of C and H to escaping CO and H_2O. Furthermore iron was transported in the vapor phase, was mixed up

and recrystallized in breccias, and was generally remobilized during all the complex processes in the lunar crust. There is no need to belabor the problems resulting from oxidation-reduction reactions in view of earlier comments. However, it is necessary to emphasize the problems of determining the amount of metallic Fe,Ni,Co resulting from meteoritic contamination.

Recent evidence from oxygen isotopes (Clayton and Mayeda, 1975) indicates that the precursors of the Earth, Moon, and "differentiated meteorites" (*i.e.* eucrite, howardite, hypersthene achondrite, enstatite chondrite and achondrite, and nakhlite) could have been genetically related in the solar nebula, whereas the ordinary chondrites (types H, L and LL), carbonaceous chondrites (C2 and C3), and ureilites must have formed separately. The simplest explanation is that the Earth, Moon, and differentiated meteorites formed largely from material which was originally interacting in the same general region of the solar nebula, whereas the other meteorites formed elsewhere, but other possibilities must be considered including a time variation. There is considerable argument and some observations in favor of present-day meteorites arising from either the asteroid belt or cometary debris or both. Because the capture cross-section depends strongly on the relative orbital elements, the relative population of meteorites impacting the Earth and the Moon should have changed considerably with time. A search for meteoritic debris on the lunar surface must bear in mind how the surface developed with time. In terms of our favored model, most of the Moon would have accreted about −4.5Gy, and shortly afterwards severe differentiation would have resulted in sinking of most of the Fe°, Co°, Ni°, and other siderophile elements into the lunar interior. The nature of the remaining metal phase in the upper mantle may be revealed by the ultrabasic fragments emphasized earlier, or by the mare basalts if they really derive from late remelting of early deep-seated cumulates. Down to −3.9Gy the lunar surface would be changed drastically by a flux of incoming projectiles of which the large basins would provide the most dramatic evidence. Each ejecta blanket should contain some of the projectile greatly diluted by excavated crustal materials, the ratio probably varying considerably from place to place. Scouring of the lunar surface by the debris cloud, metamorphism, reduction, and vapor transfer should cause further complications. Smaller impacts would rework the ejecta blankets, and melting would produce plagioclase-rich and other rocks. Flooding of the maria by internally-derived basalts would provide fresh surfaces which should receive only minor amounts of earlier debris from late impacts in the highlands. The regolith on the mare surfaces should be especially suitable for recording meteoritic contamination since about −3Gy. In the context of this complex situation, (a) Ganapathy *et al.* (1970) and others noted the very strong depletion of certain elements including Ir and Au in Apollo 11 mare basalts, and calculated that the higher abundance of these elements in Apollo 11 fines could be produced by about 2 percent undifferentiated material from the solar nebula such as carbonaceous chondrite, (b) Morgan *et al.* (1974) interpreted the Au, Ir, Ge, Re, and Sb contents of rock fragments from highland soils in terms of debris believed to have arisen from 6 basin-forming projectiles of distinctive chemical composition, and (c) Goldstein and co-workers (latest papers: Goldstein *et al.*, 1974; Hewins and Goldstein, 1975b) interpreted the Ni and Co contents of lunar metal in terms of five components (meteoritic, high-Fe and high-Co basaltic, supermeteoritic, and submeteoritic—to be defined later). The (c) data were obtained by electron microprobe analysis of individual metal grains, whereas the former data were obtained by neutron activation analysis of bulk fragments whose very minor component of metal undoubtedly carries the trace siderophile metals (Wänke *et al.*, 1971; Wlotzka *et al.*, 1972). Particularly important is the conclusion by Morgan *et al.* (1974) from plots of Au,Ge,Ir and Au,Sb,Re that the basin-forming projectiles do not resemble iron meteorites and show little resemblance to chondrites which have recently impacted the Earth. Wlotzka *et al.* (1972, 1973) made neutron activation analyses of Ir,Au,As,W and other trace elements of bulk metal separated from Apollo 14, 15, and 16 fines and breccias, and also made electron microprobe analyses of Co and Ni for individual particles. After reviewing several possibilities, they concluded that, although the meteoritic component added during the past 3 to 4 Gy had a siderophile content like that of undifferentiated solar material, earlier meteoritic component had a different composition. Wasson *et al.* (1975) concluded that earlier meteoritic contamination was richer in siderophile elements than material arriving after −3.7Gy, and went on to question the identification of debris from basin-forming projectiles by Morgan *et al.* Although several fragments of stony meteorites were discovered in lunar fines (*e.g.* a carbonaceous chondrite, Wood *et al.*, 1971; an enstatite chondrite, Haggerty, 1972d), and many iron-rich

fragments appear to be heated relics of iron meteorites (*e.g.* Goldstein and Axon, 1973; Goldstein *et al.*, 1975), most meteoritic debris may have been transformed during incorporation into lunar regolith. It is obvious that great caution is needed in attempting to interpret the chemistry of lunar iron, and indeed in using the term "meteoritic."

The magnetic properties of lunar specimens are largely determined by the metallic iron minerals. Much iron in unmetamorphosed breccias, glasses, and fines occurs as tiny particles peppering a glassy matrix, as displayed in transmission electron micrographs (*e.g.* Agrell *et al.*, 1970; Lally *et al.*, 1972; Housley *et al.*, 1973). Widely-separated iron particles about 0.01μm across in a diamagnetic matrix are superparamagnetic and show viscous remanent magnetization (*e.g.* Gose *et al.*, 1972). For increasing grain size, the magnetic phenomena are governed first by a single domain ($\sim$0.03μm) and then by multi-domain assemblages ($>1\mu$m) typical of ferromagnets. Gose *et al.* (1972), Cisowski *et al.* (1974), and others correlated the increasing grain size of iron in metamorphosed breccias with the metamorphic grade deduced from the silicate and oxide minerals, and Pearce *et al.* (1972), Tsay and Live (1974), and others mimicked the observed phenomena with measurements on glassy fines or synthetic glasses annealed at 600 to 1045° C. Wasilewski (1974) pointed out the possible magnetic effects from antiferromagnetic γ-Fe,Ni, and referred to the demonstrated occurrence of γ-iron in lunar breccias (Lally *et al.*, 1972). Early interpretations of Mössbauer and electron ferromagnetic resonance spectra in terms of magnetite or other Fe^{3+}-bearing phases appear to have been replaced satisfactorily by new interpretations (*e.g.* Tsay *et al.*, 1973b) based on tiny grains of superparamagnetic iron; however, the controversy hinges on subtle arguments involving computer simulation of resonance profiles, chemical composition, and shape, and on observed temperature variation. Some relevant recent papers are: Forester (1973), Griscom *et al.* (1973), Tsay *et al.* (1973b), Weeks (1973), Weeks and Prestel (1974), Friebele *et al.* (1974), and Tsay and Live (1974). Many mineralogical properties of lunar fines and breccias require a high state of reduction, and any ferric–oxide phases should tend to be reduced to either ferrous phases or iron metal.

Dunlop *et al.* (1973) concluded that single-domain particles of iron, 10–20nm across, are the major carriers of natural magnetic remanence in soil breccia 14313. From detailed analysis of viscous remanence, thermoremanence and magnetic granulometry, they also concluded that the population frequency varies approximately as the inverse square of the grain volume, and that there are two separate populations, one nearly equidimensional with coercive forces >2000 Oe and one very elongated. The former can be identified with spheres enclosed in glass, and the latter perhaps with needles or whiskers observed in several optical and electron microscopic studies.

Electron microprobe analyses of submicroscopic particles are difficult, but some analyses indicate low Ni and Co for iron particles in glasses. The Curie points for pure Fe, Co, and Ni are 770, 1131, and 358° C, respectively. The latest thermomagnetic data (Nagata *et al.*, 1974, 1975) show Curie points of lunar samples straddling the 770° C transition for pure iron. Because of the opposite temperature effects of the subsitution of Co and Ni, all interpretations are completely ambiguous: however, the histograms are consistent with all lunar rocks containing some pure iron, and with the breccias, fines, and some but not all igneous rocks containing Ni-bearing iron as well (see later). Mössbauer resonance measurements of the hyperfine field allowed Housley *et al.* (1972) to conclude that the iron metal in 10084 fines contained less than 1.5 percent Ni *on average* and perhaps none at all; because electron microprobe analyses of coarse particles from 10084 fines showed particles with up to 16 percent Ni (see later), the fine iron particles should be very low in Ni.

Although there are some technical subtleties, the amount of Fe° was estimated from the saturation magnetization, the ferromagnetic resonance, and the Mössbauer spectrum. The principal features of the data given by Housley *et al.* (1974), Huffman *et al.* (1974), Pearce *et al.* (1974), Cisowski *et al.* (1974), and Pearce *et al.* (1975) are: (a) low values (<0.05) of $Fe°/(Fe° + Fe^{2+})$ in most mare basalts, (b) diverse values for highland rocks (0 to 0.15), (c) relatively small range for lunar soils (0.02 to 0.08) no matter whether they derive from highland or mare locations, and (d) increasing values as the grain size of the *soil* decreases and the grain size of the *iron* increases, with a specific trend for each of the Apollo 14, 16, and 17 suites. The latter trends were explained by increasing reduction of the iron as a soil became more mature during meteorite bombardment.

The formation of iron minerals in breccias and soils must involve many complex problems (*e.g.* Agrell *et al.*, 1970). Reduction of ferrous iron from the silicates, oxides, and sulfides augments the iron already available from pre-existing lunar rocks and meteoritic debris. Such reduction can occur as the re-

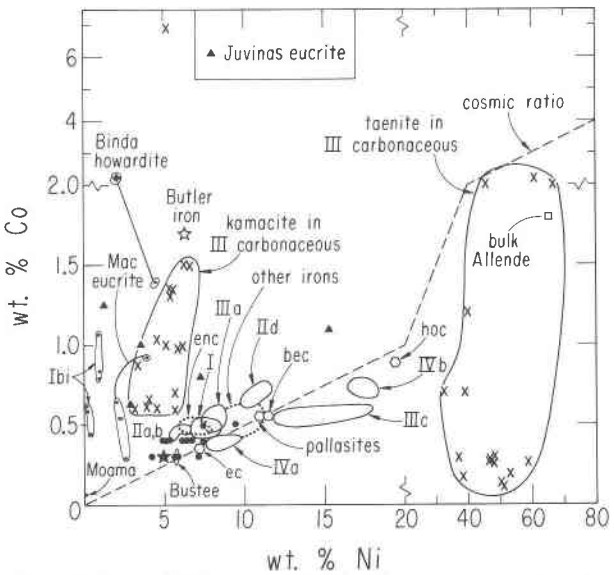

FIG. 18. Co and Ni content of nickel–iron: summary of meteoritic material. Note change of scale for Ni at 20 wt.% and for Co at 2 wt.%.

Irons: data for *bulk* compositions taken from Scott (1972, Fig. 16) with principal regions for types I, IIa, b, IId, IIIa, IIIc, IVa, IVb, and others outlined. The unusual Butler iron with Co-rich kamacite (Ni 6–6.5 Co 1.7), taenite (Ni 16–45 Co 0.6), and plessite is shown separately (Goldstein, 1966). *Eucrites and howardites*: data for homogeneous kamacite grains from the Binda howardite and Macibini eucrite from Lovering (1964). Five grains from the Juvinas eucrite showed diverse bulk compositions (filled triangles; Wänke *et al.*, 1971). Iron in micrometer intergrowth with troilite in the Moama eucrite has Ni 0.04 Co 0.16 wt.% (Lovering, 1975). Duke (1965) reported Ni for Ni–Fe metal in 10 basaltic achondrites, but Co was not measured: 6 have Ni <1 wt.%, 3 have 2–4% Ni, and one contains taenite (38%) with kamacite (4%). We obtained new data for iron in the Ibitira eucrite described by Wilkening and Anders (1975): iron associated with troilite has Ni 0.9 Co 0.8–1.1, and that with ilmenite and spinel has Ni 0.1–0.3 Co 0.4–0.6.

Carbonaceous chondrites: large filled circles are for metal grains (high Cr 0.16–1.0 and high P 0–3.2 wt.%) usually enclosed in forsterite crystals in black matrix of Type II (C2) carbonaceous chondrites (Olsen *et al.*, 1973a). Inclined crosses show compositions of kamacite and taenite (some as aggregates) in 7 Type III carbonaceous chondrites (Fuchs and Olsen, 1973). Kamacite dominates in 5 specimens, but in Allende and Ornans the metal is mostly taenite giving bulk compositions near 67 and 61 wt.% Ni. Note that one cross for kamacite lies outside the ringed area at Ni 5.2 Co 6.9.

Other meteorites: the hexagons show compositions of bulk Ni–Fe metal in enstatite chondrites (ec), pallasites, bronzite–enstatite chondrites (bec) and hypersthene–olivine chondrites (hoc) as reported by Lovering (1964) from a Ph.D. thesis by Greenland. The dotted line labeled enc shows the composition range for Ni–Fe in enstatite chondrites (Keil, 1968) which lies at higher Co than the mean reported by Lovering (1964); the horizontal cross at Ni 3.3 Co 0.61 is for the Kota-Kota enstatite chondrite. The only Ni–Co pair for an enstatite *achondrite* is for the Bustee specimen (Wai and Knowles, 1972), but Ni analyses and general chemical properties suggest that enstatite achondrites have a similar range of Co–Ni to enstatite chondrites (Wasson and Wai, 1970). An abstract by Gooley and Moore (1973) reported generally low Ni in diogenites (<3%; 0.1% in Garland and Shalka; up to 52% in Ibbenbüren) and high Co (>1%; up to 8% in Ibbenbüren and 27% in Roda). The metal phases of the ordinary chondrites show complex textures and zoning profiles of Ni and Fe, but detailed data are not available for Co (*e.g.* Wood, 1967; Taylor and Heymann, 1971; Dodd, 1971; Goldstein and Doan, 1972). The Ni contents of bulk metal from mesosiderites range from 7.0 to 9.0 wt.% (Powell, 1969; Wasson *et al.*, 1974); although no specific Co analyses were made, general chemical relations indicate similar levels to those in the iron meteorites.

The star at Ni 5 Co 0.3 is the predicted value for conversion of all Fe to the metallic state in normal or carbonaceous chondrites (Wlotzka *et al.*, 1972). Not plotted are the following data for bulk metal analyzed by neutron activation (Wänke *et al.*, 1970): Juvinas eucrite Ni 2.9 Co 0.62, Norton County aubrite 10.3, 0.27 and 9.1, 0.29, Pultusk H-chondrite: 9.1, 0.46, Ramsdorf L-chondrite 13.9 0.63.

sult of loss of CO, S, H_2O, and O_2 either upon meteoritic impact or from thermal metamorphism. Increasing grade of metamorphism and recycling of lunar breccias by fresh impacts should result in a tendency towards hybridization of all the different types of iron. Reduction of silicate, oxide, and sulfide could yield iron low in Ni and Co, and this could dilute the Ni and Co concentrations of iron from most meteoritic debris and most lunar rocks. The solar wind implants the outer 0.1μm with protons and carbon atoms, and the present-day flux of protons could reduce about 10^3g/cm^2 Fe during the past 3 Gy if no protons were lost during the impact. However, the escape velocity for the Moon is only 2.4 km/sec, and some impacting bodies, especially present-day micrometeorites, should hit at such a high velocity (10–25 km/sec) that a substantial fraction of material is lost. The situation before −4Gy is especially uncertain, but processes associated with impacts must have caused substantial reduction of iron in rocks, breccias, and fines perhaps for depths in the range of kilometers.

The next sections describe some of the mineralogical properties of iron metal in lunar rocks in the context of the above introduction. Emphasis will be placed on the Co and Ni content. Data for meteoritic specimens recently fallen on Earth are shown in Figure 18 to provide a possible reference point. For convenience, the scales for Ni and Co change at 20 and 2 weight percent respectively, causing two kinks in the line for the cosmic ratio Ni/Co ~ 20. A detailed explanation is given in the figure legend. The *bulk* compositions of metal from irons and non-carbonaceous chondrites have more than 5 percent Ni, and the Ni/Co trend cuts across the line for the

cosmic ratio. Reduction of all the Fe to the metallic state would bring all the chondritic metal close to the star at Ni 5 Co 0.3 weight percent (Wlotzka *et al.*, 1972), but only partial reduction is to be expected for chondrites incorporated into lunar surface rocks, because some Fe should remain in the silicates; indeed the enstatite chondrites should become oxidized with loss of the Si from the metal to form silicate. Kamacite and taenite in Type III carbonaceous chondrites are respectively poorer and richer in Ni/Co than the cosmic ratio, and the bulk composition of the metal from the Allende meteorite is very rich in Ni. The metal from most eucrites and howardites has relatively low Ni and high Co, but metal from the Moama eucrite has no detectable Ni and only a little Co. In general the metals from the eucrites and howardites except for the Macibini eucrite can be matched with those from the mare basalts.

Mare basalts. Two types of metal occur in mare basalts (Fig. 19). That in the Ti-rich mare basalts found at Apollo 11 and 17 sites occurs only as blebs in troilite (see earlier). The final liquid should be very low in Ni and fairly low in Co as a result of prior crystallization of olivine and/or pyroxene. Although few analyses were made, Co apparently ranges from 1.4 to 0 weight percent while Ni decreases slightly from 0.4 to 0.00 weight percent. The metal in the relatively low-Ti basalts from Apollo 12 and 15 sites crystallized throughout the entire crystallization range of the silicates, and its Ni content drops from as high as 30 weight percent for inclusions in early olivine to as low as 0 weight percent for crystals in the final residuum where a little troilite may occur. Different rocks show different composition ranges, and different investigators reported inconsistent ranges for the same rock (*e.g.* for 12004). However, the general trend is clear, and the data can be explained by the expected tendency for the early ferromagnesian minerals to extract Mg and Ni out of the liquid, allowing Fe to increase, while Co tended to be intermediate in behavior (Hewins and Goldstein, 1974). Idiosyncrasies may ultimately be correlated with the complex behavior of the other minerals, especially pyroxene and oxide minerals (see earlier). Whether the negative correlations between S and Fe° in mare basalts result from loss of S during crystallization or whether they result from inheritance of properties of the source region of mare basalts (perhaps early cumulates) is undecided (Gibson *et al.*, 1975). Taylor *et al.* (1973a) correlated the Cr content of Fe,Ni metal in 15536 basalt with that of coexisting oxides and other minerals; the highest values of 0.2 to 0.7 weight percent were for metal coexisting with chromite, but fluorescence error must be considered.

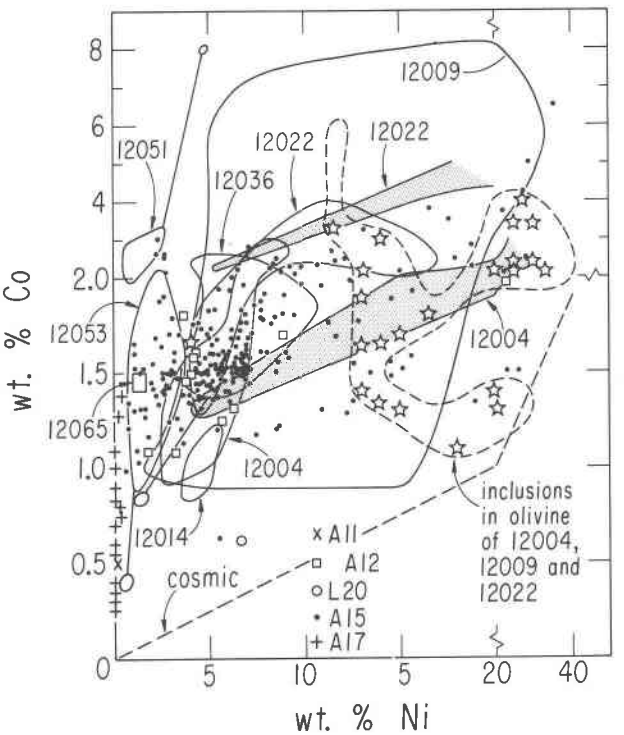

FIG. 19. Co and Ni content of nickel-iron: mare basalts. Note change of scale for Ni at 20 wt.% and for Co at 2 wt.%. *Apollo 11*: numerous general statements that Ni is very low (<0.1) and Co variable between 0 and 0.7; 1 datum from Simpson and Bowie (1970). *Apollo 12*: ranges given by different authors for same rock do not agree completely; ranges for various rocks are outlined from data of Brett *et al.* (1971), Busche *et al.* (1971), Cameron (1971), El Goresy *et al.* (1971), Reid *et al.* (1970), Taylor *et al.* (1971), Wlotzka *et al.* (1972), and Wood *et al.* (1971); inclusions in olivines from 12004, 12009, and 12022 are shown by special symbol; ranges for metal enclosed by olivine from 12004 and 12022 (Hewins and Goldstein, 1974) are stippled. *Luna 20*: one datum, Tarasov *et al.* (1973). *Apollo 15*: rake samples, Dowty *et al.* (1973b); Fig. 8 shows plots for individual rocks; olivine-phyric samples tend to have Ni-rich metal compared to pyroxene-phyric ones. Four gabbros show similar composition ranges but extending to lower Co contents when Ni is zero (Taylor *et al.*, 1975; Taylor and Misra, 1975). *Apollo 17*: Taylor and Williams (1974), Meyer and Boctor (1974).

Selected non-mare rocks. Figure 20 shows the Co/Ni contents of metal from some of the key rocks mentioned earlier. The metal in mosaic assemblages of the troctolitic granulite 76535 consists of both high-Ni and low-Ni varieties. Most particles consist of one or the other, but some form a 2-phase assemblage similar to the "clear taenite" found in ordinary chondrites (Taylor and Heymann, 1971) and in lunar soils (Axon and Goldstein, 1973). A strong diffusion profile was found at the 76535 kamacite-taenite

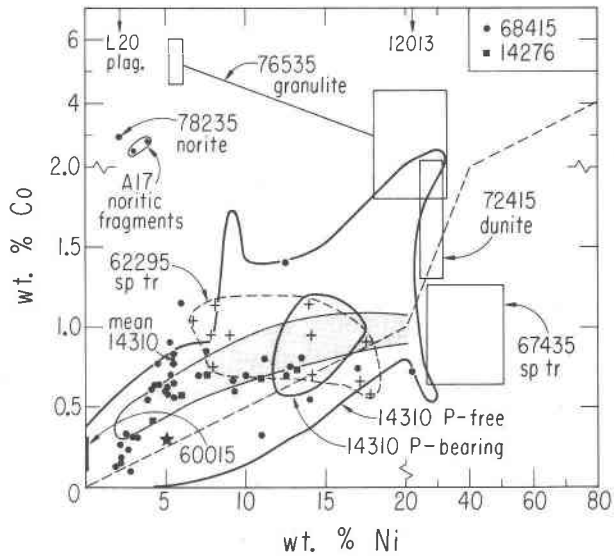

FIG. 20. Co and Ni content of nickel-iron: selected non-mare rocks. Note change of scale for Ni at 20 wt.% and for Co at 2 wt.%. 76535 troctolitic granulite, single grains and kamacite–taenite assemblages, Gooley *et al.* (1974), oriented particles in the interior of plagioclase grains contain Ni 5–15 Co up to 5%; 72415 dunite clast, Albee *et al.* (1974b); 78235 norite, interstitial grains associated with whitlockite, apatite, rutile, baddeleyite, chromite, and troilite, McCallum *et al.* (1975a); "noritic" fragments in Apollo 17 soil appear to be similar to 78235, metal in vein and as inclusion in orthopyroxene, Irving *et al.* (1974); 67435 spinel troctolite fragment with coarse texture, Prinz *et al.* (1973); 62295 spinel troctolite with quench texture, metal associated with schreibersite, Brown *et al.* (1973), Misra and Taylor (1975), horizontal crosses show individual data; 14310 plagioclase-rich basalt, many data, heavy lines outline ranges for P-bearing and P-free metal measured by James (1973), stippled area shows range obtained by El Goresy *et al.* (1971) as reported by Hewins and Goldstein (1975a, Fig. 1), cross shows mean value of range Ni 5.5±5.4 Co 0.8±0.4 obtained by Ridley *et al.* (1972), see also Gancarz *et al.* (1971); 68415 plagioclase-rich basalt, large filled circles show data obtained by Taylor *et al.* (1973a) and Gancarz *et al.* (1972); 14276 plagioclase-rich basalt, filled squares, Gancarz *et al.* (1972); granitic part of 12013 KREEP-rich polymict breccia contained metal with 21.5–23% Ni but no data for Co, Drake *et al.* (1970); metal in fine-grained aggregates of plagioclase in 60015 anorthosite believed to result from shock melting, Ni 0.11–0.13 Co 0.20–0.32, Sclar and Baur (1974).

boundaries. Metal also occurs as oriented needles in the interior but not at the grain margins of the plagioclase. If analogy with the pure Fe–Ni system is valid, the kamacite–taenite assemblages reacted down to 400°C, and the inferred cooling rate is a few tens of degrees per million years for the range 800 to 400°C. The 72415 dunite clast contains metal with Co and Ni ranges which overlap those for the troctolite. The metal from the 78235 norite and Apollo 17 "noritic" fragments has only 2 percent Ni but relatively high Co (2.5–3.0). All these composition ranges fall in the high-Co part of the range for mare basalts, and one might conclude generally that the metal in the upper mantle and lower crust has equilibrated with the Fe,Mg silicates and tends to be relatively rich in Ni and Co. The 67435 spinel troctolite has very Ni-rich metal, while the 62295 spinel troctolite has metal with 7–17 weight percent Ni and 0.7–1.1 percent Co whose range overlaps that for the 14310 plagioclase-rich basalt. Unfortunately the data for this basalt are somewhat inconsistent. James (1973) showed two rather wide ranges, one for P-free metal fairly close to the cosmic line and centered on Ni 14 Co 0.9, and a particularly wide range for P-bearing metal which tends to straddle the cosmic line and which extends to pure Fe. Hewins and Goldstein (1975b) explained a narrow trend obtained by El Goresy *et al.* (1971) in terms of fractional crystallization involving simultaneous crystallization of metal and silicate. The mean value of 14310 metal given by Ridley *et al.* (1972) appears relatively high in Co. Data for metal in plagioclase-rich basalts 14276 and 68415 mostly lie in the range for 14310 metal. Perhaps all three are derived from melted regolith, and are somewhat inhomogeneous.

Plagioclase crystals in Luna 20 fines also contain rods of Fe about 0.5μm wide and several to 100μm long (Brett *et al.*, 1973; Bell and Mao, 1973). Up to four orientations of the rods occur. Rounded blebs formed when the rods reached the surface. Electron microprobe analyses revealed about 1 percent Ni (Brett *et al.*) and 2.1 percent Ni (Bell and Mao). Exsolution of Fe from plagioclase is the favored mechanism for growth of these rods because they occur in the interior but not at margins of plagioclase grains in the 76535 granulite. Presumably Fe exsolved from grain margins migrated into the mosaic assemblages. Exsolution of Fe requires a reduction mechanism. Many lunar rocks, fragments, and clasts contain veins or intergranular clots of complex assemblages containing several of the following phases: iron, troilite, baddeleyite, apatite, whitlockite, several silicates including diopside. Perhaps the whole crust is pervaded by vapors which react in subtle ways with the main minerals. Metal grains in the granitic part of 12013 KREEP-rich polymict breccia contain 22 percent Ni (Drake *et al.*, 1970), and the Co content should be measured.

Anorthosites (sensu stricto) contain little or no metal. Most workers did not report iron metal in the 15415 anorthosite (Genesis Rock), but Hewins and Goldstein (1975b) located very tiny grains devoid of Ni and Co, possibly attributable to shock reduction.

Indeed Sclar and Baur (1974) reported only 0.1 Ni and 0.3 weight percent Co in metal enclosed in fine-grained aggregates of plagioclase believed to have resulted from shock melting of 60015 anorthosite. Figure 21 shows ranges of Co and Ni for metal in "anorthositic" rocks studied by Hewins and Goldstein (1975b). Those for coarse-grained specimens mostly fall in the range for metal in mare basalts (Fig. 19), whereas those for recrystallized specimens tend to be richer in Ni and lower in Co. Considerable overlap occurs for the latter and the metal in the plagioclase-rich basalts and 62295 spinel troctolite (Fig. 20).

Fines. The iron in the fines ranges from coarse fragments up to ~1mm across down to submicroscopic particles enclosed in glass. As described in the introduction, the latter appear to be essentially pure iron formed by reduction of silicate. Many morphologies were reported (*e.g.* Frondel *et al.*, 1970). This section is concerned principally with the coarse particles for which extensive metallographic and electron microprobe studies were made mostly by J. I. Goldstein, F. Wlotzka, and their respective co-workers. Figures 22, 24, 25, and 26 summarize the analyses of the *bulk* Co and Ni for several hundred particles from soils at the Apollo sites, while Figure 23 shows the assignment scheme proposed by Goldstein *et al.* (1974). Because of space restrictions, we have combined together data for soils of similar nature, but there are subtle differences discussed in detail by Goldstein *et al.* Although we agree with the general conclusions, we adopt a rather more sceptical attitude to assignment of metal in lunar fines. Based on the data plotted in Figures 18, 19, 20, and 21, we conclude that (a) the high-Fe and high-Co basaltic ranges are continuous, and the lower limit of the high-Co basaltic field should be placed horizontally at Co ~ 1 weight percent, (b) the meteorite field applies only to a restricted group of relatively "undifferentiated" meteorites with Co/Ni near the cosmic ratio, and does not encompass the very differentiated eucrites and howardites which tend to overlap the lunar basalts, (c) non-basaltic lunar rocks such as anorthosite, norite, and granulite contain iron in the basaltic high-Co range, (d) recrystallized rocks such as 14310 and the recrystallized "anorthositic" rocks of Figure 21 occupy wide ranges of uncertain meaning. Furthermore we note that shock-reduced lunar iron has low Ni from magnetic data, and probably falls in the high-Fe basaltic range of Goldstein *et al.*

Metallic spherules, 50μm–5mm across, from Apollo 11, 12, 14, 15, and 16 fines show complex

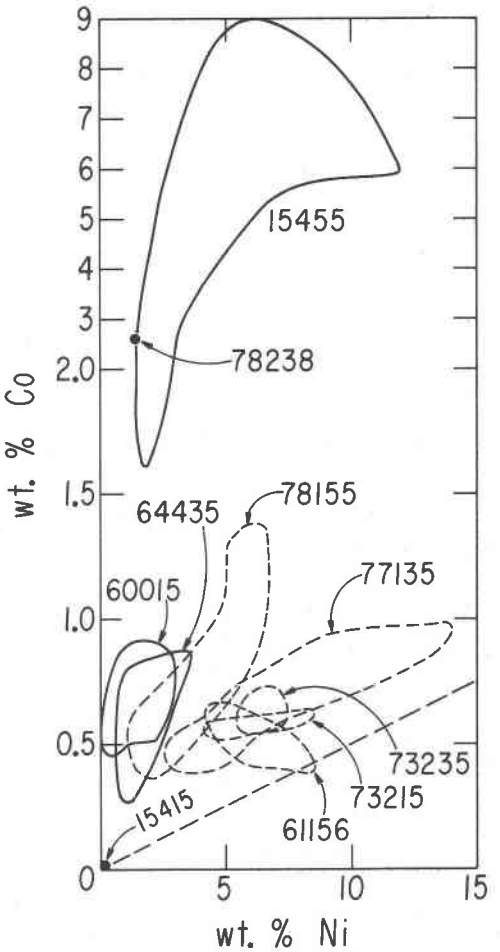

FIG. 21. Co and Ni content of nickel-iron: feldspar-rich (anorthositic) specimens. Note change of scale for Co at 2 wt.%. Described in abstract (Hewins and Goldstein, 1975b). Full lines show ranges for coarse anorthosites and dashed ones for recrystallized anorthosites.

microtextures which were studied systematically by Blau and Goldstein (1975) using optical and scanning electron microscopy plus electron microprobe analysis. Cooling rates were deduced by comparing textures with those of quenched droplets of synthetic molten alloys. About 30 percent of the lunar spherules had dendritic or cellular textures indicative of rapid quenching, and Blau and Goldstein concluded that 6 out of 65 spherules partially or completely solidified by radiation loss during flight in the lunar vacuum, that 3 solidified upon conduction loss to a silicate substrate, and that about 9 cooled by both radiation and conduction. The remaining 70 percent had globular metal areas, and some had solid-state precipitates; a variety of processes including relatively slow cooling or even reheating in an ejecta

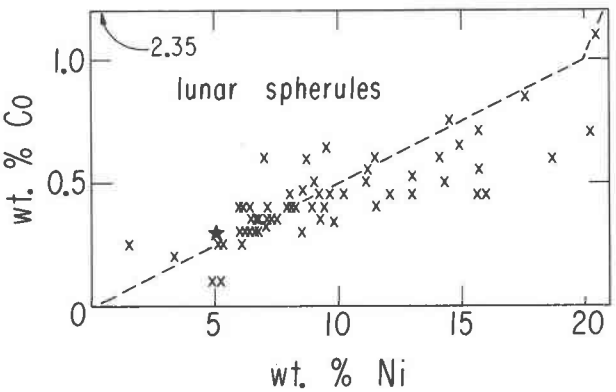

FIG. 22. Co and Ni content of nickel–iron: lunar spherules. Bulk compositions. Many textural and chemical details in Blau and Goldstein (1975). One datum at Ni 0.2 Co 2.35 omitted.

blanket could be possible. The Co and Ni contents mostly lie in a band (Fig. 22) from Ni 6 Co 0.35 to Ni 20 Co 0.8, which closely matches the band for irons and non-carbonaceous chondrites (Fig. 18), including the tendency for low Ni specimens to have more Co than the cosmic ratio while the high Ni ones have less Co than the cosmic ratio. The simplest explanation is that the spherules mostly result from bulk iron in a range of meteorites, and that contamination with lunar iron is insignificant. Three spherules with Ni < 5, one with high Co(2.3), and two with low Co(0.2) may result from lunar or meteoritic sources or a mixture of both; for example the one at Ni 3 Co 0.25 falls near the range for the Macibini eucrite.

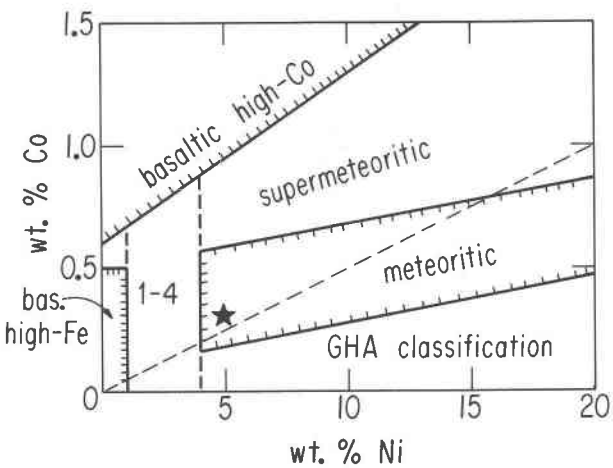

FIG. 23. Metal classification of Goldstein *et al.* (1974) based on Ni and Co content. Abbreviated as M (meteoritic), SM (supermeteoritic), Fe (basaltic high-Fe), Co (basaltic high-Co), and 1–4 (submeteoritic with Ni 1–4% and Co below basaltic high-Co). See their Figures 6 and 7 for histograms of metal in lunar soils.

The S and P contents average at 2.7 and 3.5 weight percent with most values below 8 and 10 weight percent. All six radiation-cooled spherules are S-rich. Phosphorus could have derived from either reduction of phosphate or from original phosphide. Experimental data indicated that Fe,Ni,Co,S,P alloy forms two immiscible liquids upon melting. This explained both the sulfide husks found around many lunar spherules and the enrichment of Co and Ni in the phosphide-rich areas. That the spherules occur in all Apollo soils, irrespective of whether they are of mare or highland type, confirms assignment to a meteoritic origin. Because most spherules have Ni > 5, hybridism with reduced metal from lunar silicate sources should be small. Furthermore the extreme paucity of high-Co metal argues against formation of spherules from lunar rocks except in rare instances. This study of large lunar spherules gives confidence in attempting to interpret the more complex data for other types of iron in lunar soils.

Blau and Goldstein (1975) listed the many references to small metal spherules in and on glasses of which the mounds revealed by scanning electron microscopy are particularly spectacular. Although requiring further study, it is likely that the smaller spherules tend to be poorer in Ni and Co, and to have formed by reduction of Fe^{2+} in silicates. Carter and McKay (1972) simulated the mounds experimentally.

As a crude approximation, we brought together the numerous data for large irregular particles in fines from highland sites (Apollo 14, Apollo 16, and Luna 20; Fig 24), sites with high-Ti mare basalt (Apollo 11 and 17; Fig. 25), and sites with low-Ti mare basalt (Apollo 12 and 15; Fig. 26). It must be emphasized that in the later Apollo missions, the fines from the different subregions should and do vary considerably. The crystallization ages of the basalts at the sites are Apollo 14 (Al-rich) −4.0Gy, Apollo 11 (Ti-rich) −3.8 to −3.6, Apollo 17 (Ti-rich) −3.8 to −3.7, Apollo 12 (quartz and olivine) −3.4 to −3.2, and Apollo 15 (quartz and olivine) −3.4 to −3.3 (Taylor, 1975). Naively one might test whether meteoritic contamination had changed with time by comparing the metal from the various fines, but the uncertainties are immense. All the plotted data are for large metal particles mostly near 100μm across, but the size populations are different for each soil (*e.g.* Apollo 14 and 15 soils, Wlotzka *et al.*, 1972, between 20 and 100μm after grinding the soils; Apollo 15, Goldstein and Axon, 1972, 50–250μm; Apollo 16, Goldstein and Axon, 1973, over 200μm).

For these relatively large, irregular particles, the

simple distribution for spherules is replaced by complex distributions. Immediately obvious is a strong tendency for all soils to have a concentration of metal particles with bulk compositions near Ni 6 Co 0.45, and indeed the tendency is so high that individual points could not be plotted therein without overlap. Actually the cluster for each Apollo site occupies a slightly different region, and the clusters for the older sites tend to center about Ni 6, whereas those for the younger Apollo 12 and 15 sites center about Ni 5. The reason for the clustering is unclear. Certainly there is no simple match with the spherules, and one might speculate that an early meteoritic component tends to be dominated by relatively Ni-poor material, whereas a later meteoritic component shows a wide range of Ni like that for meteorites now impacting the Earth. Wlotzka *et al.* (1972) pointed out that complete reduction of all Fe^{2+} to Fe° in a "normal or carbonaceous chondrite" would give iron with 5 percent Ni and 0.3 percent Co (star in several of Figs. 18–26.) Neutron activation analyses of Co, Cu, Ga, Ge, As, Pd, Ir, and Au for bulk metal from 14163 fines matched quite well with calculated values for either a reduced carbonaceous chondrite or for a hexahedrite. The details are complex, but in general the agreement results because all these types of meteorite are relatively undifferentiated.

The highland soils contain very little iron with Co > 1, indicating little contribution from high-Co basaltic, anorthositic, noritic, and granulitic rocks. The fairly strong concentration of pure iron may result more from reduction of Fe^{2+} than from contribution of high-Fe basaltic component. Most of the data fall in a parallelogram from Ni 0 Co 0 weight percent to 10,0.3; 10,0.9; and 0,0.6. Much of this range overlaps those for recrystallized "anorthosites" in Figure 21 and feldspar-rich basalts in Figure 20. The simplest explanation is that the iron of these highland soils consists mainly of a complex mixture of metals from an ancient meteoritic component and a variety of feldspar-rich rocks. Perhaps thorough study of the chemical composition of silicates and glasses adhering to some of the metal particles would allow further progress to be made.

The soils from Apollo 12 and 15 mare regions contain much Co-rich metal, and there is a high concentration for 15601 soil centered on Co 1.3 Ni 0.25. A high concentration of pure Fe occurs in all these soils. Soil 15601 obtained from the edge of Hadley Rille is shown separately from the other Apollo 15 soils because it has no concentration of metal grains near Ni 5 Co 0.5 and is presumably

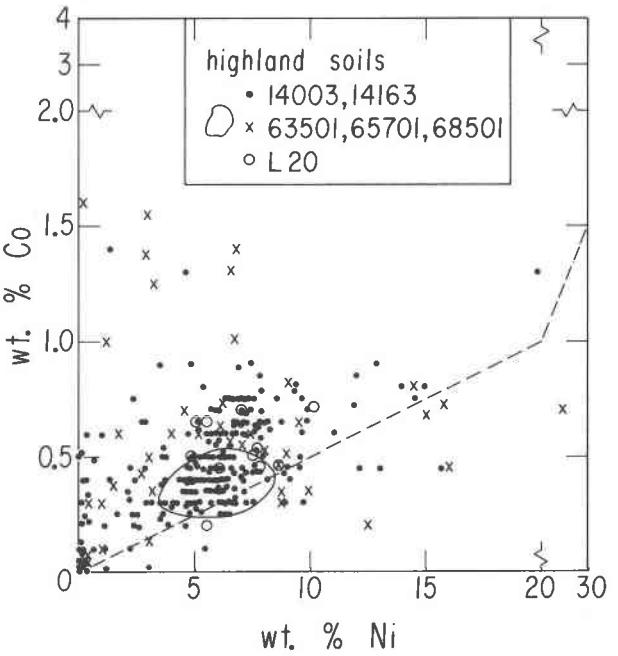

FIG. 24. Co and Ni content of nickel-iron: soils from highland sites. Note change of scale for Ni at 20 wt.% and for Co at 2 wt.%. Apollo 14 (Goldstein *et al.*, 1972; Wlotzka *et al.*, (1972). Apollo 16 (Goldstein and Axon, 1973). Luna 20 (Goldstein and Blau, 1973). The ring outlines a very heavy concentration in all three Apollo 16 soils.

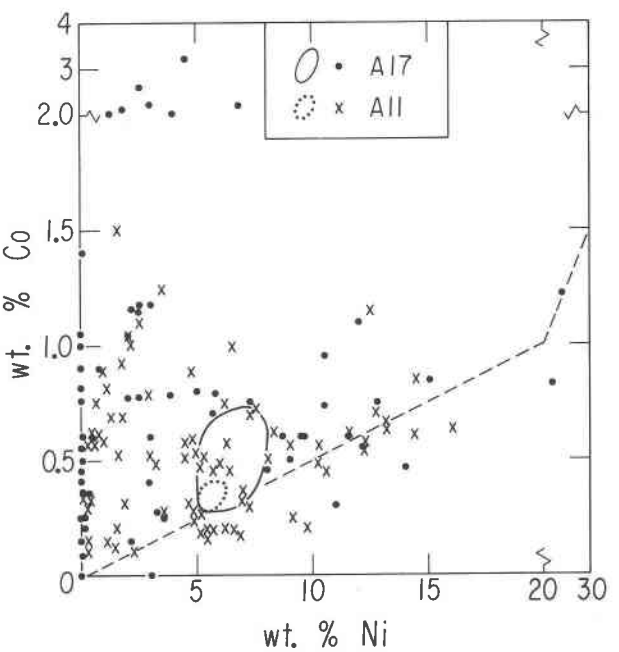

FIG. 25. Co and Ni content of nickel-iron: soils from Apollo 11 and 17. Note change of scale for Ni at 20 wt.% and for Co at 2 wt.%. 10084 (Wlotzka et al., 1972). 78501 and 78510 (Goldstein *et al.*, 1974). Strong concentrations are ringed.

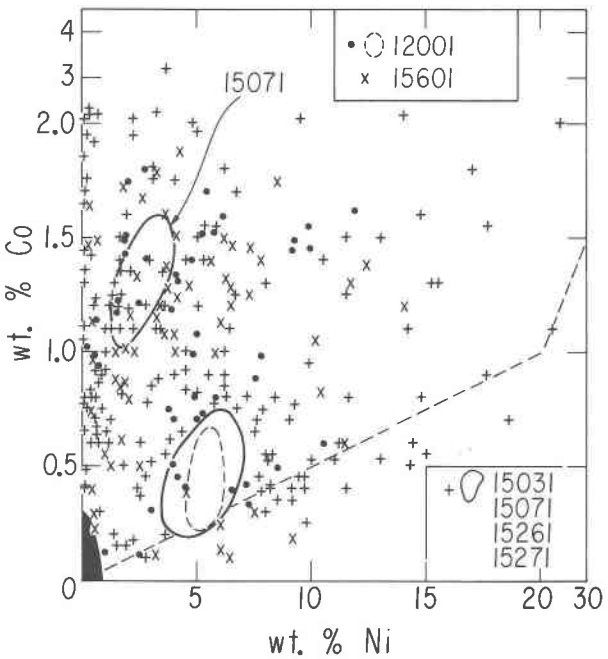

FIG. 26. Co and Ni content of nickel–iron: soils from Apollo 12 and 15. Note change of scale for Ni at 20 wt.% and for Co at 2 wt.%. 12001 (Wlotzka *et al.*, 1972). Apollo 15 (Goldstein and Axon, 1972). Strong concentrations are ringed. The one labeled 15071 occurs only for that soil. The concentration at the origin occurs for all soils. See Axon and Goldstein (1973) and text for data on 2-phase Co-rich particles.

dominated by mare basalt. The soils from Apollo 11 and 17 mare regions contain a wide range of metal compositions even though the local rocks are high Ti basalts whose metal has Ni ~0 and Co <~1. Substantial contribution from either lunar non-mare rocks or "differentiated" meteorites is indicated; of course, fragments of feldspar-rich rocks including anorthosites and norites have been reported by many workers.

Goldstein and co-workers reported many textures and chemical variations too complex to discuss here in detail: among those reported are structureless metal (usually kamacite), kamacite + isothermal taenite, ragged α_2, acicular martensite, zoned taenite, $\alpha + \gamma +$ interstitial phosphide, metal + massive phosphide, metal + phosphide eutectic, and metal + sulfide. In general, some grains have equilibrated to low-temperature assemblages such as coexisting kamacite and taenite, whereas others show different levels of adjustment to lower temperature. Particularly important was the conclusion (Axon and Goldstein, 1973) that some high-Co particles in Apollo 15 soils had annealed to 350°C at conditions probably found only at a depth of 10–20km. Silicon contents are below 0.2 weight percent, thereby ruling out simple addition of Si-rich metal from enstatite chondrites. Sulfur and P are also very low except for metal particles quenched from high temperature. Tungsten contents are much higher than for metal in "undifferentiated" meteorites (Wlotzka *et al.*, 1972), and addition consequent upon reduction of W in lunar rocks is indicated. Chromium is usually low, but one particle from Apollo 14 soils contained 17 weight percent Cr (Goldstein *et al.*, 1972).

Because most data were obtained on coarse particles or on bulk samples, the role of the smaller particles is rather undefined. Electron microprobe analyses could be extended to particles only a few micrometers or less in diameter. Systematic study of the composition and texture of adhering or containing silicate or glass is mostly lacking, though Goldstein *et al.* have provided some qualitative indications (*e.g.* Goldstein and Axon, 1972). Because silicate should be more abundant than metal in the average product of the solar nebula, several percent of meteoritic silicate should occur in the lunar regolith. Perhaps criteria can be developed for recognizing such material when attached to iron of meteoritic origin.

Breccia. Although there are many data on the composition of iron in breccias, we have not found any obvious patterns different from those in fines. As mentioned repeatedly, metamorphism of mixed debris has yielded very complex materials ranging from weakly metamorphosed breccias up to partially-melted rocks. Many of the fines are merely disrupted breccias. Recrystallization and vapor transport have modified the iron metal in breccias, and the grain size and chemical properties give information on the metamorphic grade. Detailed studies of iron and associated silicate and other minerals in relatively unmetamorphosed breccias may allow decipherment of early processes at the lunar surface.

Conclusion

This review of the mineralogy of the Moon has been set deliberately in a petrological–geochemical context with auxiliary use of geophysical parameters. Although the mineralogy can be interpreted plausibly in the context of an early differentiated Moon whose surface was extensively reworked by various igneous and metamorphic processes, the provenance of most samples is too uncertain for definitive interpretations. The clues provided by the ultrabasic and basic rocks and fragments are very tantalizing, and combined with the equally fragmentary and tantalizing geophysical data, allow speculation about the lunar interior.

In recent years increasing emphasis on igneous and metamorphic processes in meteorites has been coupled with theoretical arguments for catastrophic dynamics to favor high-temperature processes in early bodies in the solar system. Such high-temperature processes unfortunately tend to reduce the number of clues to the mineralogy of the early solar system and to the origin of the planets. In a good detective story, the clues lead inexorably to a unique conclusion, but the case of the Origin of the Moon is still open. The lunar detectives have hauled in excellent clues, but many remain undiscovered. Further exploration of the lunar surface with detailed sample collection is needed when reconnaissance has been completed of other targets in the Solar System; perhaps mankind will learn the futility of expenditures on dreadful war machines and will direct its aggressions to colonization of parts of the Solar System. Scientific study of the Moon might then enter a new phase in which field and laboratory studies would consolidate and extend present knowledge. In the meantime substantial advances should come from the following studies of lunar mineralogy: (a) careful surface study of all lunar samples now in storage for further coarse-grained rocks or clasts, (b) detailed study of all the Mg-rich specimens, especially the "periodotitic" ones, with particular emphasis on those minor and trace elements which undergo substantial fractionation, (c) coordinated study of unmetamorphosed polymict breccias to search for mineralogic and geochemical clues leading to a hierarchy of processes, (d) study of redox conditions as a function of crystallization age to test for an over-all tendency to progressive reduction, (e) detailed study of the chemistry of coexisting iron and silicate minerals in fines and breccias to obtain further clues to the amount and type of meteoritic contamination as a function of time, (f) laboratory studies of potential geochemical indicators such as the partition of transition metals between silicate, metal, and liquid as a function of temperature and redox state. These and many other studies to be invented by ingenious investigators should reduce the uncertainties so often mentioned in this review.

Few scientific endeavors can have been so exciting and so full of good fellowship as the study of the mineralogy of the Moon. We are greatly indebted to our scientific colleagues for their brilliant studies which made this review possible. Scientific historians will probably evaluate the scientific exploration of the Moon as one of the most productive advances in the geological sciences and indeed in the whole of science. Certainly in the specific field of mineralogy, the implications of lunar mineralogy for the origin and development of meteorites and planets will be mined for a very long time indeed.

Perhaps some readers will feel that we have attempted to make too much of the slender clues in lunar minerals to which we reply with a phrase from Robert Browning's famous soliloquy by the Florentine painter Andrea del Sarto: "Ah but a man's reach should exceed his grasp/Or what's a heaven for."

Appendix: Additional lunar minerals

The following minerals extend the list in Part I: *cordierite* (Albee *et al.*, 1974a), inclusion in spinel grain of a plagioclase-rich lithic clast of sample 72435, no chemical or optical data listed; *molybdenite* (Jedwab, 1973), micrometer-size particles in fines, probably contaminant from lubricant in sample cabinets; *farringtonite* (Dowty *et al.*, 1974b), $<4\mu$m grain associated with nickel–iron, troilite, and a Ca–silicate (probably plagioclase) all enclosed by spinel in spinel troctolite clast 65785, chemical analysis showed 51 percent P_2O_5, 41 percent MgO, 4 percent FeO; *akaganéite* (Taylor *et al.*, 1974a,b), identified by X-ray and optical spectra in the "rusty" material previously ascribed to goethite(?) in references listed in Part I, attributed to terrestrial oxyhydration of probably precursors Fe metal and lawrencite in Apollo 16 specimens; *unidentified Cl,Fe,Zn-bearing phases,* probably a sulfate and a phosphate associated with akaganéite; still uncharacterized mineralogically (El Goresy *et al.*, 1973b; see also Taylor *et al.*, 1973b); *bornite*(?) (Carter and Padovani, 1973), chemical identification during SEM study of metallic spherule in 68841 fines, occurs with FeS between interlocking crystals of schreibersite and metallic iron; *aluminum oxycarbide* (?) (Tarasov *et al.*, 1973), 20μm grain in troctolitic fragment from Luna 20, electron microprobe analysis gave 74 percent Al, 20 percent C, and 4 percent 0; *monazite* (Lovering *et al.*, 1974), 10μm grain identified chemically by electron microprobe from mesostasis of 10047 mare basalt; *thorite*(?) (Haines *et al.*, 1972), abstract reporting chemical identification of one U-rich grain in 14259,97 soil; *pyrochlore* (?) (Hinthorne *et al.*, 1975), abstract describing chemical identification of 5μm grain in 76535 granulite, 20 percent UO_2 + ThO_2. *Titanite,* alias sphene, reported in Part I as a doubtful mineral, was chemically identified by Grieve *et al.* (1975), and occurs as anhedral, $<5\mu$m grains associated with ilmenite and troilite in basaltic mesostasis of polymict breccia 14321. Zr-rich phases

show even further complexities, and Brown *et al.* (1975) now record 8 contrasted compositions for zirkelite-type phases. *Graphite* was found with FeS as a nodule in an α-iron fragment of soil 14003 (Goldstein *et al.*, 1972).

Acknowlegments

We thank all our colleagues at the University of Chicago for help and advice, particularly E. Anders, A. T. Anderson, R. N. Clayton, R. Ganapathy and L. Grossman. Technical help from I. Baltuska, R. Banovich, O. Draughn and T. Solberg was much appreciated. We thank B. Mason and R. Brett for helpful criticism and the Publications and Executive Committees of MSA for their difficult decisions on this unusually long manuscript. Generous financial aid came from NASA grant NGL 14-001-171 Res, but the research could not have been carried out without electron microprobe and X-ray facilities built up from NSF grants including the grant to the Materials Research Laboratory (NSF DMR72-03028 A04). The cost of publishing this paper has been met by a special grant from the National Aeronautics and Space Administration.

References

The following reference abbreviations are used throughout:

Apollo 15: The Apollo 15 Lunar Samples (Lunar Science Institute, Houston, Texas)

LS III, IV, V, VI Lunar Science III, IV, V, VI (Lunar Science Institute, Houston, Texas)

PLC 1 Proceedings Apollo 11 Lunar Science Conference, Geochim. Cosmochim. Acta Suppl. 1

PLC 2,3,4,5,6: Proceedings 2nd etc. Lunar Science Conference, Geochim. Cosmochim. Acta Suppl. 2, etc.

AGRELL, S. O., J. E. AGRELL, A. R. ARNOLD AND J. V. P. LONG (1973) Some observations on rock 62295. *LS IV,* 15–17.

———, J. H. SCOON, I. D. MUIR, J. V. P. LONG, J. D. C. MCCONNELL AND A. PECKETT (1970) Observations on the chemistry, mineralogy and petrology of some Apollo 11 lunar samples. *PLC 1,* 93–128.

ALBEE, A. L., A. A. CHODOS, R. F. DYMEK, A. J. GANCARZ AND D. S. GOLDMAN (1974a) Preliminary investigation of boulders 2 and 3, Apollo 17, Station 2: Petrology and Rb–Sr Model Ages. *LS V,* 6–8.

———, ———, ———, ———, ———, D. A. PAPANASTASSIOU AND G. J. WASSERBURG (1974b) Dunite from the lunar highlands: Petrography, deformational history, Rb–Sr age. *LS V,* 3–5.

———, R. F. DYMEK AND D. J. DEPAOLA (1975) Spinel symplectites: high-pressure solid-state reaction or late-stage magmatic crystallization? *LS VI,* 1–3.

———, A. J. GANCARZ AND A. A. CHODOS (1973) Metamorphism of Apollo 16 and 17 and Luna 20 metaclastic rocks at about 3.95 AE: samples 61156, 64423,14-2, 65015, 67483,15-2, 76055, 22006, 22007. *PLC 4,* 569–595.

ANDERSEN, O, (1915) The system anorthite–forsterite–silica. *Am. J. Sci., 4th ser.,* **39,** 407–454.

ANDERSON, A. T. (1973) The texture and mineralogy of lunar periodotite, 15445,10. *J. Geol.* **81,** 219–226.

———, T. F. BRAZIUNAS, J. JACOBY AND J. V. SMITH (1972) Thermal and mechanical history of breccias 14306, 14063, 14270, and 14321. *PLC 3,* 819–835.

——— AND J. V. SMITH (1971) Nature, occurrence, and exotic origin of "gray mottled" (Luny Rock) basalts in Apollo 12 soils and breccias. *PLC 2,* 431–438.

——— AND 10 OTHERS (1970) Armalcolite: a new mineral from the Apollo 11 samples. *PLC 1,* 55–63.

ANDERSON, D. L. (1975) On the composition of the lunar interior. *J. Geophys. Res.* **80,** 1555–1557.

ARRHENIUS, G., J. E. EVERSON, R. W. FITZGERALD AND H. FUJITA (1971) Zirconium fractionation in Apollo 11 and 12 rocks. *PLC 2,* 169–176.

AXON, H. J. AND J. I. GOLDSTEIN (1972) Temperature-time relationships from lunar two phase metallic particles (14310, 14163, 14003). *Earth Planet. Sci. Lett.* **16,** 439–447.

——— AND ——— (1973) Metallic particles of high cobalt content in Apollo 15 soil samples. *Earth Planet. Sci. Lett.* **18,** 173–180.

BASU, A. R. AND I. D. MACGREGOR (1975) Chromite spinels from ultramafic xenoliths. *Geochim. Cosmochim. Acta,* **39,** 937–945.

BAYER, C., J. FELSCHE, H. SCHULZ AND P. RÜEGSEGGER (1972) X-ray study and Mössbauer spectroscopy on lunar ilmenites (Apollo 11). *Earth. Planet. Sci. Lett.* **16,** 273–274.

BELL, P. M. AND H. K. MAO (1973) Optical and chemical analysis of iron in Luna 20 plagioclase. *Geochim. Cosmochim. Acta,* **37,** 755–759.

——— AND ——— (1975) Cataclastic plutonites: possible keys to the evolutionary history of the early Moon. *LS VI,* 34–35. See also *PLC 6,* 231–248.

BENCE, A. E. AND B. AUTIER (1972) Secondary ion analysis of pyroxenes from two porphyritic lunar basalts. *Apollo 15,* 191–194.

———, J. W. DELANO, J. J. PAPIKE AND K. L. CAMERON (1974) Petrology of the highlands massif at Tauris-Littrow: an analysis of the 2–4mm soil fraction. *PLC 5,* 785–827.

——— AND J. J. PAPIKE (1972) Pyroxenes as recorders of lunar basalt petrogenesis: chemical trends due to crystal–liquid interaction. *PLC 3,* 431–469.

———, ——— AND D. H. LINDSLEY (1971) Crystallization histories of clinopyroxenes in two porphyritic rocks from Oceanus Procellarum. *PLC 2,* 559–574.

———, ———, S. SUENO AND J. W. DELANO (1973) Pyroxene poikiloblastic rocks from the lunar highlands. *PLC 4,* 597–611.

BISHOP, F. C., J. V., SMITH AND J. B. DAWSON (1975) Pentlandite–magnetite intergrowth in De Beers spinel lherzolite: review of sulphides in nodules. *Phys. Chem. Earth,* **9,** 323–337.

BLAU, P. J. AND J. I. GOLDSTEIN (1975) Investigation and simulation of metallic spherules from lunar soils. *Geochim. Cosmochim, Acta,* **39,** 309–324.

BOYD, F. R. AND D. SMITH (1971) Compositional zoning in pyroxenes from lunar rock 12021, Oceanus Procellarum. *J. Petrol.* **12,** 439–464.

BRETT, R. (1973) A lunar core of Fe–Ni–S. *Geochim. Cosmochim. Acta,* **37,** 165–170.

——— (1975) Reduction of mare basalts by sulfur loss. *LS VI,*89–91.

———, P. BUTLER, JR., C. MEYER, JR., A. M. REID, H. TAKEDA AND R. WILLIAMS (1971) Apollo 12 igneous rocks 12004, 12008, 12009, and 12022: a mineralogical and petrological study. *PLC 2,* 301–317.

———, R. C. GOOLEY, E. DOWTY, M. PRINZ AND K. KEIL (1973)

Oxide minerals in lithic fragments from Luna 20 fines. *Geochim. Cosmochim. Acta,* **37,** 761–773.

BROWN, G. E. AND B. A. WECHSLER (1973) Crystallography of pigeonites from basaltic vitrophyre 15597. *PLC 4,* 887–900.

BROWN G. M., C. H. EMELEUS, J. G. HOLLAND, A. PECKETT AND R. PHILLIPS (1971) Picrite basalts, ferrobasalts, feldspathic norites, and rhyolites in a strongly fractionated lunar crust. *PLC 2,* 583–600.

———, ———, ———, ——— AND ——— (1972) Mineral-chemical variations in Apollo 14 and Apollo 15 basalts and granitic fractions. *PLC 3,*141–157.

———, A. PECKETT, R. PHILLIPS AND C. H. EMELEUS (1973) Mineral-chemical variations in The Apollo 16 magnesio-feldspathic highland rocks. *PLC 4,* 505–518.

———, ———, C. H. EMELEUS AND R. PHILLIPS (1974) Mineral-chemical properties of Apollo 17 mare basalts and terra fragments. *LS V,* 89–91.

———,———, R. PHILLIPS AND C. H. EMELEUS (1975) Mineralogy and petrology of Apollo 17 basalts. *LS VI,* 95–97 and *PLC 6,* 1–13.

BRYAN, W. B. (1974) Fe–Mg relationships in sector-zoned submarine basalt plagioclase. *Earth Planet. Sci. Lett.* **24,** 157–165.

BUNCH, T. E. AND K. KEIL (1971) Chromite and ilmenite in nonchondritic meteorites. *Am. Mineral.* **56,** 146–157.

———, ——— AND K. G. SNETSINGER (1967) Chromite composition in relation to chemistry and texture of ordinary chondrites. *Geochim. Cosmochim. Acta,* **31,** 1569–1582.

——— AND E. OLSEN (1975) Distribution and significance of chromium in meteorites. *Geochim. Cosmochim. Acta,* **39,** 911–927.

BURNHAM, C. W. (1971) The crystal structure of pyroxferroite from Mare Tranquillitatis. *PLC 2,* 47–57.

BURNS, R. G., D. J. VAUGHAN, R. M. ABU-EID AND M. WITNER (1973) Spectral evidence for Cr^{3+}, Ti^{3+} and Fe^{2+} rather than Cr^{2+} and Fe^{3+} in lunar ferromagnesian silicates. *PLC 4,* 983–994.

BUSCHE, F. D., G. H. CONRAD, K. KEIL, M. PRINZ, T. E. BUNCH, J. ERLICHMAN AND W. L. QUAIDE (1971) Electron microprobe analyses of minerals from Apollo 12 lunar samples. *Univ. New Mexico Inst. Meteorit., Spec. Pub.* **3.**

———, M. PRINZ, K. KEIL AND T. E. BUNCH (1972) Spinels and the petrogenesis of some Apollo 12 igneous rocks. *Am. Mineral.* **57,** 1729–1747.

CAMERON, E. N. (1970) Opaque minerals in certain lunar rocks from Apollo 11. *PLC 1,* 221–245.

——— (1971) Opaque minerals in certain lunar rocks from Apollo 12. *PLC 2,* 193–206.

——— (1975) Postcumulus and subsolidus equilibration of chromite and coexisting silicates in the Eastern Bushveld Complex. *Geochim. Cosmochim. Acta,* **39,** 1021–1033.

CAMERON, K. L. AND M. CAMERON (1973) Mineralogy of ultramafic nodules from Knippa Quarry, near Uvalde, Texas. *Geol. Soc. Am. Abstr. Programs,* **5,** 566.

——— AND J. W. DELANO (1973) Petrology of Apollo 15 consortium breccia 15465. *PLC 4,* 461–466.

———, ———, A. E. BENCE AND J. J. PAPIKE (1973) Petrology of the 2–4mm soil fraction from the Hadley-Apennine region of the Moon. *Earth Planet. Sci. Lett.* **19,** 9–21.

——— AND G. W. FISHER (1975) Olivine-matrix reactions in thermally-metamorphosed Apollo 14 breccias. *Earth Planet. Sci. Lett.* **25,** 197–207.

CARTER, J. L. AND D. S. MCKAY (1972) Metallic mounds produced by reduction of material of simulated lunar composition and implications on the origin of metallic mounds on lunar glasses. *PLC 3,* 953–970.

——— AND E. PADOVANI (1973) Genetic implications of some unusual particles in Apollo 16 less than 1mm fines 668841,11 and 69941,13. *PLC 4,* 323–332.

CARTER, N. L., L. A. FERNANDEZ, H. G. AVE'LALLEMANT AND I. S. LEUNG (1971) Pyroxenes and olivines in crystalline rocks from the Ocean of Storms. *PLC 2,* 775–795.

———, I. S. LEUNG, H. G. AVE'LALLEMANT AND L. A. FERNANDEZ (1970) Growth and deformational structures in silicates from Mare Tranquillitatis. *PLC 1,* 267–285.

CHAMPNESS, P. E., A. C. DUNHAM, F. G. F. GIBB, H. N. GILES, W. S. MACKENZIE, E. F. STUMPFL AND J. ZUSSMAN (1971) Mineralogy and petrology of some Apollo 12 lunar samples. *PLC 2,* 359–376.

——— AND G. W. LORIMER (1971) An electron microscopic study of a lunar pyroxene. *Contrib. Mineral. Petrol.* **33,** 171–183.

CHAO, E. C. T. (1973) The petrology of 76055,10, a thermally metamorphosed fragment-laden olivine micronorite hornfels. *PLC 4,* 645–664.

——— AND 14 OTHERS (1970) Pyroxferroite, a new calcium-bearing iron silicate from Tranquillity Base. *PLC 1,* 65–79.

CHARLES, R. W., D. A. HEWITT AND D. R. WONES (1971) H_2O in lunar processes: The stability of hydrous phases in lunar samples 10058 and 12013. *PLC 2,* 645–664.

CHRISTIE, J. M., J. S. LALLY, A. H. HEUER, R. M. FISHER, D. T. GRIGGS AND S. V. RADCLIFFE (1971) Comparative electron petrography of Apollo 11, Apollo 12, and terrestrial rocks. *PLC 2,* 69–89.

CHRISTOPHE-MICHEL-LEVY, M., C. LEVY, R. CAYE AND R. PIERROT (1972) The magnesian spinel-bearing rocks from the Fra Mauro formation. *PLC 3,* 887-894. Given incorrectly as (1973) in Part I.

CISOWSKI, C. S., J. R. DUNN, M. FULLER, M. F. ROSE AND P. J. WASILEWSKI (1974) Impact processes and lunar magnetism. *PLC 5,* 2841–2858.

CLANTON, U. S., J. L. CARTER AND D. S. MCKAY (1975) Vapor-phase crystallization of sulfides? *LS VI,* 152–154. See also *PLC 6,* 719–728.

CLAYTON, R. N. AND T. K. MAYEDA (1975) Genetic relations between the Moon and meteorites. *LS VI,* 155–157 and *PLC 6,* 1761–1769.

COMPSTON, W., M. J. VERNON, H. BERRY, R. RUDOWSKI, C. M. GRAY AND N. WARE (1972) Age and petrogenesis of Apollo 14 basalts. *LS III,* 151–153.

CRAWFORD, M. L. (1973) Crystallization of plagioclase in mare basalts. *PLC 4,* 705–717.

——— AND L. S. HOLLISTER (1974) KREEP basalt: A possible partial melt from the lunar interior. *PLC 5,* 399–419.

DALTON, J. AND L. S. HOLLISTER (1974) Spinel–silicate co-crystallization relations in sample 15555. *PLC 5,* 421–429.

DAWSON, J. B. AND J. V. SMITH (1975) Chromite–silicate intergrowths in upper-mantle peridotites. *Phys. Chem. Earth,* **9,** 339–350.

DELANO, J. W., A. E. BENCE, J. J. PAPIKE AND K. L. CAMERON (1973) Petrology of the 2–4mm soil fraction from the Descartes region of the Moon and stratigraphic implications. *PLC 4,* 537–551.

DENCE, M. R., J. A. V. DOUGLAS, A. G. PLANT AND R. J. TRAILL (1970) Petrology, mineralogy and deformation of Apollo 11 samples. *PLC 1,* 315–340.

———, ———, ——— AND ——— (1971) Mineralogy and petrology of some Apollo 12 samples. *PLC 2,* 285–299.

DIXON, J. R. AND J. J. PAPIKE (1975) Petrology of cataclastic anorthosites from the Descartes region of the Moon: Apollo 16. *LS VI,* 190–192.

DOAN, A. S. AND J. I. GOLDSTEIN (1970) The ternary phase diagram, Fe–Ni–P. *Metal. Trans.* **1,** 1759–1767.

DODD, R. T. (1971) The petrology of chondrules in the Sharps meteorite. *Contrib. Mineral. Petrol.* **31,** 201–227.

DOWTY, E., K. KEIL AND M. PRINZ (1972a) Anorthosite in the Apollo 15 rake sample from Spur Crater. *Apollo 15,* 62–66.

———, ——— AND ——— (1973a) Major-element vapor fractionation on the lunar surface: an unusual lithic fragment from the Luna 20 fines. *Earth Planet. Sci. Lett.* **21,** 91–96.

———, ——— AND——— (1974a) Plagioclase twin laws in lunar highland rocks; possible petrogenetic significance. *Meteoritics,* **9,** 183–197.

———, ——— AND ——— (1974b) Igneous rocks from Apollo 16 rake samples. *PLC 5,* 431–445.

———, ——— AND ——— (1974c) Lunar pyroxene–phyric basalts: crystallization under supercooled conditions. *J. Petrol.* **15,** 419–453.

———, M. PRINZ AND K. KEIL (1973b) Composition, mineralogy, and petrology of 28 mare basalts from Apollo 15 rake samples. *PLC 4,* 423–444.

———, ——— AND ——— (1974d) Ferroan anorthosite: A widespread and distinctive lunar rock type. *Earth Planet. Sci. Lett.* **24,** 15–25.

———, M. ROSS AND F. CUTTITTA (1972b) Fe^{2+}–Mg site distribution in Apollo 12021 clinopyroxenes: evidence for bias in Mössbauer measurements, and relation of ordering to exsolution. *PLC 3,* 481–492.

DRAKE, M. J., I. S. MCCALLUM, G. A. MCKAY AND D. F. WEILL (1970) Mineralogy and petrology of Apollo 12 sample No. 12013: A progress report. *Earth Planet. Sci. Lett.* **9,** 103–123.

DUBA, A., H. C. HEARD AND R. N. SCHOCK (1974) Electrical conductivity of olivine at high pressure and under controlled oxygen fugacity. *J. Geophys. Res.* **79,** 1667–1673.

DUKE, M. B. (1965) Metallic iron in basaltic achondrites. *J. Geophys. Res.* **70,** 1523–1527.

DUNLOP, D. J., W. A. GOSE, G. W. PEARCE AND D. W. STRANGWAY (1973) Magnetic properties and granulometry of metallic iron in lunar breccia 14313. *PLC 4,* 2977–2990.

DWORNIK, E. J., C. S. ANNELL, R. P. CHRISTIAN, F. CUTTITTA, R. B. FINKELMAN, D. T. LIGON, JR. AND H. J. ROSE, JR. (1974) Chemical and mineralogical composition of Surveyor 3 scoop sample 12029,9. *PLC 5,* 1009–1014.

DYAL, P., C. W. PARKIN AND W. D. DAILY (1974) Temperature and electrical conductivity of the lunar interior from magnetic transient measurements in the geomagnetic tail. *PLC 5,* 3059–3071.

EL GORESY, A., M. PRINZ AND P. RAMDOHR (1975) Zoning in spinels as an indicator of the crystallization histories of Apollo 12 and 15 mare basalts. *Geol. Soc. Am., Abstracts with Programs,* **7,** 1067.

———, P. RAMDOHR AND O. MEDENBACH (1973a) Lunar samples from Descartes sites: opaque mineralogy and geochemistry. *PLC 4,* 733–750.

———, ———, ——— AND H. J. BERNHARDT (1974) Taurus-Littrow TiO_2-rich basalts: opaque mineralogy and geochemistry. *PLC 5,* 627–652.

———, ———, M. PAVIĆEVIĆ, O. MEDENBACH, O. MÜLLER AND W. GENTNER (1973b) Zinc, lead, chlorine and FeOOH-bearing assemblages in the Apollo 16 sample 66095: origin by impact of a comet or a carbonaceous chondrite. *Earth Planet. Sci. Lett.* **18,** 411–419.

———, P. RAMDOHR AND L. A. TAYLOR (1971) The opaque minerals in the lunar rocks from Oceanus Procellarum. *PLC 2,* 219–235.

———, L. A. TAYLOR AND P. RAMDOHR (1972) Fra Mauro crystalline rocks: mineralogy, geochemistry and subsolidus reduction of the opaque minerals. *PLC 3,* 333–349.

ENGELHARDT, W. VON, J. ARNDT, W. F. MÜLLER AND D. STÖFFLER (1970) Shock metamorphism of lunar rocks and origin of the regolith at the Apollo 11 landing site. *PLC 1,* 363–384.

EVANS, H. T. JR. (1970) The crystallography of lunar troilite. *PLC 1,* 399–408.

FLORAN, R. J., K. L. CAMERON, A. E. BENCE AND J. J. PAPIKE (1972) Apollo 14 breccia 14313: A mineralogic and petrologic report. *PLC 3,* 661–671.

FORESTER, D. W. (1973) Mössbauer search for ferric oxide phases in lunar materials and simulated lunar materials. *PLC 4,* 2697–2707.

FRIEBELE, E. J., D. L. GRISCOM, C. L. MARQUARDT, R. A. WEEKS AND D. PRESTEL (1974) Temperature dependence of the ferromagnetic resonance linewidth of lunar soils, iron and magnetite precipitates in simulated lunar glasses, and nonspherical metallic iron particles. *PLC 5,* 2729–2736.

FRONDEL, C., C. KLEIN JR., J. ITO AND J. C. DRAKE (1970) Mineralogical and chemical studies of Apollo 11 lunar fines and selected rocks. *PLC 1,* 445–474.

FRONDEL, J. W. (1975) *Lunar Mineralogy.* Wiley-Interscience. New York.

FUCHS, L. H. (1968) The phosphate mineralogy of meteorites. In, P. M. Millman, Ed., *Meteorite Research,* Reidel, Dordrecht.

——— (1971) Orthopyroxene and orthopyroxene-bearing rock fragments rich in K, REE, and P in Apollo 14 soil samples 14163. *Earth Planet. Sci. Lett.* **12,** 170–174.

———AND E. OLSEN (1973) Composition of metal in Type III carbonaceous chondrites and its relevance to the source-assignment of lunar metal. *Earth Planet. Sci. Lett.* **18,** 379–384.

———, ——— AND K. J. JENSEN (1973) Mineralogy, mineral-chemistry, and composition of the Murchison (C2) meteorite. *Smithsonian Contrib. Earth Sci.,* No. *10,* 1–39.

GANAPATHY, R., R. R. KEAYS, J. C. LAUL AND E. ANDERS (1970) Trace elements in Apollo 11 lunar rocks: implications for meteorite influx and origin of Moon. *PLC 1,* 1117–1142.

———, J. W. MORGAN, H. HIGUCHI, E. ANDERS AND A. T. ANDERSON (1974) Meteoritic and volatile elements in Apollo 16 rocks and in separated phases from 14306. *PLC 5,* 1659–1683.

GANCARZ, A. J., A. L. ALBEE AND A. A. CHODOS (1971) Petrologic and mineralogic investigation of some crystalline rocks returned by the Apollo 14 mission. *Earth Planet. Sci. Lett.* **12,** 1–18.

———, ——— AND ——— (1972) Comparative petrology of Apollo 16 sample 68415 and Apollo 14 samples 14276 and 14310. *Earth Planet. Sci. Lett.* **16,** 307–330.

GAY, P., G. M. BANCROFT AND M. G. BOWN (1970) Diffraction and Mössbauer studies of minerals from lunar soils and rocks. *PLC 1,* 481–497.

———, M. G. BOWN AND I. D. MUIR (1972) Mineralogical and petrographic features of two Apollo 14 rocks. *PLC 3,* 351–362.

———, ———, ———, G. M. BANCROFT AND P. G. L. WILLIAMS (1971) Mineralogical and petrographic investigation of some Apollo 12 samples. *PLC 2,* 377–392.

GHOSE, S., I. S. MCCALLUM AND E. TIDY (1973) Luna 20 pyroxenes: exsolution and phase transformation as indicators of petrologic history. *Geochim. Cosmochim. Acta,* **37,** 831–839.

———, G. NG AND L. S. WALTER (1972) Clinopyroxenes from Apollo 12 and 14: exsolution, domain structure and cation order. *PLC 3,* 507–531.

———, C. WAN AND I. S. MCCALLUM (1975) Late thermal history of lunar anorthosite 67075: Evidence from cation order in olivine and orthopyroxene. *LS VI,* 282–283.

GIBB, F. G. F. (1974) Supercooling and the crystallization of plagioclase from a basaltic magma. *Mineral. Mag.* **39,** 641–653.

GIBSON, E. K. JR., S. CHANG, K. LENNON, G. W. MOORE AND G. W. PEARCE (1975) Carbon, sulfur, hydrogen and metallic iron abundances in Apollo 15 and 17 basalts. *LS VI,* 290–292. See also *PLC 6,* 1287–1301.

——— AND G. W. MOORE (1973) Carbon and sulfur distributions and abundances in lunar fines. *PLC 4,* 1577–1586.

——— AND ——— (1974) Sulfur abundances and distributions in the valley of Taurus-Littrow. *PLC 5,* 1823–1837.

GOLDSTEIN, J. I. (1966) Butler, Missouri: an unusual iron meteorite. *Science* **153,** 975.

——— AND H. J. AXON (1972) Metallic particles from 3 Apollo 15 soils. *Apollo 15,* 78–81.

——— AND ——— (1973) Composition, structure, and thermal history of metallic particles from 3 Apollo 16 soils, 65701, 68501, and 63501. *PLC 4,* 751–775.

———, ——— AND S. O. AGRELL (1975) The structure and thermal history of five large metal particles from the lunar regolith. *LS VI,* 303–305.

———, ——— AND C. F. YEN (1972) Metallic particles in the Apollo 14 lunar soil. *PLC 3,* 1037–1064.

——— AND P. J. BLAU (1973) Chemistry and thermal history of metal particles in Luna 20 soils. *Geochim. Cosmochim. Acta,* **37,** 847–855.

——— AND A. S. DOAN, JR. (1972) The effect of phosphorus on the formation of the Widmänstatten pattern in iron meteorites. *Geochim. Cosmochim. Acta,* **36,** 51–69.

———, E. P. HENDERSON AND H. YAKOWITZ (1970) Investigation of lunar metal particles. *PLC 1,* 499–512.

———, R. H. HEWINS AND H. J. AXON (1974) Metal silicate relationships in Apollo 17 soils. *PLC 5,* 653–671.

——— AND H. YAKOWITZ (1971) Metallic inclusions and metal particles in the Apollo 12 lunar soil. *PLC 2,* 177–191.

GOOLEY, R. C., R. BRETT AND J. L. WARNER (1973) Crystallization history of metal particles in Apollo 16 rake samples. *PLC 4,* 799–810.

———, ———, ——— AND J. R. SMYTH (1974) A lunar rock of deep crustal origin: sample 76535. *Geochim. Cosmochim. Acta,* **38,** 1329–1339.

——— AND C. B. MOORE (1973) The metal in diogenites. *Meteoritics,* **8,** 41 (abstr.).

GOSE, W. A., G. W. PEARCE, D. W. STRANGWAY AND E. E. LARSON (1972) Magnetic properties of Apollo 14 breccias and their correlation with metamorphism. *PLC 3,* 2387–2395.

GREEN, D. H. (1975) Genesis of Archean peridotitic magmas and constraints on Archean geothermal gradients and tectonics. *Geology,* **2,** 15–18.

GRIEVE, R. A. F., G. A. MCKAY, H. D. SMITH AND D. F. WEILL (1975) Lunar polymict breccia 14321: a petrographic study. *Geochim. Cosmochim. Acta,* **39,** 229–245.

——— AND A. G. PLANT (1973) Partial melting on the lunar surface, as observed in glass coated Apollo 16 samples. *PLC 4,* 667–679.

GRIFFIN, W. L., R. ÅMLI AND K. S. HEIER (1972) Whitlockite and apatite from lunar rock 14310 and from Ödegården, Norway. *Earth Planet. Sci. Lett.* **15,** 53–58.

GRISCOM, D. L., E. J. FRIEBELE AND C. L. MARQUARDT (1973) Evidence for a ubiquitous, sub-microscopic "magnetite-like" constituent in the lunar soils. *PLC 4,* 2709–2727.

GROSSMAN, L. (1975) Petrography and mineral chemistry of Ca-rich inclusions in the Allende meteorite. *Geochim. Cosmochim. Acta,* **39,** 433–454.

HAFNER, S. S., D. VIRGO AND D. WARBURTON (1971) Cation distributions and cooling history of clinopyroxenes from Oceanus Procellarum. *PLC 2,* 91–108.

HAGGERTY, S. E. (1971a) Compositional variations in lunar spinels. *Nature Phys. Sci.* **233,** 156–160.

——— (1971b) Subsolidus reduction of lunar spinels. *Nature Phys. Sci.* **234,** 113–117.

——— (1972a) Apollo 14: subsolidus reduction and compositional variations of spinels. *PLC 3,* 305–332.

——— (1972b) Luna 16: an opaque mineral study and a systematic examination of compositional variations of spinels from Mare Fecunditatis. *Earth Planet. Sci. Lett.* **13,** 328–352.

——— (1972c) The mineral chemistry of some decomposition and reaction assemblages associated with Cr–Zr, Ca–Zr and Fe–Mg–Zr titanates. *Apollo 15,* 88–91.

——— (1972d) An enstatite chondrite from Hadley Rille. *Apollo 15,* 85–87.

——— (1973a) Luna 20: mineral chemistry of spinel, pleonaste, chromite, ulvöspinel, ilmenite and rutile. *Geochim. Cosmochim. Acta,* **37,** 857–867.

——— (1973b) Armalcolite and genetically associated opaque minerals in the lunar samples. *PLC 4,* 777–797.

——— (1973c) The chemistry and genesis of opaque minerals in kimberlites. *Intl. Conf. Kimberlites, Extended Abstr.* 147–149.

——— (1973d) Ortho- and para-armalcolite samples in Apollo 17. *Nature Phys. Sci.* **242,** 123–125.

——— (1975) The chemistry and genesis of opaque minerals in kimberlites. *Phys. Chem. Earth,* **9,** 245–307.

HAINES, E. L., A. L. ALBEE, A. A. CHODOS AND G. J. WASSERBURG (1971) Uranium-bearing minerals of lunar rock 12013. *Earth Planet. Sci. Lett.* **12,** 145–154.

———, A. J. GANCARZ, A. L. ALBEE AND G. J. WASSERBURG (1972) The uranium distribution in lunar soils and rocks 12013 and 14310. *LS III,* 350–351.

HARGRAVES, R. B. AND L. S. HOLLISTER (1972) Mineralogic and petrologic study of lunar anorthosite slide 15415,18. *Science,* **175,** 430–432.

HASKIN, L. A., C.-Y. SHIH, B. M. BANSAL, J. M. RHODES, H. WIESMANN AND L. E. NYQUIST (1974) Chemical evidence for the origin of 76535 as a cumulate. *PLC 5,* 1213–1225.

HEARD, H. C., A. DUBA, A. J. PIWINSKII AND R. N. SCHOCK (1975) Electrical conductivity studies: refinement of the selenotherm. *LS VI,* 355–357.

HEIKEN, G. (1975) Petrology of lunar soils. *Rev. Geophys. Space Phys.* **13,** 567–587.

HELZ, R. T. (1972) Rock 14068: an unusual lunar breccia. *PLC 3,* 865–886.

HENDERSON, P. (1975) Reaction trends shown by chrome-spinels of the Rhum layered intrusion. *Geochim. Cosmochim. Acta,* **39,** 1035–1044.

HEUER, A. H., J. M. CHRISTIE, J. S. LALLY AND G. L. NORD, JR.

(1974) Electron petrographic study of some Apollo 17 breccias. *PLC 5,* 275–286.

HEWINS, R. H. AND J. I. GOLDSTEIN (19774) Metal–olivine associations and Ni–Co contents in two Apollo 12 mare basalts. *Earth Planet. Sci. Lett.* **24,** 59–70.

——— AND ——— (1975a) Comparison of silicate and metal geothermometers for lunar rocks. *LS VI,* 356–357.

——— AND ——— (1975b) The provenance of metal in anorthositic rocks. *LS VI,* 358–360 and *PLC 6,* 343–362.

HINTHORNE, J. E., R. CONRAD AND C. A. ANDERSEN (1975) Lead–lead age and trace element abundances in lunar troctolite, 76535. *LS VI,* 373–375.

HLAVA, P. F., M. PRINZ AND K. KEIL (1972) Niobian rutile in an Apollo 14 KREEP fragment. *Meteoritics,* **7,** 479–485.

HODGES, F. N. AND I. KUSHIRO (1973) Petrology of Apollo 16 lunar highlands rocks. *PLC 4,* 1033–1048.

HOLLISTER, L. S., W. E. TRZCIENSKI, JR., R. B. HARGRAVES AND C. G. KULICK (1971) Petrogenetic significance of pyroxenes in two Apollo 12 samples. *PLC 2,* 529–557.

HOUSLEY, R. M., E. H. CIRLIN, N. E. PATON AND I. B. GOLDBERG (1974) Solar wind and micrometeorite alteration of the lunar regolith. *PLC 5,* 2623–2642.

———, R. W. GRANT AND M. ABDEL-GAWAD (1972) Study of excess Fe metal in the lunar fines by magnetic separation, Mössbauer spectroscopy, and microscopic examination. *PLC 3,* 1065–1076.

———, ——— AND N. E. PATON (1973) Origin and characteristics of excess Fe metal in lunar glass welded aggregates. *PLC 4,* 2737–2749.

HUBBARD, N. J., J. M. RHODES, H. WIESMANN, C.-Y. SHIH AND B. M. BANSAL (1974) The chemical definition and interpretation of rock types returned from the non-mare regions of the Moon. *PLC 5,* 1227–1246.

HUFFMAN, G. P., G. R. DUNMYRE AND R. M. FISHER (1975) Superparamagnetic clusters of Fe^{2+} spins in lunar olivines. *LS VI,* 414–416. See also *PLC 6,* 757–772.

———, F. C. SCHWERER, R. M. FISHER AND T. NAGATA (1974) Iron distributions and metallic–ferrous ratios for Apollo lunar samples: Mössbauer and magnetic analyses. *PLC 5,* 2779–2794.

IRVINE, T. N. (1974) Petrology of the Duke Island ultramafic complex, Southeastern Alaska. *Geol. Soc. Am. Mem.* **138.**

IRVING, A. J., I. M. STEELE AND J. V. SMITH (1974) Lunar noritic fragments and associated diopside veins. *Am. Mineral.* **59,** 1062–1068.

JAGODZINSKI, H. AND M. KOREKAWA (1973) Diffuse X-ray scattering by lunar minerals. *PLC 4,* 933–951.

——— AND ——— (1975) Diffuse scattering by domains in lunar and terrestrial plagioclase. *LS VI,* 429–431.

JAMES, O. (1972) Lunar anorthosite 15415: texture, mineralogy and metamorphic history. *Science,* **175,** 432–436.

——— (1973) Crystallization history of lunar feldspathic basalt 14310. *U. S. Geol. Surv. Prof. Pap.* **841.**

JEDWAB, J. (1971) Surface morphology of free-growing ilmenites and chromites from vuggy rocks 10072,31 and 12036,2. *PLC 2,* 923–935.

——— (1973) Rare-micron-size minerals in lunar fines. *PLC 4,* 861–874.

——— AND A. HERBOSCH (1970) Tentative estimation of the contribution of Type I carbonaceous meteorites to the lunar soil. *PLC 1,* 551–559.

JOHNSON, R. E., E. WOERMANN AND A. MUAN (1971) Equilibrium studies in the system MgO–"FeO"–TiO_2. *Am. J. Sci.* **271,** 278–292.

KEIL, K. (1968) Mineralogical and chemical relationships among enstatite chondrites. *J. Geophys. Res.* **73,** 6945–6976.

———, T. E. BUNCH AND M. PRINZ (1970) Mineralogy and composition of Apollo 11 lunar samples. *PLC 1,* 561–598.

———, M. PRINZ AND T. E. BUNCH (1971) Mineralogy, petrology, and chemistry of some Apollo 12 samples. *PLC 2,* 319–341.

KESSON, S. E. AND D. H. LINDSLEY (1975) The effects of Al^{+3}, Cr^{+3}, and Ti^{+3} on the stability of armalcolite in vacuum and at 7.5 kbar. *LS VI,* 472–474. See also *PLC 6,* 911–920.

——— AND A. E. RINGWOOD (1976) Mare basalt petrogenesis in a dynamic Moon. *Earth Planet. Sci. Lett.* **30,** 155–163.

KLEIN, C. JR. AND J. C. DRAKE (1972) Mineralogy, petrology, and surface features of some fragmental material from the Fra Mauro site. *PLC 3,* 1095–1113.

KLEINMANN, B. AND P. RAMDOHR (1971) Alpha-corundum from the lunar dust. *Earth Planet. Sci. Lett.* **13,** 19–22.

KURAT, G., K. KEIL AND M. PRINZ (1974) Rock 14318: a polymict lunar breccia with chondritic texture. *Geochim. Cosmochim. Acta,* **38,** 1133–1146.

KUSHIRO, I. AND H. S. YODER, JR. (1966) Anorthite–forsterite and anorthite–enstatite reactions and their bearing on the basalt eclogite transformation. *J. Petrol.* **7,** 337–362.

LALLY, J. S., A. H. HEUER, G. L. NORD, JR. AND J. M. CHRISTIE (1975) Subsolidus reactions in lunar pyroxenes: an electron petrographic study. *Contrib. Mineral. Petrol.* **51,** 263–281.

———, R. M. FISHER, J. M. CHRISTIE, D. T. GRIGGS, A. H. HEUER, G. L. NORD, JR. AND S. V. RADCLIFFE (1972) Electron petrography of Apollo 14 and 15 rocks. *PLC 3,* 401–422.

LEVY, C., M. CHRISTOPHE-MICHEL-LEVY, P. PICOT AND R. CAYE (1972) A new titanium and zirconium oxide from the Apollo 14 samples. *PLC 3,* 1115–1120.

LINDSLEY, D. H. AND C. W. BURNHAM (1970) Pyroxferroite: stability and X-ray crystallography of synthetic $Ca_{0.15}Fe_{0.85}SiO_3$ pyroxenoid. *Science,* **168,** 364–367.

———, S. E. KESSON, M. J. HARTZMAN AND M. K. CUSHMAN (1974a) The stability of armalcolite: experimental studies in the system MgO–Fe–Ti–O. *PLC 5,* 521–534.

———, H. E. KING AND A. C. TURNOCK (1974b) Compositions of synthetic augite and hypersthene coexisting at 810°C: applications to pyroxenes from lunar highlands rocks. *Geophys. Res. Lett.* **1,** 134–136.

LIPIN, B. R. (1975) The system anorthite–olivine–silica and its bearing on the petrogenesis of lunar crustal rocks. *Geol. Soc. Am. Abstr. with Programs,* **7,** 1172.

——— AND A. MUAN (1974) Equilibria bearing on the behavior of titanate phases during crystallization of iron silicate melts under strongly reducing conditions. *PLC 5,* 535–548.

LOFGREN, G., C. H. DONALDSON, R. J. WILLIAMS, O. MULLINS AND T. M. USSELMAN (1974) Experimentally reproduced textures and mineral chemistry of Apollo 15 quartz normative basalts. *PLC 5,* 549–567.

LONGHI, J., D. WALKER, T. L. GROVE, E. M. STOLPER AND J. F. HAYS (1974) The petrology of the Apollo 17 mare basalts. *PLC 5,* 447–469.

LOVERING, J. F. (1964) Electron microprobe analyses of the metallic phase in basaltic achondrites. *Nature,* **203,** 70.

——— (1975) The Moama eucrite—a pyroxene–plagioclase–plagioclase–adcumulate. *Meteoritics,* **10,** 101–114.

——— AND 14 OTHERS (1971) Tranquillityite: A new silicate mineral from Apollo 11 and Apollo 12 basaltic rocks. *PLC 2,* 39–45.

———, D. A. WARK, A. J. W. GLEADOW AND R. BRITTEN (1974) Lunar monazite: a late-stage (mesostasis) phase in mare basalt. *Earth Planet. Sci. Lett.* **21,** 164–168.

LUNATIC ASYLUM (1970) Mineralogic and isotopic investigations on lunar rock 12013. *Earth Planet. Sci. Lett.* **9,** 137–163.

MAO, H. K., A. EL GORESY AND P. M. BELL (1974) Evidence of extensive chemical reduction in lunar regolith samples from the Apollo 17 site. *PLC 5,* 673–683.

MARVIN, U. B. (1971) Lunar niobian rutile. *Earth Planet. Sci. Lett.* **11,** 7–9.

———, J. A. WOOD, G. J. TAYLOR, J. B. REID, JR., B. N. POWELL, J. S. DICKEY, JR. AND J. F. BOWER (1971) Relative proportions and probable sources of rock fragments in the Apollo 12 soil samples. *PLC 2,* 679–699.

MASON, B. (1972) Mineralogy and petrology of lunar samples 15264,19, 15274,12, and 15314,59. *Apollo 15,* 135–136.

———, W. G. MELSON AND J. NELEN (1972) Spinel and hornblende in Apollo 14 fines. *LS III,* 512–514.

MASSON, C. R., I. B. SMITH, W. D. JAMIESON, J. L. MCLAUCHLAN AND A. VOLBORTH (1972) Chromatographic and mineralogical study of Apollo 14 fines. *PLC 3,* 1029–1036.

MCCALLISTER, R. H. AND L. A. TAYLOR (1973) The kinetics of ulvöspinel reduction: synthetic study and applications to lunar rocks. *Earth Planet. Sci. Lett.* **17,** 357–364.

MCCALLUM, I. S., E. A. MATHEZ, F. P. OKAMURA AND S. GHOSE (1974) Petrology and crystal chemistry of poikilitic anorthositic gabbro 77017. *PLC 5,* 287–302.

———, ———, ——— AND ——— (1975a) Petrology of noritic cumulates: samples 78235 and 78238. *LS VI,* 534–536. See also *PLC 6,* 395–414.

———, F. P. OKAMURA AND S. GHOSE (1975b) Mineralogy and petrology of sample 67075 and the origin of lunar anorthosites. *Earth Planet. Sci. Lett.* **26,** 36–53.

MCKAY, D. S., U. S. CLANTON, D. A. MORRISON AND G. H. LADLE (1972) Vapor phase crystallization in Apollo 14 breccia. *PLC 3,* 739–752.

MCKAY, G. A., S. J. KRIDELBAUCH AND D. F. WEILL (1973) The occurrence and origin of schreibersite–kamacite intergrowths in microbreccia 66055. *PLC 4,* 811–818.

MERCIER, J-C. C. AND A. NICOLAS (1975) Textures and fabrics of upper-mantle peridotites as illustrated by xenoliths from basalts. *J. Petrol.* **16,** 454–487.

MEYER, C., JR., D. H. ANDERSON AND J. G. BRADLEY (1974) Ion microprobe mass analysis of plagioclase from "non-mare" lunar samples. *PLC 5,* 685–706.

———, R. BRETT, N. J. HUBBARD, D. A. MORRISON, D. S. MCKAY, F. K. AITKEN, H. TAKEDA AND E. SCHONDFELD (1971) Mineralogy, chemistry, and origin of the KREEP component in soil samples from the Ocean of Storms. *PLC 2,* 393–411.

MEYER, C. E. AND H. G. WILSHIRE (1974) "Dunite" inclusion in lunar basalt 74275. *LS V,* 503–505.

MEYER, H. O. A. AND N. Z. BOCTOR (1974) Opaque mineralogy: Apollo 17, rock 75035. *PLC 5,* 707–716.

——— AND R. H. MCCALLISTER (1973) Mineralogy and petrology of Apollo 16: Rock 60215,13. *PLC 4,* 661–665.

MINKIN, J. A. AND E. C. T. CHAO (1971) Single crystal X-ray investigation of deformation in terrestrial and lunar ilmenite. *PLC 2,* 237–246.

MISRA, K. C. AND L. A. TAYLOR (1975) Correlation between native metal compositions and the petrology of Apollo 16 rocks. *LS VI,* 566–568. See also *PLC 6,* 615–639.

MOORE, C. B., C. F. LEWIS AND J. D. CRIPE (1974) Total carbon and sulfur contents of Apollo 17 lunar samples. *PLC 5,* 1897–1906.

MORGAN, J. W., R. GANAPATHY, H. HIGUCHI, U. KRÄHENBÜHL AND E. ANDERS (1974) Lunar basins: tenative characterization of projectiles, from meteoritic elements in Apollo 17 boulders. *PLC 5,* 1703–1736.

MUAN, A., J. HAUCK AND T. LÖFALL (1972) Equilibrium studies with a bearing on lunar rocks. *PLC 3,* 185–196.

MURTHY, V. R., N. M. EVENSON AND H. T. HALL (1971) Model of early lunar differentiation. *Nature,* **234,** 267 and 290.

MYSEN, B. (1975) Partitioning of iron and magnesium between crystals and partial melts in peridotite upper mantle. *Contrib. Mineral. Petrol.* **52,** 69–76.

NAGATA, T., R. M. FISHER, F. C. SCHWERER, M. D. FULLER AND J. R. DUNN (1975) Effects of meteorite impacts on magnetic properties of Apollo lunar materials. *LS VI,* 587–589 and *PLC 6,* 3111–3122.

———, N. SUGIURA, R. M. FISHER, F. C. SCHWERER, M. D. FULLER AND J. R. DUNN (1974) Magnetic properties of Apollo 11–17 lunar materials with special reference to effects of meteorite impact. *PLC 5,* 2827–2839.

NEHRU, C. E., M. PRINZ, E. DOWTY AND K. KEIL (1973) Electron microprobe analyses of spinel group minerals and ilmenite in Apollo 15 rake samples of igneous origin. *Inst. Meteorit., Univ. New Mexico, Spec. Publ.* **10.**

———, ———, ——— AND ——— (1974) Spinel-group minerals and ilmenite in Apollo 15 rake samples. *Am. Mineral.* **59,** 1220–1235.

NIEBUHR, H. H., S. ZEIRA AND S. S. HAFNER (1973) Ferric iron in plagioclase crystals from anorthosite 15415. *PLC 4,* 971–982.

O'HARA, M. J. AND D. J. HUMPHRIES (1975) Armalcolite crystallization, phenocryst assemblages, eruption conditions and origin of eleven high titanium basalts from Taurus Littrow. *LS VI,* 619–621.

OLSEN, E. AND L. H. FUCHS (1967) The state of oxidation of some iron meteorites. *Icarus,* **6,** 242–253.

———, ——— AND W. C. FORBES (1973a) Chromium and phosphorus enrichment in the metal of Type II (C2) carbonaceous chondrites. *Geochim. Cosmochim. Acta,* **37,** 2037–2042.

———, J. S. HUEBNER, J. A. V. DOUGLAS AND A. G. PLANT (1973b) Meteoritic amphiboles. *Am. Mineral.* **58,** 869–872.

PAPIKE, J. J. AND A. E. BENCE (1972) Apollo 14 inverted pigeonites: possible samples of lunar plutonic rocks. *Earth Planet. Sci. Lett.* **14,** 176–182.

———, ——— AND D. H. LINDSLEY (1974) Mare basalts from the Taurus-Littrow region of the Moon. *PLC 5,* 471–504.

———, C. T. PREWITT, S. SUENO AND M. CAMERON (1973) Pyroxenes: comparison of real and ideal structural topologies. *Z. Kristallogr.* **138,** 254–273.

PAVIĆEVIĆ, M., P. RAMDOHR AND A. EL GORESY (1972) Electron microprobe investigations of the oxidation states of Fe and Ti in ilmenite in Apollo 11, Apollo 12, and Apollo 14 crystalline rocks. *PLC 3,* 295–303.

PEARCE, G. W., W. A. GOSE AND J. LINDSAY (1975) Reduction of iron and regolith soil maturity. *LS VI,* 634–636.

———, D. W. STRANGWAY AND W. A. GOSE (1974) Magnetic properties of Apollo samples and implications for regolith formation. *PLC 5,* 2815–2826.

———, R. J. WILLIAMS AND D. S. MCKAY (1972) The magnetic properties and morphology of metallic iron produced by subsolidus reduction of synthetic Apollo 11 composition glasses. *Earth Planet. Sci. Lett.* **17,** 95–104.

PECKETT, A., R. PHILLIPS AND G. M. BROWN (1972) New zirconium-rich minerals from Apollo 14 and 15 lunar rocks. *Nature,* **236,** 215–217.

PILLINGER, C. T., P. R. DAVIS, G. EGLINTON, A. P. GOWAR, A. J. T. JULL, J. R. MAXWELL, R. M. HOUSLEY AND E. H. CIRLIN

(1974) The association between carbide and finely divided metallic iron in lunar fines. *PLC 5,* 1949–1961.

POWELL, B. N. (1969) Petrology and chemistry of the mesosiderites—I. Textures and composition of nickel-iron. *Geochim. Cosmochim. Acta,* **33,** 789–810.

———, F. K. AITKEN AND P. W. WEIBLEN (1973) Classification, distribution, and origin of lithic fragments from the Hadley-Apennine region. *PLC 4,* 445–460.

———, AND P. W. WEIBLEN (1972) Petrology and origin of lithic fragments in the Apollo 14 regolith. *PLC 3,* 837–852.

PREWITT, C. T., G. E. BROWN AND J. J. PAPIKE (1971) Apollo 12 clinopyroxenes: high temperature X-ray diffraction studies. *PLC 2,* 59–68.

——— AND D. R. ROTHBARD (1975) Crystal structures of meteoritic and lunar whitlockites. *LS VI,* 646–648.

PRINZ, M., E. DOWTY, K. KEIL AND T. E. BUNCH (1973a) Mineralogy, petrology and chemistry of lithic fragments from Luna 20 fines: origin of the cumulate ANT suite and its relationships to high-alumina and mare basalts. *Geochim. Cosmochim. Acta,* **37,** 979–1006.

———, ———, ——— AND ——— (1973b) Spinel troctolite and anorthosite in Apollo 16 samples. *Science,* **179,** 74–76.

QUAIDE, W., V. OBERBECK, T. BUNCH AND G. POLKOWSKI (1971) Investigations of the natural history of the regolith at the Apollo 12 site. *PLC 2,* 701–718.

RAYMOND, K. N. AND H. R. WENK (1971) Lunar ilmenite (refinement of the crystal structure). *Contrib. Mineral. Petrol.* **30,** 135–140.

REED, S. J. B. AND S. R. TAYLOR (1974) Meteoritic metal in Apollo 16 samples. *Meteoritics,* **9,** 23–34.

REID, A. M., J. Z. FRAZER, H. FUJITA AND J. E. EVERSON (1970) Apollo 11 samples: major mineral chemistry. *PLC 1,* 749–761.

REID, J. B. JR. (1972) Olivine-rich, true spinel-bearing anorthosites from Apollo 15 and Luna 20 soils—possible fragments of the earliest formed lunar crust. *Apollo 15,* 154–157.

RIDLEY, W. I., R. BRETT, R. J. WILLIAMS, H. TAKEDA AND R. W. BROWN (1972) Petrology of Fra Mauro basalt 14310. *PLC 3,* 159–170.

———, N. J. HUBBARD, J. M. RHODES, H. WEISMANN AND B. BANSAL (1973) The petrology of lunar breccia 15445 and petrogenetic implications. *J. Geol.* **81,** 621–631.

RINGWOOD, A. E. AND E. ESSENE (1970) Petrogenesis of Apollo 11 basalts, internal constitution and origin of the Moon. *PLC 1,* 769–799.

ROEDDER, E. AND P. W. WEIBLEN (1971) Petrology of silicate melt inclusions, Apollo 11 and Apollo 12 and terrestrial equivalents. *PLC 2,* 507–528.

——— AND ——— (1972a) Occurrence of chromian, hercynitic spinel ("pleonaste") in Apollo 14 samples and its petrologic implications. *Earth Planet. Sci. Lett.* **15,** 376–402.

——— AND ——— (1972b) Petrographic features and petrologic significance of melt inclusions in Apollo 14 and 15 rocks. *PLC 3,* 251–279.

——— AND ——— (1974) Petrology of clasts in lunar breccia 67915. *PLC 5,* 303–318.

ROEDER, P. L. AND R. F. EMSLIE (1970) Olivine–liquid equilibrium. *Contrib. Mineral. Petrol.* **29,** 275–289.

ROSS, M., J. S. HUEBNER AND E. DOWTY (1973) Delineation of the one atmosphere augite–pigeonite miscibility gap for pyroxenes from lunar basalt 12021 *Am. Mineral.* **58,** 619–635.

RYDER, G., D. B. STOESER, U. B. MARVIN AND J. F. BOWER (1975) Lunar granites with unique ternary feldspars. *PLC 6,* 435–449.

SATO, M., N. L. HICKLING AND J. E. MCLANE (1973) Oxygen fugacity values of Apollo 12, 14, and 15 lunar samples and reduced state of lunar magmas. *PLC 4,* 1061–1079.

SCHÜRMANN, K. AND S. S. HAFNER (1972) Distinct subsolidus cooling histories of Apollo 14 basalts. *PLC 3,* 493–506.

SCLAR, C. B. (1971) Shock-induced features of Apollo 12 microbreccias. *PLC 2,* 817–832.

——— AND J. F. BAUER (1974) Shock-induced melting in anorthositic rock 60015 and a fragment of anorthositic breccia from the "picking pot" (70052). *PLC 5,* 319–336.

———, ———, S. J. PICKART AND H. A. ALPERIN (1973) Shock effects in experimentally shocked terrestrial ilmenite, lunar ilmenite of rock fragments in 1–10mm fines (10085,19), and lunar rock 60015,127. *PLC 4,* 841–859.

SCOTT, E. R. D. (1972) Chemical fractionation in iron meteorites and its interpretation. *Geochim. Cosmochim. Acta,* **36,** 1205–1236.

SHANKLAND, T. J. (1975) Electrical conduction in rocks and minerals: parameters for interpretation. *Phys. Earth Planet. Interiors,* **10,** 209–219.

SIMKIN, T., A. F. NOONAN, G. S. SWITZER, B. MASON, J. A. NELEN AND W. G. MELSON (1973) Composition of Apollo 16 fines 60051, 60052, 64811, 64812, 67711, 67712, 68821, and 68822. *PLC 4,* 279–289.

SIMONDS, C. H., W. C. PHINNEY AND J. L. WARNER (1974) Petrography and classification of Apollo 17 non-mare rocks with emphasis on samples from the Station 6 boulder. *PLC 5,* 337–353.

———, J. L. WARNER AND W. C. PHINNEY (1973) Petrology of Apollo 16 poikilitic rocks. *PLC 4,* 613–632.

SIMPSON, P. R. AND S. H. U. BOWIE (1970) Quantitative optical and electron-probe studies of opaque phases in Apollo 11 samples. *PLC 1,* 873–890.

SKINNER, B. J. (1970) High crystallization temperatures indicated for igneous rocks from Tranquillity Base. *PLC 1,* 891–895.

SMITH, J. V. (1974) Lunar mineralogy: A heavenly detective story. Presidential Address, Part 1. *Am. Mineral.* **59,** 231–243.

——— (1976) Development of the Earth–Moon system with implications for the geology of the early Earth. In, B. F. Windley, Ed., *Proc. NATO Adv. Study Inst.* Leicester, 1975. John Wiley and Sons, London.

———, A. T. ANDERSON, R. C. NEWTON, E. J. OLSEN, P. J. WYLLIE, A. V. CREWE, M. S. ISAACSON AND D. JOHNSON (1970) Petrologic history of the Moon inferred from petrography, mineralogy, and petrogenesis of Apollo 11 rocks. *PLC 1,* 897–925.

——— AND J. B. DAWSON (1975) Chemistry of Ti-poor spinels, ilmenites and rutiles from peridotite and eclogite xenoliths. *Phys. Chem. Earth,* **9,** 309–322.

——— AND I. M. STEELE (1974) Intergrowths in lunar and terrestrial anorthosites with implications for lunar differentiation. *Am. Mineral.* **59,** 673–680.

SMYTH, J. R. (1974a) Low orthopyroxene from a lunar deep crustal rock: a new pyroxene polymorph of space group $P2_1ca$. *Geophy. Res. Lett.* **1,** 27–29. See also *PLC 6,* 821–832.

——— (1974b) The crystal chemistry of armalcolites from Apollo 17. *Earth Planet. Sci. Lett.* **24,** 262–270.

——— (1975) A crystal structure refinement of an anomalous lunar anorthite. *LS VI,* 756–758. See also *PLC 6,* 821–832.

SNETSINGER, K. G., K. KEIL AND T. E. BUNCH (1967) Chromite from "equilibrated" chondrites. *Am. Mineral.* **52,** 1322–1331.

SONETT, C. P. (1975) Solar-wind induction and lunar conductivity. *Phys. Earth Planet. Interiors,* **10,** 313–322.

STEELE, I. M. (1972) Chromian spinels from Apollo 14 rocks. *Earth Planet. Sci. Lett.* **14,** 190–194.

——— (1974) Ilmenite and armalcolite in Apollo 17 breccias. *Am. Mineral.* **59,** 681–689.

——— (1975) Mineralogy of lunar norite 78235: second lunar occurrence of $P2_1ca$ pyroxene from Apollo 17 soils. *Am. Mineral.* **60,** 1086–1091.

——— AND J. V. SMITH (1971) Mineralogy of Apollo 15415 "Genesis rock": source of anorthosite on Moon. *Nature,* **234,** 138–140.

——— AND ——— (1972) Ultrabasic lunar samples. *Nature Phys. Sci.* **240,** 5–6.

——— AND ——— (1973) Mineralogy and petrology of some Apollo 16 rocks and fines: general petrologic model of Moon. *PLC 4,* 519–536.

——— AND ——— (1975a) Lunar touchstones: I Minerals, II Rock Types. *LS VI,* 765–770.

——— AND ——— (1975b) Minor elements in lunar olivine as a petrologic indicator. *PLC 6,* 451–467.

———, ——— AND L. GROSSMAN (1972) Mineralogy and petrology of Apollo 15 rake samples. *Apollo 15,* 161–164.

STEWART, D. B., M. ROSS, B. A. MORGAN, D. E. APPLEMAN, J. S. HUEBNER AND R. F. COMMEAU (1972) Mineralogy and petrology of lunar anorthosite 15415. *LS III,* 726–728.

STOESER, D. B., U. B. MARVIN, J. A. WOOD, R. W. WOLFE AND J. F. BOWER (1974) Petrology of a stratified boulder from South Massif, Taurus-Littrow. *PLC 5,* 355–377.

SUNG, C., R. M. ABU-EID AND R. G. BURNS (1974) Ti^{3+}/Ti^{4+} ratios in lunar pyroxenes: implications to depth of origin of mare basalt magma. *PLC 5,* 717–726.

TAKEDA, H. (1973) Inverted pigeonites from a clast of rock 15459 and basaltic achondrites. *PLC 4,* 875–885.

———, M. MIYAMOTO AND A. M. REID (1974) Crystal chemical control of element partitioning for coexisting chromite–ulvöspinel and pigeonite–augite in lunar rocks. *PLC 5,* 727–741.

TARASOV, L. S., M. A. NASAROV, I. D. SHEVALEEVSKY, E. S. MAKAROV AND V. I. IVANOV (1973) Mineralogy of anorthositic rocks from the region of the crater Apollonius C (Luna-20). *PLC 4,* 333–349.

TAYLOR, G. J., M. J. DRAKE, M. E. HALLAM, U. B. MARVIN AND J. A. WOOD (1973) Apollo 16 stratigraphy: the ANT hills, the Cayley Plains and a pre-Imbrian regolith. *PLC 4,* 553–568.

——— AND D. HEYMANN (1971) The formation of clear taenite in ordinary chondrites. *Geochim. Cosmochim. Acta,* **35,** 175–188.

TAYLOR, L. A. AND R. H. MCCALLISTER (1972) An experimental investigation of the significance of zirconium partitioning in lunar ilmenite and ulvöspinel. *Earth Planet. Sci. Lett.* **17,** 105–109.

———, ——— AND O. SARDI (1973a) Cooling histories of lunar rocks based on opaque mineral geothermometers. *PLC 4,* 819–828.

———, H. K. MAO AND P. M. BELL (1973b) "Rust" in the Apollo 16 rocks. *PLC 4,* 829–839.

———, ——— AND ——— (1974a) Identification of the hydrated iron oxide mineral akaganéite in Apollo 16 lunar rocks. *Geology,* **1,** 429–432.

———, ——— AND ——— (1974b) β-FeOOH, akaganéite, in lunar rocks. *PLC 5,* 743–748.

———, G. KULLERUD AND W. B. BRYAN (1971) Opaque mineralogy and textural features of Apollo 12 samples and a comparison with Apollo 11 rocks. *PLC 2,* 855–871.

——— AND K. C. MISRA (1975) Mineralogy and petrology of Apollo 15 rock 15075. *LS VI,* 801–803. See also *PLC 6,* 165–179.

———, D. R. UHLMANN, R. W. HOPPER AND K. C. MISRA (1975) Absolute cooling rates of lunar rocks based on the kinetics of Zr diffusion in opaque oxides: applications to Apollo 15 rocks from Elbow Crater. *LS VI,* 798–800. See also *PLC 6,* 181–191.

——— AND K. L. WILLIAMS (1973) Cu–Fe–S phases in lunar rocks. *Am. Mineral.* **58,** 952–954.

——— AND ——— (1974) Formational history of lunar rocks: applications of experimental geochemistry of the opaque minerals. *PLC 5,* 585–596.

———, ——— AND R. H. MCCALLISTER (1972) Stability relations of ilmenite and ulvöspinel in the Fe–Ti–O system and application of these data to lunar mineral assemblages. *Earth Planet. Sci. Lett.* **16,** 282–288.

TAYLOR, S. R. (1975) *Lunar Science: A Post-Apollo View.* Pergamon, New York.

TRAILL, R. J., A. G. PLANT AND J. A. V. DOUGLAS (1970) Garnet: first occurrence in the lunar rocks. *Science,* **169,** 981–982.

TSAY, F. AND D. H. LIVE (1974) Ferromagnetic resonance studies of thermal effects on lunar metallic Fe phases. *PLC 5,* 2737–2746.

———, S. L. MANATT AND S. I. CHAN (1973a) Magnetic phases in lunar fines: metallic Fe or ferric oxides? *Geochim. Cosmochim. Acta,* **37,** 1201–1211.

———, ———, D. H. LIVE AND S. I. CHAN (1973b) Metallic Fe phases in Apollo 16 fines: Their origin and characteristics as revealed by electron spin resonance studies. *PLC 4,* 2751–2761.

USSELMAN, T. N. (1975) Experimental approach to the state of the core: Part 1. The liquidus relations of the Fe-rich portion of the Fe–Ni–S system from 30 to 100kb. *Am. J. Sci.* **275,** 278–290.

———, G. E. LOFGREN, C. DONALDSON AND R. J. WILLIAMS (1975) Experimentally reproduced textures and mineral chemistries of high titanium mare basalts. *LS VI, 835–837. See also PLC 6,* 997–1020.

WAI, C. M. AND C. R. KNOWLES (1972) The metal phase of the Bustee enstatite achondrite. *Mineral. Mag.* **38,** 627–629.

WALKER, D., T. L. GROVE, J. LONGHI, E. M. STOLPER AND J. F. HAYS (1973a) Origin of lunar feldspathic rocks. *Earth Planet. Sci. Lett.* **20,** 1325–1336.

———, J. LONGHI, T. L. GROVE, E. STOLPER AND J. F. HAYS (1973b) Experimental petrology and origin of rocks from the Descartes Highlands. *PLC 4,* 1013–1032.

———, ———, E. M. STOLPER, T. L. GROVE AND J. F. HAYS (1975) Origin of titaniferous lunar basalts. *Geochim. Cosmochim. Acta,* **39,** 1219–1235.

WALTER, L. S., B. M. FRENCH, K. F. J. HEINRICH, P. D. LOWMAN, JR., A. S. DOAN AN I. ADLER (1971) Mineralogical studies of Apollo 12 samples. *PLC 2,* 343–358.

WÄNKE, H., F. WLOTZKA, E. JAGOUTZ AND F. BEGEMANN (1970) Composition and structure of metallic iron particles in lunar "fines." *PLC 1,* 931–935.

——— AND 9 OTHERS (1971) Apollo 12 samples: Chemical composition and its relation to sample locations and exposure ages, the two component origin of the various soil samples and studies on lunar metallic particles. *PLC 2,* 1187–1208.

WARK, D. A., A. F. REID, J. F. LOVERING AND A. EL GORESY (1973) Zirconolite (versus zirkelite) in lunar rocks. *LS IV,* 764–766.

WARNER, J. L. (1972) Metamorphism of Apollo 14 breccias. *PLC 3,* 623–643.

———, C. H. SIMONDS AND W. C. PHINNEY (1974) Impact-induced fractionation in the lunar highlands. *PLC 5,* 379–397.

WASILEWSKI, P. (1974) Possible magnetic effects due to fine particle metal and intergrown phases in lunar samples. *The Moon,* **11,** 301–311.

WASSON, J. T., C. CHOU AND W. V. BOYNTON (1975) Temporal decrease of siderophile/iridium ratios in mature lunar soils. *LS VI,* 857–859.

———, R. SCHAUDY, R. W. BILD AND C. CHOU (1974) Mesosiderites I. Compositions of their metallic portions and possible relationship to other metal-rich meteorite groups. *Geochim. Cosmochim. Acta,* **38,** 135–149.

——— AND C. M. WAI (1970) Composition of the metal, schreibersite and perryite of enstatite achondrites and the origin of enstatite chondrites and achondrites. *Geochim. Cosmochim. Acta,* **34,** 169–184.

WECHSLER, B. A., C. T. PREWITT AND J. J. PAPIKE (1975) Structure and chemistry of lunar and synthetic armalcolite. *LS VI, 860–862.*

WEEKS, R. A. (1973) Ferromagnetic phases of lunar fines and breccias: electron magnetic resonance spectra of Apollo 16 samples. *PLC 4,* 2763–2781.

——— AND D. PRESTEL (1974) Ferromagnetic resonance properties of lunar fines and comparison with the properties of lunar analogues. *PLC 5,* 2709–2728.

WEIBLEN, P. W., B. N. POWELL AND F. K. AITKEN (1974) Spinel-bearing feldspathic–lithic fragments in Apollo 16 and 17 soil samples: clues to processes of early lunar crustal evolution. *PLC 5,* 749–767.

——— AND E. ROEDDER (1973) Petrology of melt inclusions in Apollo samples 15598 and 62295, and of clasts in 67915 and several lunar soils. *PLC 4,* 681–703.

WENK, E., A. GLAUSER, H. SCHWANDER AND V. TROMMSDORFF (1972) Twin laws, optic orientation, and composition of plagioclases from rocks 12051, 14053 and 14310. *PLC 3,* 581–589.

WENK, H.-R., W. F. MÜLLER AND G. THOMAS (1973) Antiphase domains in lunar plagioclase. *PLC 4,* 909–923.

WILKENING, L. L. AND E. ANDERS (1975) Some studies of an unusual eucrite: Ibitira. *Geochim. Cosmochim. Acta,* **39,** 1205–1210.

WILLIAMS, K. L. AND L. A. TAYLOR (1974) Optical properties and chemical compositions of Apollo 17 armalcolites. *Geology,* **1,** 5–8.

WLOTZKA, F., E. JAGOUTZ, B. SPETTEL, H. BADDEHAUSEN, A. BALACESCU AND H. WÄNKE (1972) On lunar metallic particles and their contribution to the trace element content of Apollo 14 and 15 soils. *PLC 3,* 1077–1084.

———, B. SPETTEL AND H. WÄNKE (1973) On the composition of metal from Apollo 16 fines and the meteoritic component. *PLC 4,* 1483–1491.

WOOD, J. A. (1967) Chondrites: their metallic minerals, thermal histories, and parent planets. *Icarus,* **6,** 1–49.

——— (1975) Lunar petrogenesis in a well-stirred magma ocean. *PLC 6,* 1087–1102.

———, U. B. MARVIN, J. B. REID, JR., G. J. TAYLOR, J. F. BOWER, B. N. POWELL AND J. S. DICKEY, JR. (1971) Mineralogy and petrology of the Apollo 12 lunar samples. *Smithsonian Astrophysical Observatory Spec. Rep.* **333.**

YAJIMA, T. AND S. S. HAFNER (1974) Cation distribution and equilibrium temperature of pigeonite from basalt 15065. *PLC 5,* 769–784.

YODER, H. S. JR. (1973) Melilite stability and paragenesis. *Fortschr. Mineral.* **50,** 140–173.

Manuscript received, January 12, 1976; accepted for publication, May 11, 1976.